ArevaEPRDCPEm Resource

From: WILLIFORD Dennis (AREVA) [Dennis.Williford@areva.com]
Sent: Thursday, November 29, 2012 12:10 PM
To: Snyder, Amy
Cc: BENNETT Kathy (AREVA); DELANO Karen (AREVA); LEIGHLITER John (AREVA); ROMINE Judy (AREVA); RYAN Tom (AREVA)
Subject: Response to U.S. EPR Design Certification Application RAI No. 547 (6499, 6359), FSAR Ch. 3 - NEW PHASE 4 RAI, Supplement 3
Attachments: RAI 547 Supplement 3 Response US EPR DC.pdf

Amy,

AREVA NP Inc. provided a schedule for a technically correct and complete response to the four questions in RAI No. 547 on July 11, 2012. On October 4, 2012, AREVA NP submitted Supplement 1 which provided a technically correct and complete final response to one (03.07.02-77) of the four remaining questions. On November 27, 2012, AREVA NP submitted Supplement 2 which changed the schedule for one of the three remaining questions.

The attached file, "RAI 547 Supplement 3 Response US EPR DC.pdf" provides a technically correct and complete final response to one of the three remaining questions.

The following table indicates the respective pages in the response document, "RAI 547 Supplement 3 Response US EPR DC.pdf," that contain AREVA NP's response to the subject question. Appended to this file are affected pages of the U.S. EPR Final Safety Analysis Report in redline-strikeout format which support the response to RAI 547, Question 03.07.02-76.

Question #	Start Page	End Page
RAI 547 — 03.07.02-76	2	14

The schedule for a technically correct and complete response to the remaining 2 questions is unchanged and is provided below.

Question #	Response Date
RAI 547 — 03.06.01-14	January 31, 2013
RAI 547 — 03.07.02-78	April 30, 2013

Sincerely,

Dennis Williford, P.E.
U.S. EPR Design Certification Licensing Manager
AREVA NP Inc.
7207 IBM Drive, Mail Code CLT 2B
Charlotte, NC 28262
Phone: 704-805-2223
Email: Dennis.Williford@areva.com

From: WILLIFORD Dennis (RS/NB)
Sent: Tuesday, November 27, 2012 12:40 PM
To: Amy.Snyder@nrc.gov
Cc: BENNETT Kathy (RS/NB); DELANO Karen (RS/NB); LEIGHLITER John (RS/NB); ROMINE Judy (RS/NB); RYAN Tom (RS/NB); WELLS Russell (RS/NB)
Subject: Response to U.S. EPR Design Certification Application RAI No. 547 (6499, 6359), FSAR Ch. 3 - NEW PHASE 4 RAI, Supplement 2

Amy,

AREVA NP Inc. provided a schedule for a technically correct and complete response to the four questions in RAI No. 547 on July 11, 2012. On October 4, 2012, AREVA NP submitted Supplement 1 which provided a technically correct and complete final response to one (03.07.02-77) of the four remaining questions.

The schedule for a technically correct and complete response to the 1 of the remaining 3 questions has been changed as provided below.

Question #	Response Date
RAI 547 — 03.06.01-14	**January 31, 2013**
RAI 547 — 03.07.02-76	November 29, 2012
RAI 547 — 03.07.02-78	April 30, 2013

Sincerely,

Dennis Williford, P.E.
U.S. EPR Design Certification Licensing Manager
AREVA NP Inc.
7207 IBM Drive, Mail Code CLT 2B
Charlotte, NC 28262
Phone: 704-805-2223
Email: Dennis.Williford@areva.com

From: WILLIFORD Dennis (RS/NB)
Sent: Wednesday, October 17, 2012 2:07 PM
To: Amy.Snyder@nrc.gov
Cc: Michael.Miernicki@nrc.gov; BENNETT Kathy (RS/NB); DELANO Karen (RS/NB); LEIGHLITER John (RS/NB); ROMINE Judy (RS/NB); RYAN Tom (RS/NB); GARDNER Darrell (RS/NB) (Darrell.Gardner@areva.com); VANCE Brian (RS/NB); WELLS Russell (RS/NB)
Subject: Response to U.S. EPR Design Certification Application RAI No. 547 (6499, 6359), FSAR Ch. 3 - NEW PHASE 4 RAI, Question 03.06.01-14 - STATUS

Amy,
AREVA appreciates the initial comments received from NRC staff during our telecon on September 25th, the e-mail with additional comments received on September 27th, and the additional comments and status update on the review status of the DRAFT RAI 547 Question 03.06.01-14 response (submitted on August 17, 2012) which were provided by Mike Miernicki on October 15th. We understand that the NRC staff needs additional time to complete their review and provide final comments on the Draft response. AREVA will provide a revised schedule for submittal of the final response to this question after receipt and evaluation of all NRC staff comments.

The schedule for a technically correct and complete final response to the other 2 questions remains unchanged as shown below.

Question #	Response Date
RAI 547 — 03.06.01-14	**TBD**
RAI 547 — 03.07.02-76	November 29, 2012
RAI 547 — 03.07.02-78	April 30, 2013

Sincerely,

Dennis Williford, P.E.
U.S. EPR Design Certification Licensing Manager
AREVA NP Inc.
7207 IBM Drive, Mail Code CLT 2B
Charlotte, NC 28262
Phone: 704-805-2223
Email: Dennis.Williford@areva.com

From: RYAN Tom (RS/NB)
Sent: Thursday, October 04, 2012 1:33 PM
To: Tesfaye, Getachew
Cc: BENNETT Kathy (RS/NB); DELANO Karen (RS/NB); LEIGHLITER John (RS/NB); ROMINE Judy (RS/NB); WILLIFORD Dennis (RS/NB); ABAYAN Victor (EP/PE)
Subject: Response to U.S. EPR Design Certification Application RAI No. 547 (6499, 6359), FSAR Ch. 3 - NEW PHASE 4 RAI, Supplement 1

Getachew,

AREVA NP Inc. provided a schedule for a technically correct and complete response to the four questions in RAI No. 547 on July 11, 2012.

The attached file, "RAI 547 Supplement 1 Response US EPR DC.pdf" provides a technically correct and complete final response to one of the four remaining questions.

The following table indicates the respective pages in the response document, "RAI 547 Supplement 1 Response US EPR DC.pdf," that contain AREVA NP's response to the subject question. Appended to this file are affected pages of the U.S. EPR Final Safety Analysis Report in redline-strikeout format which support the responses to RAI 547 Question 03.07.02-77.

Question #	Start Page	End Page
RAI 547 — 03.07.02-77	2	2

The schedule for a technically correct and complete response to the remaining 3 questions is unchanged and is provided below.

Question #	Response Date

RAI 547 — 03.06.01-14	**October 17, 2012**
RAI 547 — 03.07.02-76	**November 29, 2012**
RAI 547 — 03.07.02-78	**April 30, 2013**

Sincerely,

Tom Ryan for
Dennis Williford, P.E.
U.S. EPR Design Certification Licensing Manager
AREVA NP Inc.
7207 IBM Drive, Mail Code CLT 2B
Charlotte, NC 28262
Phone: 704-805-2223
Email: Dennis.Williford@areva.com

From: WILLIFORD Dennis (RS/NB)
Sent: Wednesday, July 11, 2012 2:52 PM
To: Getachew.Tesfaye@nrc.gov
Cc: BENNETT Kathy (RS/NB); DELANO Karen (RS/NB); ROMINE Judy (RS/NB); RYAN Tom (RS/NB); Michael.Miernicki@nrc.gov; WELLS Russell (RS/NB)
Subject: Response to U.S. EPR Design Certification Application RAI No. 547 (6499, 6359), FSAR Ch. 3 - NEW PHASE 4 RAI

Getachew,

Attached please find AREVA NP Inc.'s response to the subject request for additional information (RAI). The attached file, "RAI 547 Response US EPR DC.pdf," provides a schedule since a technically correct and complete response to the four questions cannot be provided at this time.

The following table indicates the respective pages in the response document, "RAI 547 Response US EPR DC.pdf," that contain AREVA NP's response to the subject questions.

Question #	Start Page	End Page
RAI 547 — 03.06.01-14	2	2
RAI 547 — 03.07.02-76	3	4
RAI 547 — 03.07.02-77	5	5
RAI 547 — 03.07.02-78	6	12

The schedule for a technically correct and complete response to these 4 questions is provided below.

Question #	Response Date
RAI 547 — 03.06.01-14	**October 17, 2012**
RAI 547 — 03.07.02-76	**November 29, 2012**
RAI 547 — 03.07.02-77	**November 14, 2012**
RAI 547 — 03.07.02-78	**April 30, 2013**

Sincerely,

Dennis Williford, P.E.
U.S. EPR Design Certification Licensing Manager
AREVA NP Inc.
7207 IBM Drive, Mail Code CLT 2B
Charlotte, NC 28262
Phone: 704-805-2223
Email: Dennis.Williford@areva.com

From: Tesfaye, Getachew [mailto:Getachew.Tesfaye@nrc.gov]
Sent: Friday, June 15, 2012 2:45 AM
To: ZZ-DL-A-USEPR-DL
Cc: Xu, Jim; Thomas, Brian; Miernicki, Michael; Clark, Phyllis; Segala, John; ArevaEPRDCPEm Resource
Subject: U.S. EPR Design Certification Application RAI No. 547 (6499, 6359), FSAR Ch. 3 - NEW PHASE 4 RAI

Attached please find the subject request for additional information (RAI). A draft of the RAI was provided to you on May 17, 2012, and June 12, 2012, you informed us that the RAI is clear and no further clarification is needed. As a result, no change is made to the draft RAI. The schedule we have established for review of your application assumes technically correct and complete responses within 30 days of receipt of RAIs. For any RAIs that cannot be answered within 30 days, it is expected that a date for receipt of this information will be provided to the staff within the 30 day period so that the staff can assess how this information will impact the published schedule.

Thanks,
Getachew Tesfaye
Sr. Project Manager
NRO/DNRL/LB1
(301) 415-3361

Hearing Identifier: AREVA_EPR_DC_RAIs
Email Number: 4116

Mail Envelope Properties (2FBE1051AEB2E748A0F98DF9EEE5A5D4F6FBC8)

Subject: Response to U.S. EPR Design Certification Application RAI No. 547 (6499, 6359), FSAR Ch. 3 - NEW PHASE 4 RAI, Supplement 3
Sent Date: 11/29/2012 12:09:50 PM
Received Date: 11/29/2012 12:10:26 PM
From: WILLIFORD Dennis (AREVA)

Created By: Dennis.Williford@areva.com

Recipients:
"BENNETT Kathy (AREVA)" <Kathy.Bennett@areva.com>
Tracking Status: None
"DELANO Karen (AREVA)" <Karen.Delano@areva.com>
Tracking Status: None
"LEIGHLITER John (AREVA)" <John.Leighliter@areva.com>
Tracking Status: None
"ROMINE Judy (AREVA)" <Judy.Romine@areva.com>
Tracking Status: None
"RYAN Tom (AREVA)" <Tom.Ryan@areva.com>
Tracking Status: None
"Snyder, Amy" <Amy.Snyder@nrc.gov>
Tracking Status: None

Post Office: auscharmx02.adom.ad.corp

Files	**Size**	**Date & Time**
MESSAGE	9661	11/29/2012 12:10:26 PM
RAI 547 Supplement 3 Response US EPR DC.pdf	2506159	

Options
Priority: Standard
Return Notification: No
Reply Requested: No
Sensitivity: Normal
Expiration Date:
Recipients Received:

Response to

Request for Additional Information No. 547, Supplement 3

9/28/2012

U. S. EPR Standard Design Certification
AREVA NP Inc.
Docket No. 52-020

SRP Section: 03.07.02 - Seismic System Analysis

QUESTIONS for Structural Engineering Branch 2 (ESBWR/ABWR Projects) (SEB2)

Question 03.07.02-76:

Open Item

Follow-up RAI 371, Question 03-07-02-67 (Supplement 24 Response)

In RAI 371, Question 03.07.02-67, the staff asked the applicant to provide a comparison of NI Common Basemat Structure ISRS computed from a fixed base ANSYS model with that of ISRS computed from a fixed base SASSI model. Since the ANSYS 3D Finite Element Model (FEM) used for static analysis serves as the basis for the SASSI FEM, the comparison was requested to determine if the SASSI model is dynamically equivalent to the more detailed ANSYS model. In its response the applicant provided comparisons of ISRS for a number of locations on the NI. Most of the ISRS comparisons show only slight differences between the two models. However there were a number of cases in which the ANSYS result was noticeably higher than the SASSI result. These are discussed below:

1. The applicant has noted that there is a discrepancy in the dome ISRS of the Shield Building. At a frequency of approximately 15 Hz the static model results exceed the dynamic model results by about 23 percent. Although the applicant claims this is due to a small deviation in the ANSYS model from the perfect dome geometry around the apex of the dome and due to irregularities in the dome surface geometry, it is not clear why this would lead to a difference of over 20 percent in the results for the two models. In addition the ZPA for the static model exceeds that of the dynamic model by about 14 percent.
2. A comparison of ISRS for the Reactor Building Internal Structure (RBIS) at elevation 63 feet, 11 ¾ inches for the Z or vertical direction (Figure 03.07.02-67-36) shows the static model result at a frequency of about 15 Hz to be 31 percent higher than the dynamic model result. In addition, at 15 Hz both results exceed the ISRS envelope shown on FSAR Figure 3.7.2-79 (Revision 3). At this same elevation a similar result is observed for the X direction (Figure 03.07.02-67-34) where the static model result at a frequency of about 10 Hz is 44 percent higher than the dynamic model result. At 10 Hz, both results exceed the ISRS envelope shown on FSAR Figure 3.7.2-79 (Revision 3). The ZPA for the static model in the X direction is 20 percent higher than that of the dynamic model. Since the ISRS envelope includes soil case 5ae which has a shear wave velocity of 13,123 ft/sec and in effect provides a rigid support for the NI, it is not clear why the fixed base SASSI result exceeds the results for case 5ae.
3. A comparison of ISRS for the RBIS at elevation 16 feet, 10 ¾ inches for the Y direction (Figure 03.07.02-67-38) shows the static model result at about 15 Hz is 24 percent higher than the dynamic model result. At 15 Hz, both results exceed the ISRS shown on FSAR Figure 3.7.2-75 (Revision 3). For the Z direction at about the same frequency the static model result exceeds the dynamic model result by about 14 percent.
4. A comparison of ISRS for the Fuel Building at elevation 23 feet, 7 ½ inches for the Z direction (Figure 03.07.02-67-27) shows the static model result at a frequency of about 7 Hz to be 15 percent higher than the dynamic model result.
5. A comparison of Y-direction ISRS for Safeguard Building 1 (Figure 03.07.02-67-8) and X-direction ISRS for Safeguard Building 2/3 (Figure 03.07.02-67-19) at an elevation of 26 feet 3 inches shows that the static model results at frequencies less than 10 Hz to be 21 and 24 percent higher, respectively, than the dynamic model results. The envelope of the ISRS shown on FSAR Figures 3.7.2-81(Revision 3) for Safeguard Building 1 is about 5 percent

lower than the static result at a frequency of about 7.5 Hz. For Safeguard building 2/3 the envelope of ISRS shown on FSAR Figure 3.7.2-87 (Revision 3) exceeds both the static model and dynamic results. This might suggest that the comparison of static and dynamic results for the Safeguard Building at elevation 26 feet 3 inches are acceptable because the envelope of ISRS is approximately equal to or exceeds the static model result. However at frequencies below 10 Hz, the CSDRS for the EUR medium and soft soil cases exceed the CSDRS for the EUR hard soil case upon which the examples provided with the response are based. If the EUR medium or EUR soft time histories were used for the fixed base analyses it is likely the results at frequencies below 10 Hz would be higher than that provided with the response and might possibly exceed the envelope of the ISRS shown on FSAR Figures 3.7.2-81 and 87.

Because there are significant differences in the ISRS and ZPA's between the static model and dynamic model results as detailed in items 1 through 5 above, it cannot be concluded that the SASSI model is dynamically equivalent to the static ANSYS model. Based on its review, the staff has a concern that for certain locations on the NI the SASSI model may be under-predicting both the ZPA's used for building design and the ISRS used for the design of equipment and suspended systems. Of particular concern are the results for the RBIS which supports the reactor coolant system (RCS). The fundamental horizontal frequencies for the RCS components as reported in the response to RAI 201, Question 03.07.02-35 (Supplement 5) are:

- Reactor Vessel ≈ 10 Hz
- Steam Generator ≈ 6.5 Hz
- Reactor Coolant Pumps ≈ 14 Hz
- Pressurizer ≈ 14.5 Hz

As the difference in horizontal response between the static and dynamic models noted in item 2 above occurred at a frequency of 10 Hz and in item 3 at 15 Hz, it is possible that the seismic response for the RCS has been under-predicted. As a result, AREVA is requested to provide additional information to address the differences in the model results and provide a technical basis as to why the SASSI model and seismic results from that model are acceptable. The applicant should also identify and address other locations in the NI where the analysis results show similar differences between the ANSYS and SASSI models as noted above and address the consequences of these differences in its response. Lastly, the staff requests that AREVA provide an explanation as to why the ISRS results for case 5ae are exceeded by the results of the fixed base SASSI analysis.

Response to Question 03.07.02-76:

1. The dome of the Reactor Shield Building for the dynamic (MTR/SASSI) model is based on the latest design drawing. However, the static (ANSYS) model was developed prior to issuance of the design drawing and was therefore modeled with an approximate curvature (radius). Consequently, the in-structure response spectra (ISRS) for the dynamic and static model differed as shown in RAI 371 Question 03-07-02-67 (Supplement 24 Response). The static model dome has been modified to the same geometry shown on the design drawing, making the geometry consistent with that of the dynamic model. The resulting In-Structure Response Spectra (ISRS) match very closely as shown in updated FSAR figures 3.7.2-14 through 3.7.2-16 in the attached mark-up, demonstrating that the accurate modeling of the

dome curvature resolves the differences previously shown in RAI 371. The ZPAs are also now in agreement.

2. The ISRS comparisons provided in RAI 371 Question 03-07-02-67 (Supplement 24 Response) showed some ISRS from the static model that exceeded those from the dynamic model. Additionally, in some cases the ISRS from both the models exceeded the spectra (and ZPAs) at the corresponding building elevations shown in the US EPR FSAR.

   The ISRS comparisons between the dynamic and static model have been improved by making the following changes to the models:

   - Incorporated the Balance of NI (BONI) geometry from the static model into the dynamic model (BONI includes the Safeguard, Fuel and Shield Buildings – all but the RBIS and Containment).
   - Corrected primary shield wall thicknesses in both the static and dynamic models.
   - Mapped masses from the static model to the dynamic model.
   - Excluded the Reactor Coolant System (RCS) stick model from the dynamic model (to be consistent with the Static Model, which considers only reaction loads due to the RCS – original ISRS comparisons had an RCS stick model added to the static model).

   The static and dynamic models have the following differences:

   - Solid elements are used in the static model for the Reactor Building Internal Structures (RBIS) while shell elements are used in the dynamic model.
   - Finite element meshing is different between the two models for the RBIS and the embedded sidewalls of the BONI.
   - Mass distribution is different in the two models due to meshing differences.
   - Static model ISRS are developed using ANSYS and dynamic model results are based on MTR/SASSI, with inherent differences in finite element formulation and consideration for structural damping.

   Given the differences between the dynamic and static models, the model improvements described above have resulted in ISRS comparisons between the static and the dynamic model for the RBIS that are much improved over those presented in RAI 371. See figures 03.07.02-76-1 through 03.07.02-76-9 and updated FSAR figures 3.7.2-50 through 3.7.2-55 in the attached mark-up.

   The ISRS for the RBIS at elevation 63 feet, 11 ¾ inches are presented in updated FSAR figures 3.7.2-50 through 3.7.2-52 in the attached mark-up. Given the modeling differences which inherently exist between the static and dynamic models, the slight differences remaining in the ISRS comparisons are acceptable and dynamic compatibility has been achieved for the RBIS.

   With regard to the FSAR ISRS exceedances by the dynamic and static models at elevation 63 feet, 11 ¾ inches, it should be noted that the ISRS nodal locations used for evaluating compatibility differed from those used in the FSAR ISRS. Consequently, the comparisons between the FSAR ISRS and the static/dynamic compatibility curves were not like-for-like and differences can be expected. Likewise, the comparisons between the fixed base case

and soil case 5ae are not meaningful with the ISRS presented in AREVA's response to RAI 371, Question 03-07-02-67 for the reason mentioned above.

3. As described in Item (2), new ISRS for the RBIS at elevation 16 feet, 10 ¾ inches for the Y direction (RAI 371 Figure 03.07.02-67-38) have been generated and the comparisons are now more favorable. See updated FSAR figures 3.7.2-53 through 3.7.2-55 in the attached mark-up. Additionally, the comparisons between the FSAR ISRS and the static/dynamic compatibility curves were not like-for-like and differences can be expected, thus explaining any FSAR ISRS exceedances.
4. As described in Item (2), the BONI geometry from the static model has been incorporated into the dynamic model and new ISRS for the Fuel Building at elevation 23 feet, 7 ½ inches for the Z direction (RAI 371 Figure 03.07.02-67-27) have been generated and the ISRS comparisons are now more favorable. See updated FSAR figures 3.7.2-38 through 3.7.2-40 in the attached mark-up for elevation +23 feet, 7 ½ inches. In addition, see updated FSAR figures 3.7.2-35 through 3.7.2-37 in the attached mark-up for another comparison of Fuel Building ISRS.
5. As described in Item (2), the BONI geometry from the static model has been incorporated into the dynamic model and new ISRS for Safeguard Building 1 (Figure 03.07.02-67-8) and X-direction ISRS for Safeguard Building 2/3 (Figure 03.07.02-67-19) at an elevation of 26 feet 3 inches have been generated. The ISRS comparisons are now more favorable. See updated FSAR figures 3.7.2-17 through 3.7.2-34 in the attached mark-up for Safeguard Building ISRS comparisons.

The dynamic model also forms the basis for the development of a stick model of the RBIS that is used for a detailed Reactor Coolant System analysis, which is the subject of RAI 201. The RBIS ISRS comparisons at elevation 4 feet, 11 inches (steam generator and reactor coolant pump vertical supports), elevation 16 feet, 10 ¾ inches (reactor pressure vessel supports), and elevation 63 feet, 11 ¾ inches (steam generator lateral supports) demonstrate that the pertinent seismic responses are in good agreement between the static and dynamic model.

As noted above, the comparisons between the FSAR ISRS and the static/dynamic compatibility curves were not like-for-like and differences can be expected, thus explaining any FSAR ISRS exceedances. Additionally, comparisons between the fixed base case and soil case 5ae are not meaningful with the ISRS presented in AREVA's response to RAI 371, Question 03-07-02-67 for the same reason.

In summary, dynamic compatibility between the static and dynamic models has been demonstrated by the favorable ISRS comparisons, and it can be concluded that the dynamic model is suitable for soil-structure interaction analysis.

AREVA will address the effect that the changes in the SASSI dynamic model might have on the dynamic stick model by providing a future supplement to RAI 201 Question 3.7.2-35.

FSAR Impact:

U.S. EPR FSAR Tier 2, Section 3.7.2, Table 3.7.2-1, and Figures 3.7.2-14 through 3.7.2-46 and 3.7.2-50 through 3.7.2-55 will be revised as described in the response and indicated on the enclosed markup.

Figure 03.07.02-76-1—Static FEM vs. Dynamic FEM Spectrum Comparison at Elev. +1.50m (+4 Ft 11 In) of Reactor Building Internal Structures, 5% Damping, X-Direction

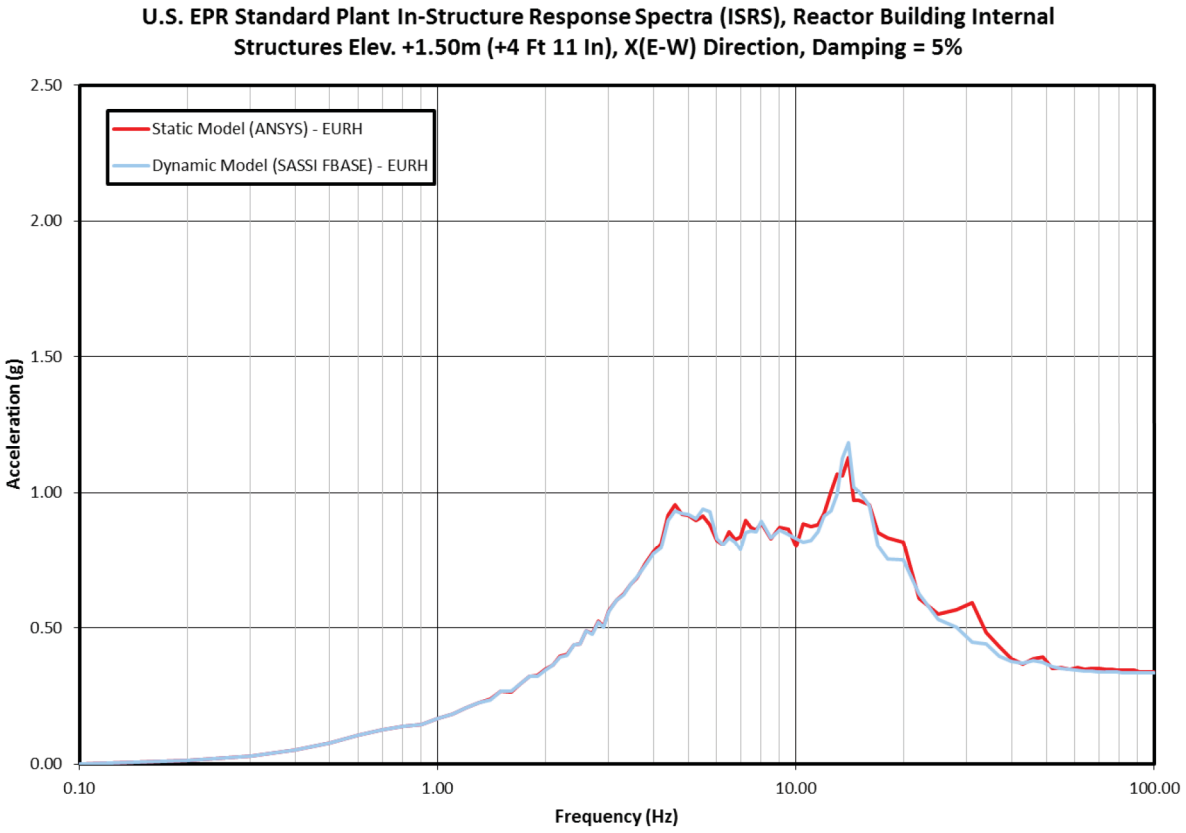

Figure 03.07.02-76-2—Static FEM vs. Dynamic FEM Spectrum Comparison at Elev. +1.50m (+4 Ft 11 In) of Reactor Building Internal Structures, 5% Damping, Y-Direction

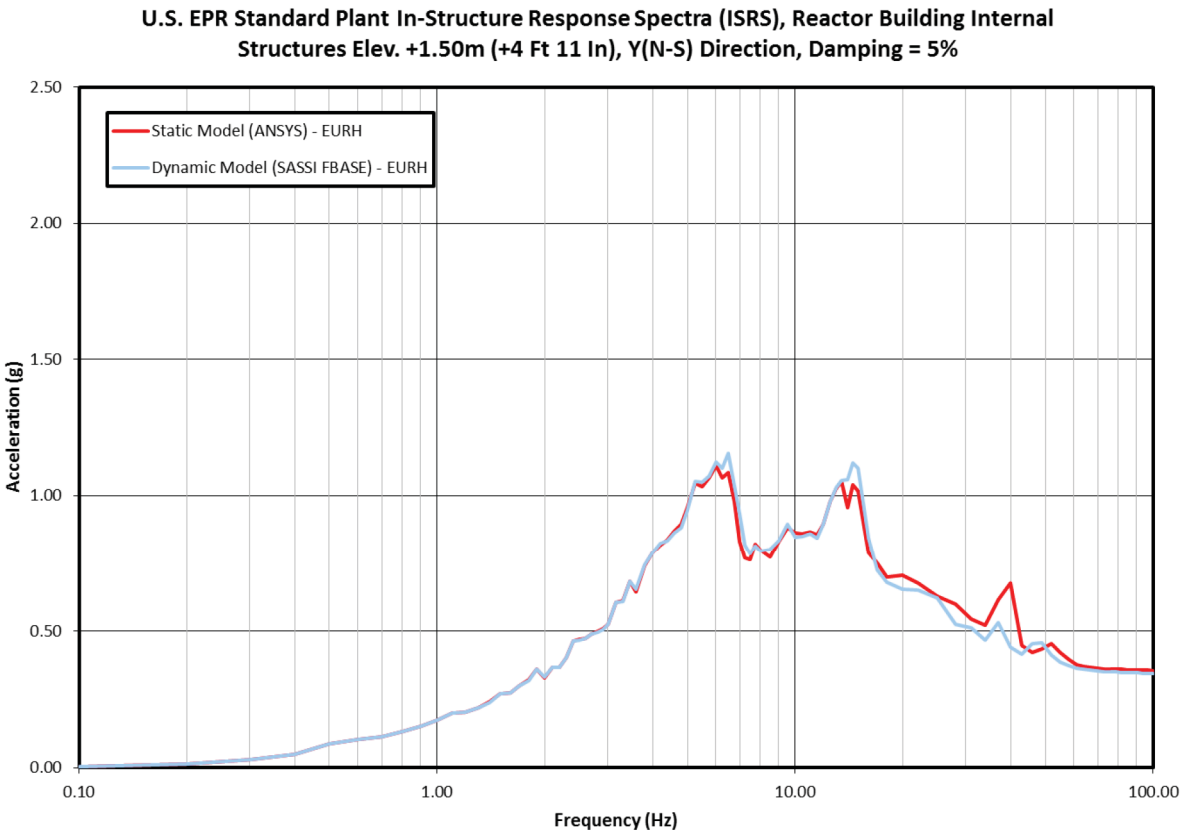

Figure 03.07.02-76-3—Static FEM vs. Dynamic FEM Spectrum Comparison at Elev. +1.50m (+4 Ft 11 In) of Reactor Building Internal Structures, 5% Damping, Z-Direction

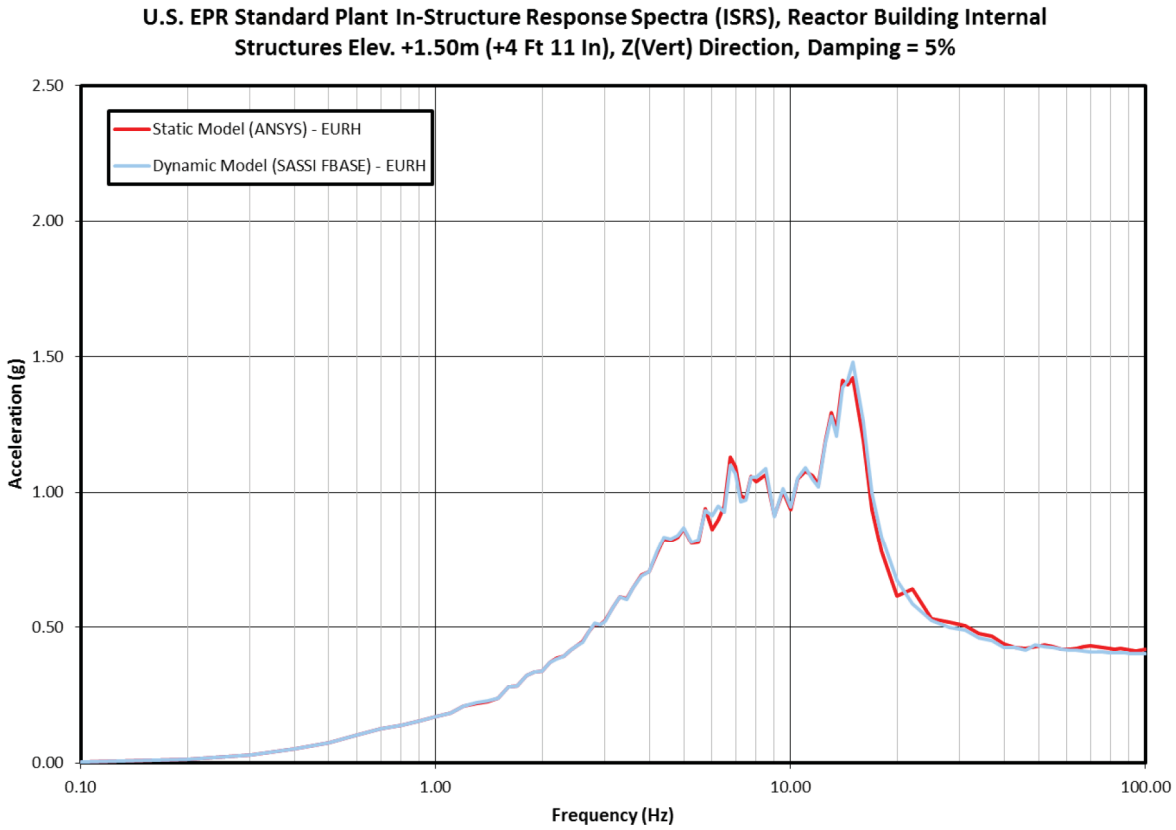

Figure 03.07.02-76-4—Static FEM vs. Dynamic FEM Spectrum Comparison at Elev. +45 ft, 3-1/4 in (+13.80m) - Reactor Building Internal Structure, 5% Damping, X-Direction

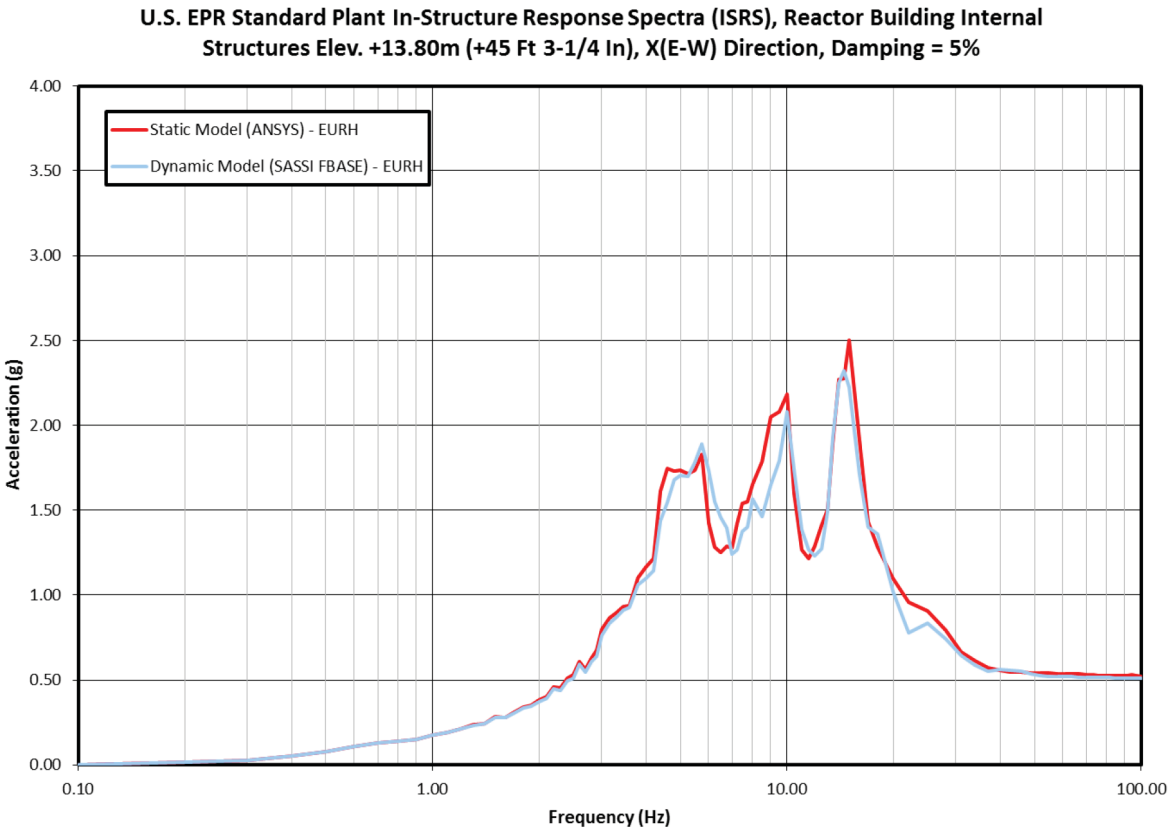

Figure 03.07.02-76-5—Static FEM vs. Dynamic FEM Spectrum Comparison at Elev. +45 ft, 3-1/4 in (+13.80m) - Reactor Building Internal Structure, 5% Damping, Y-Direction

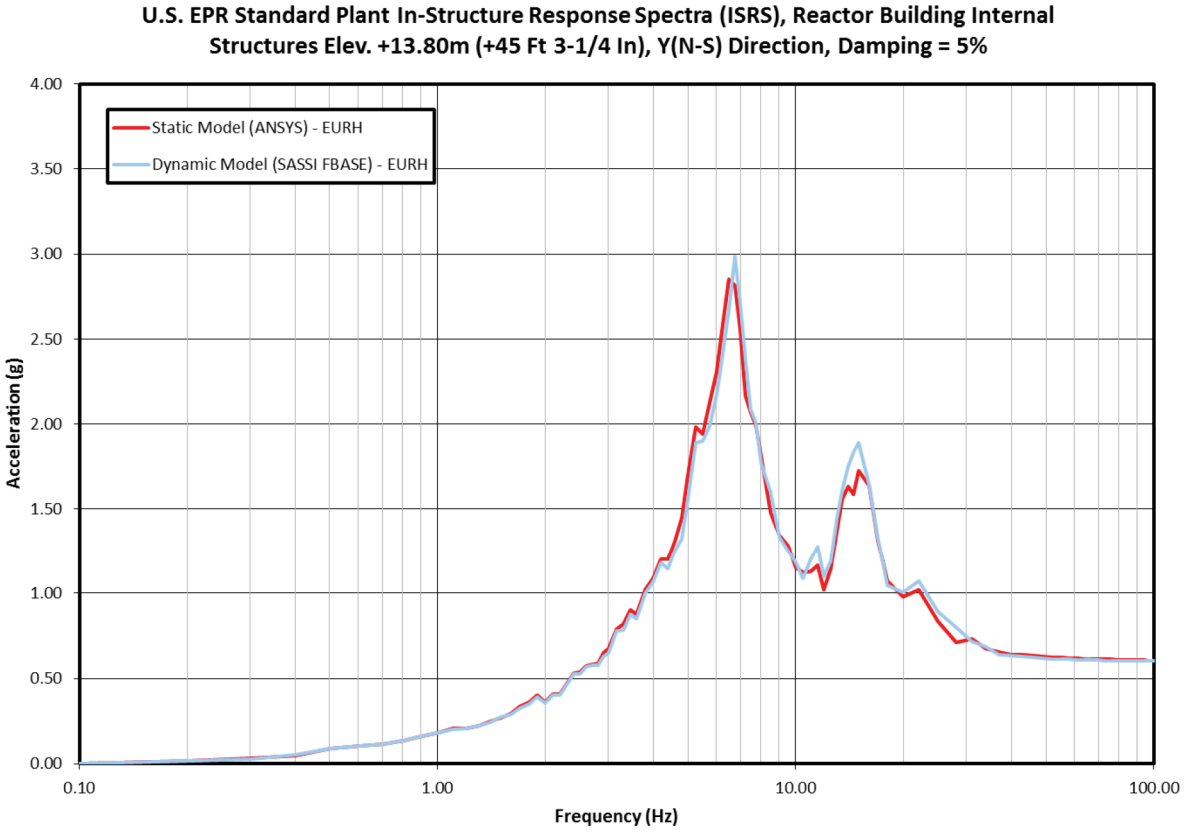

Figure 03.07.02-76-6—Static FEM vs. Dynamic FEM Spectrum Comparison at Elev. +45 ft, 3-1/4 in (+13.80m) - Reactor Building Internal Structure, 5% Damping, Z-Direction

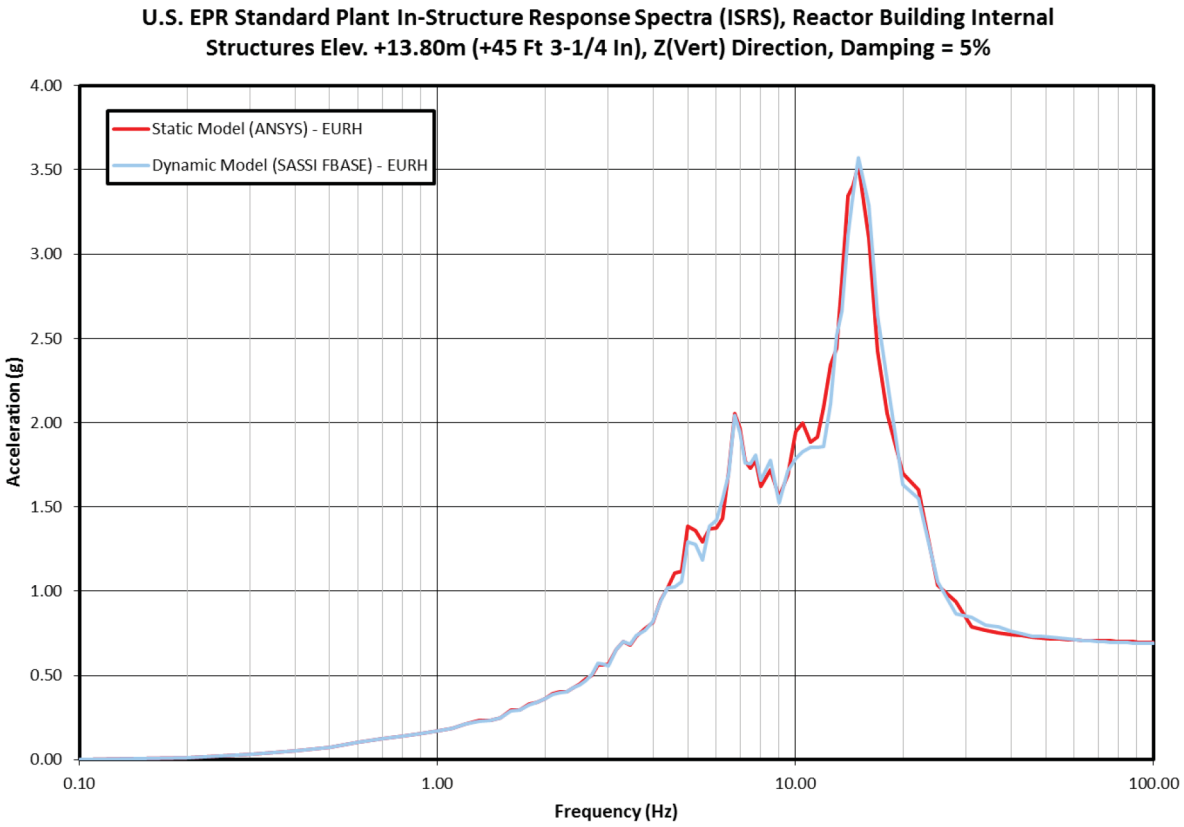

Figure 03.07.02-76-7—Static FEM vs. Dynamic FEM Spectrum Comparison at Elev. +79 ft, 0-3/4 in (+24.10m) - Reactor Building Internal Structure (west), 5% Damping, X-Direction

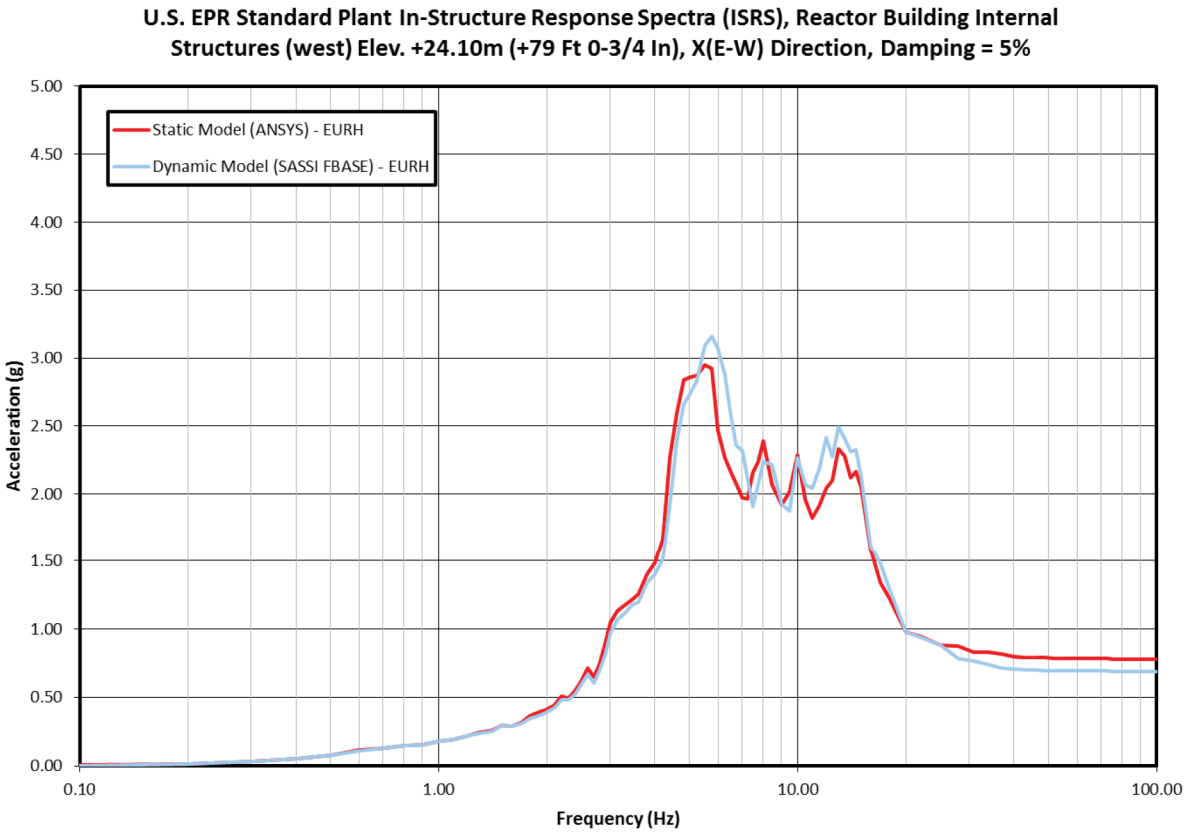

Figure 03.07.02-76-8—Static FEM vs. Dynamic FEM Spectrum Comparison at Elev. +79 ft, 0-3/4 in (+24.10m) - Reactor Building Internal Structure (west), 5% Damping, Y-Direction

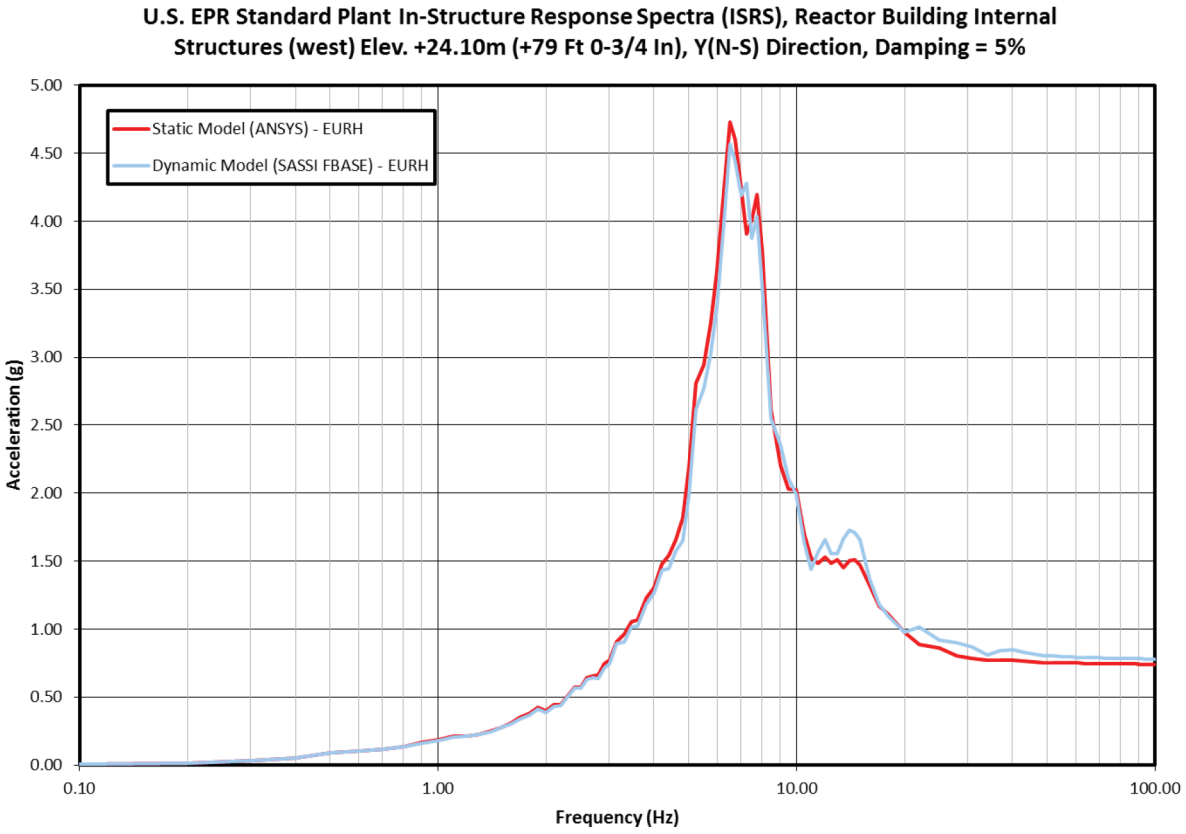

Figure 03.07.02-76-9—Static FEM vs. Dynamic FEM Spectrum Comparison at Elev. +79 ft, 0-3/4 in (+24.10m) - Reactor Building Internal Structure (west), 5% Damping, Z-Direction

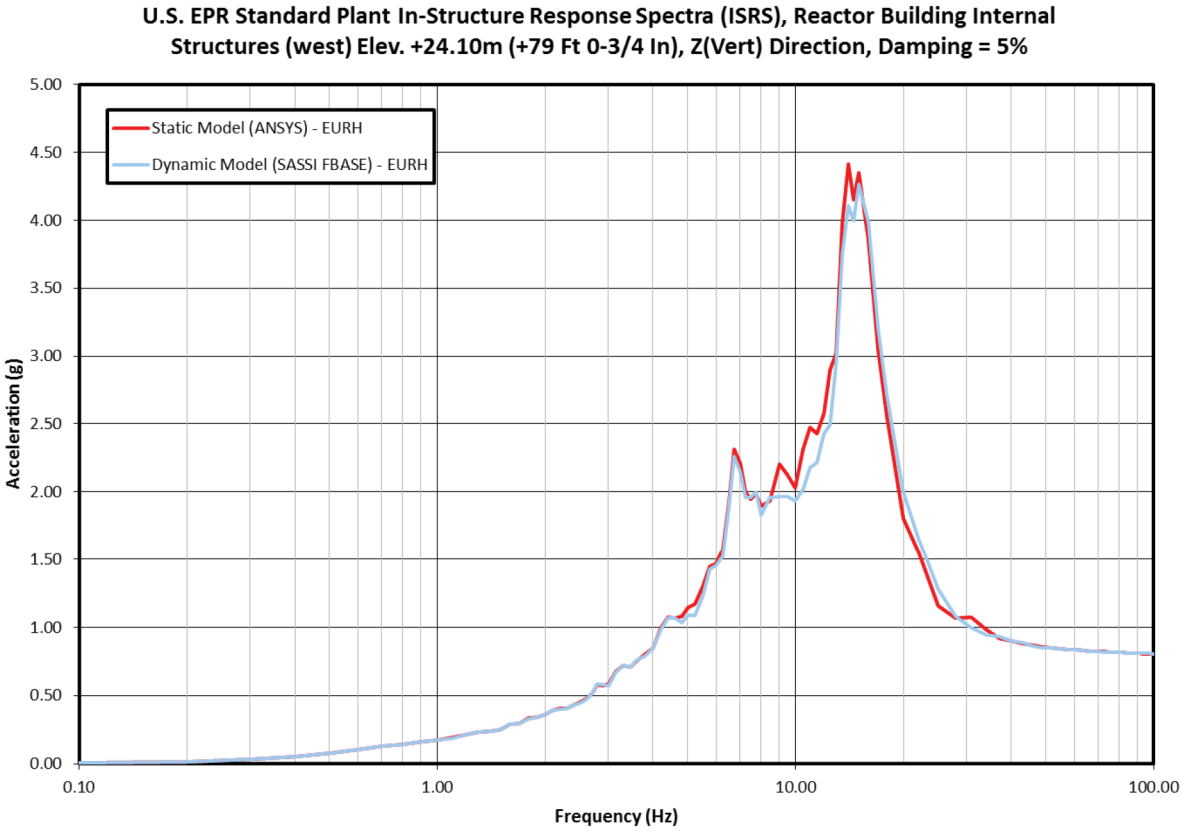

U.S. EPR Final Safety Analysis Report Markups

- SHELL43 – A four-node shell element used to model walls, slabs and the shell of the RB. This element is suitable for moderately thick shell structures and can also provide out of plane shear forces.

- BEAM44 – Used to model beams and columns.

The 3D FEM of the NAB consists of shell elements and is developed using the GTSTRUDL code, Version 29. It is used in the equivalent static analysis and serves as the basis for tuning the stick model of the NAB to ensure reasonable dynamic compatibility with the FEM.

3.7.2.3.1.2 3D Finite Element Models for Dynamic Analysis

The dynamic 3D FEM is developed for the SSI analysis of the U.S. EPR NI Common Basemat Structures. When the FEM and the degree of discretization are selected, it is ensured that the model can reliably be used to determine the structural response within the relevant frequency range. The stiffness of individual parts of the structure is represented by shell or beam finite elements, and ~~only relevant structural elements to show a correct dynamic behavior of the NI buildings are considered. To facilitate development of a structured finite element mesh for the dynamic 3D FEM, a base grid is defined for each building except the RBIS. Each base grid consists of grid axes that are in the directions of the three orthogonal axes. The distance between adjacent grid axes as well as the size of typical shell finite elements is about 1.5 m. The~~the following simplifications are made in the development of the model:

- Foundation level for all buildings is -38 ft, 10-1/2 inches (-11.85 m).

- Elements representing walls in the solid part of the basemat are considered to be rigid.

- ~~Walls, ceilings and openings are moved to the nearest axes of the base grid.~~

- Small openings and walls ~~Openings smaller than about 1.5m^2~~ are not considered.

- ~~Walls and ceilings with a thickness less than 0.30m such as staircases, landings or channels are not considered.~~

For the dynamic FEM, shell elements are used to model walls and slabs, and the solid elements used to model the basemat in the static FEM are replaced with shell elements:

- Shell elements are used to model the entire RCB.

- For the balance-of-Nuclear Island, the same geometry and mesh above the basemat used in the static FEM are incorporated.

- For the RBIS, the same geometry as for the static FEM is used with a coarser mesh, and the solid elements used to model the RPV pedestal in the static FEM are replaced with shell elements.

~~.~~ Two removable walls, which enclose the inside faces of the SG towers above Elev. +63 feet, 11-3/4 inches, are also modeled by shell elements. The two side edges and bottom edge of each removable wall is attached to the SG using pinned boundary conditions at the wall supports. Most material properties of the dynamic FEM, with the exception of the walls inside the basemat that are assumed to be rigid, remain the same as the static FEM. The elements to model the tendons and steel liner plate in the static FEM are not included in the dynamic FEM. Beam elements are used to model internal columns, ~~shield building buttresses,~~ Polar Crane (PC) beams, and RCS beams. Lumped masses are included to model the PC and NSSS equipment.

To model structural loads, the dead and live loads are applied ~~to the model~~ and solved statically. The reactions at each node are found and then converted to ~~applied to the dynamic FEM as~~ lumped masses, which include mass contributions from the following elements:

- Permanent equipment and distribution systems supported by slabs and platforms.
- Water in pools under normal operating conditions.
- Twenty-five percent of the live loads (variable loads) on floor slabs and platforms.
- Seventy-five percent of the maximum snow load on roof slabs.
- Miscellaneous dead loads of at least 50 psf.

In the dynamic FEM, the hydrodynamic loads are considered by adding the tributary water mass to the pool walls and slabs. For the static FEM, the hydrodynamic loads are developed using the method provided in TID-7024 and applied to the pool walls and slabs in the form of pressure distribution. The spent fuel racks are considered by lumping 100 percent of the spent fuel load at the bottom slab in the vertical direction and by distributing it along the height of the pool in the horizontal direction. Rack structure interaction is not considered in development of the FEM for the FB as far as global seismic response is concerned.

The sufficiency of the dynamic FEM is established by a comparison of the five percent damping ISRS envelopes between the static and dynamic fixed base FEMs at various locations within the models. The input ground motions are the three components of synthetic time histories for the EUR Hard motion. The ANSYS code, Versions 11.0 and 12.1, is used in the modal time history analysis of the static FEM, whereas the MTR/SASSI code ~~code~~ Version 9.2.2~~8.3~~, is used in the frequency response analysis of the dynamic FEM. The 0.0025 second time step is used in the modal time history analysis for the EUR Hard input motion, in which one-half the time step (0.00125

Table 3.7.2-1—Frequencies and Modal Mass Ratios for NI Common Basemat Structures with All Masses Included
Sheet 1 of 10

Mode No.	Frequency (Hz)	Modal Participating Mass Ratios		
		X	Y	Z
1	3.60	0.000	0.005	0.000
2	4.53	0.000	0.326	0.000
3	4.76	0.384	0.001	0.000
4	4.80	0.043	0.000	0.000
5	4.83	0.000	0.032	0.000
6	4.87	0.040	0.003	0.000
7	5.04	0.016	0.049	0.000
8	5.05	0.049	0.016	0.000
9	5.08	0.003	0.066	0.001
10	5.11	0.015	0.000	0.002
11	5.18	0.000	0.001	0.000
12	5.35	0.003	0.008	0.000
15	5.48	0.002	0.021	0.001
16	5.59	0.000	0.020	0.000
17	5.68	0.004	0.001	0.000
19	5.96	0.000	0.034	0.000
20	6.16	0.021	0.001	0.000
21	6.19	0.000	0.025	0.000
22	6.25	0.000	0.001	0.000
23	6.43	0.002	0.000	0.000
24	6.54	0.015	0.000	0.000
25	6.61	0.000	0.004	0.009
26	6.66	0.003	0.004	0.000
32	6.86	0.003	0.005	0.007
33	6.96	0.001	0.005	0.004
35	7.28	0.019	0.000	0.000
36	7.29	0.000	0.031	0.000
37	7.33	0.000	0.000	0.002
38	7.52	0.002	0.003	0.001
39	7.65	0.024	0.000	0.000

Table 3.7.2-1—Frequencies and Modal Mass Ratios for NI Common Basemat Structures with All Masses Included
Sheet 2 of 10

Mode No.	Frequency (Hz)	Modal Participating Mass Ratios		
		X	Y	Z
40	7.76	0.000	0.001	0.006
41	7.84	0.003	0.001	0.000
42	7.92	0.005	0.010	0.001
44	8.00	0.006	0.002	0.001
46	8.06	0.003	0.028	0.006
47	8.17	0.011	0.001	0.000
48	8.22	0.001	0.000	0.000
49	8.30	0.035	0.000	0.000
50	8.31	0.003	0.000	0.000
51	8.41	0.002	0.000	0.000
52	8.47	0.001	0.006	0.000
53	8.59	0.000	0.013	0.012
54	8.72	0.001	0.000	0.001
55	8.78	0.005	0.000	0.000
57	8.91	0.000	0.001	0.000
58	9.06	0.000	0.005	0.021
59	9.11	0.000	0.005	0.041
60	9.14	0.000	0.000	0.003
61	9.21	0.000	0.000	0.010
62	9.22	0.000	0.003	0.000
63	9.22	0.005	0.000	0.000
64	9.32	0.000	0.000	0.014
69	9.89	0.001	0.003	0.034
70	9.96	0.008	0.000	0.000
73	10.13	0.002	0.001	0.000
74	10.21	0.000	0.003	0.043
77	10.55	0.000	0.001	0.000
79	10.64	0.001	0.000	0.000
80	10.86	0.001	0.000	0.001
81	10.87	0.001	0.000	0.002
85	11.28	0.001	0.001	0.000

Table 3.7.2-1—Frequencies and Modal Mass Ratios for NI Common Basemat Structures with All Masses Included
Sheet 3 of 10

Mode No.	Frequency (Hz)	Modal Participating Mass Ratios		
		X	Y	Z
86	11.31	0.000	0.005	0.000
87	11.31	0.000	0.005	0.000
90	11.54	0.000	0.002	0.000
91	11.57	0.000	0.000	0.002
92	11.69	0.001	0.000	0.000
93	11.74	0.000	0.001	0.001
94	11.89	0.000	0.000	0.001
95	11.90	0.000	0.001	0.002
97	11.93	0.001	0.000	0.002
98	12.04	0.000	0.000	0.001
99	12.05	0.000	0.000	0.001
100	12.06	0.000	0.000	0.008
102	12.12	0.000	0.000	0.002
103	12.15	0.001	0.000	0.017
104	12.20	0.000	0.000	0.016
106	12.27	0.001	0.001	0.000
112	12.50	0.002	0.000	0.000
113	12.53	0.000	0.000	0.002
114	12.62	0.002	0.000	0.002
116	12.70	0.000	0.000	0.056
117	12.70	0.000	0.001	0.000
118	12.72	0.002	0.000	0.000
119	12.81	0.000	0.001	0.000
121	12.87	0.001	0.002	0.000
123	12.93	0.001	0.000	0.000
124	12.98	0.000	0.000	0.034
125	13.02	0.000	0.000	0.001
126	13.03	0.004	0.001	0.007
129	13.10	0.000	0.001	0.006
130	13.14	0.001	0.002	0.014
131	13.25	0.000	0.002	0.001

Table 3.7.2-1—Frequencies and Modal Mass Ratios for NI Common Basemat Structures with All Masses Included
Sheet 4 of 10

Mode No.	Frequency (Hz)	Modal Participating Mass Ratios		
		X	Y	Z
132	13.29	0.003	0.000	0.003
133	13.34	0.000	0.001	0.000
136	13.47	0.001	0.003	0.003
137	13.52	0.000	0.003	0.000
139	13.64	0.001	0.001	0.004
140	13.71	0.001	0.001	0.000
142	13.72	0.000	0.001	0.001
143	13.73	0.000	0.002	0.001
144	13.88	0.007	0.000	0.005
147	13.94	0.001	0.000	0.001
148	14.01	0.001	0.000	0.000
149	14.05	0.001	0.000	0.000
150	14.12	0.000	0.000	0.001
151	14.13	0.000	0.000	0.003
152	14.14	0.000	0.001	0.000
153	14.15	0.002	0.000	0.000
154	14.17	0.001	0.000	0.001
156	14.21	0.005	0.007	0.000
157	14.25	0.001	0.000	0.009
158	14.25	0.000	0.006	0.002
159	14.28	0.005	0.000	0.000
160	14.29	0.008	0.005	0.000
164	14.45	0.001	0.000	0.008
165	14.49	0.000	0.000	0.002
167	14.56	0.000	0.000	0.001
168	14.58	0.002	0.000	0.000
169	14.64	0.000	0.000	0.005
170	14.65	0.000	0.004	0.007
171	14.77	0.000	0.000	0.002
172	14.85	0.000	0.000	0.001
173	15.00	0.001	0.001	0.000

Table 3.7.2-1—Frequencies and Modal Mass Ratios for NI Common Basemat Structures with All Masses Included
Sheet 5 of 10

Mode No.	Frequency (Hz)	Modal Participating Mass Ratios		
		X	Y	Z
174	15.01	0.001	0.000	0.001
175	15.04	0.000	0.000	0.002
176	15.14	0.001	0.000	0.001
177	15.16	0.001	0.001	0.001
180	15.24	0.002	0.002	0.003
181	15.25	0.000	0.002	0.019
182	15.28	0.000	0.001	0.001
184	15.37	0.003	0.001	0.001
185	15.38	0.000	0.001	0.003
187	15.44	0.000	0.000	0.022
188	15.45	0.008	0.000	0.000
191	15.57	0.002	0.000	0.000
193	15.61	0.000	0.000	0.003
194	15.63	0.000	0.003	0.017
195	15.67	0.000	0.000	0.004
196	15.68	0.002	0.000	0.001
197	15.70	0.000	0.000	0.002
198	15.74	0.000	0.001	0.001
199	15.75	0.000	0.000	0.002
200	15.82	0.000	0.000	0.002
202	15.83	0.000	0.001	0.001
203	15.93	0.000	0.001	0.001
204	15.94	0.001	0.000	0.000
205	15.95	0.000	0.000	0.001
206	15.97	0.000	0.000	0.001
207	15.98	0.000	0.000	0.001
208	16.01	0.001	0.000	0.001
209	16.04	0.000	0.000	0.004
210	16.09	0.001	0.000	0.003
211	16.11	0.000	0.001	0.003
212	16.20	0.000	0.000	0.009

Table 3.7.2-1—Frequencies and Modal Mass Ratios for NI Common Basemat Structures with All Masses Included
Sheet 6 of 10

Mode No.	Frequency (Hz)	Modal Participating Mass Ratios		
		X	Y	Z
213	16.25	0.000	0.000	0.007
214	16.29	0.001	0.000	0.000
215	16.31	0.000	0.001	0.001
217	16.41	0.000	0.000	0.002
218	16.43	0.000	0.002	0.000
219	16.46	0.000	0.000	0.001
220	16.54	0.000	0.002	0.000
221	16.57	0.000	0.004	0.001
222	16.57	0.000	0.001	0.006
224	16.65	0.001	0.005	0.001
225	16.70	0.000	0.000	0.002
226	16.80	0.000	0.001	0.001
228	16.83	0.000	0.002	0.003
229	16.87	0.001	0.000	0.000
230	16.87	0.000	0.000	0.002
231	16.89	0.000	0.000	0.019
232	16.91	0.000	0.001	0.000
234	16.92	0.000	0.000	0.001
235	16.98	0.000	0.001	0.000
237	17.06	0.000	0.000	0.001
238	17.08	0.000	0.002	0.002
241	17.12	0.000	0.000	0.003
242	17.18	0.000	0.000	0.001
243	17.20	0.000	0.000	0.001
252	17.40	0.001	0.000	0.000
254	17.50	0.001	0.000	0.002
257	17.58	0.001	0.000	0.000
258	17.58	0.000	0.000	0.011
264	17.68	0.000	0.000	0.002
269	17.82	0.000	0.000	0.001
270	17.83	0.000	0.002	0.000

Table 3.7.2-1—Frequencies and Modal Mass Ratios for NI Common Basemat Structures with All Masses Included
Sheet 7 of 10

Mode No.	Frequency (Hz)	Modal Participating Mass Ratios		
		X	Y	Z
271	17.87	0.000	0.000	0.009
275	17.98	0.000	0.000	0.001
276	17.99	0.000	0.000	0.001
277	18.06	0.000	0.000	0.002
278	18.10	0.000	0.000	0.001
279	18.14	0.000	0.001	0.014
280	18.17	0.000	0.001	0.000
281	18.19	0.000	0.000	0.001
282	18.20	0.000	0.000	0.001
283	18.23	0.000	0.001	0.000
284	18.28	0.000	0.000	0.001
285	18.29	0.002	0.000	0.002
286	18.35	0.000	0.000	0.001
288	18.40	0.001	0.000	0.001
291	18.54	0.000	0.001	0.000
292	18.55	0.000	0.000	0.001
294	18.59	0.000	0.000	0.001
295	18.61	0.001	0.000	0.001
296	18.71	0.000	0.000	0.002
297	18.73	0.001	0.000	0.005
298	18.74	0.001	0.000	0.007
300	18.78	0.000	0.001	0.003
301	18.82	0.000	0.000	0.002
306	18.98	0.000	0.000	0.001
309	19.10	0.001	0.000	0.000
314	19.26	0.000	0.000	0.001
316	19.31	0.000	0.001	0.000
318	19.39	0.000	0.000	0.001
320	19.48	0.000	0.000	0.001
323	19.51	0.000	0.000	0.001
324	19.51	0.000	0.000	0.001

Table 3.7.2-1—Frequencies and Modal Mass Ratios for NI Common Basemat Structures with All Masses Included
Sheet 8 of 10

Mode No.	Frequency (Hz)	Modal Participating Mass Ratios		
		X	Y	Z
326	19.63	0.000	0.001	0.000
334	19.72	0.000	0.001	0.002
335	19.73	0.001	0.000	0.000
336	19.78	0.000	0.000	0.001
340	19.85	0.000	0.000	0.001
341	19.86	0.000	0.000	0.001
342	19.88	0.000	0.000	0.001
343	19.91	0.000	0.000	0.002
344	19.95	0.000	0.000	0.010
345	19.95	0.000	0.001	0.000
346	20.00	0.000	0.000	0.001
348	20.04	0.000	0.000	0.001
352	20.18	0.000	0.001	0.001
353	20.23	0.000	0.000	0.006
355	20.30	0.000	0.000	0.001
359	20.41	0.000	0.000	0.001
361	20.47	0.001	0.000	0.004
366	20.57	0.000	0.001	0.004
367	20.57	0.002	0.000	0.000
372	20.67	0.002	0.000	0.000
373	20.69	0.001	0.000	0.001
379	20.85	0.000	0.000	0.001
381	20.93	0.000	0.000	0.001
382	20.97	0.001	0.000	0.000
383	20.99	0.002	0.000	0.001
384	20.99	0.000	0.000	0.003
385	21.02	0.001	0.000	0.002
386	21.04	0.000	0.000	0.001
388	21.06	0.001	0.000	0.000
397	21.27	0.000	0.000	0.003
399	21.32	0.000	0.001	0.002

Table 3.7.2-1—Frequencies and Modal Mass Ratios for NI Common Basemat Structures with All Masses Included
Sheet 9 of 10

Mode No.	Frequency (Hz)	Modal Participating Mass Ratios		
		X	Y	Z
400	21.35	0.000	0.000	0.002
402	21.41	0.001	0.000	0.001
403	21.44	0.000	0.000	0.003
405	21.53	0.000	0.000	0.001
406	21.55	0.000	0.001	0.000
408	21.61	0.001	0.000	0.000
409	21.67	0.000	0.000	0.002
410	21.67	0.000	0.000	0.001
411	21.70	0.000	0.000	0.001
418	21.94	0.000	0.001	0.000
420	21.99	0.000	0.000	0.001
421	22.04	0.000	0.000	0.001
422	22.08	0.000	0.000	0.002
427	22.18	0.000	0.000	0.001
428	22.20	0.000	0.000	0.001
434	22.44	0.000	0.000	0.001
448	22.79	0.001	0.000	0.000
454	23.02	0.001	0.000	0.000
459	23.17	0.000	0.001	0.001
470	23.36	0.001	0.000	0.000
474	23.53	0.000	0.000	0.001
476	23.61	0.001	0.000	0.000
480	23.69	0.000	0.000	0.001
481	23.70	0.000	0.000	0.001
499	24.11	0.000	0.000	0.001
502	24.18	0.000	0.000	0.001
505	24.29	0.000	0.000	0.001
510	24.37	0.000	0.000	0.001
514	24.53	0.000	0.000	0.001
516	24.58	0.001	0.000	0.000
521	24.72	0.000	0.001	0.000

Table 3.7.2-1—Frequencies and Modal Mass Ratios for NI Common Basemat Structures with All Masses Included
Sheet 10 of 10

Mode No.	Frequency (Hz)	Modal Participating Mass Ratios		
		X	Y	Z
524	24.79	0.001	0.000	0.001
525	24.80	0.001	0.000	0.001
535	25.05	0.000	0.000	0.001
541	25.16	0.000	0.000	0.001
552	25.39	0.000	0.000	0.001
559	25.54	0.000	0.000	0.001
571	25.70	0.000	0.000	0.001
597	26.20	0.001	0.000	0.000
600	26.31	0.000	0.000	0.001
610	26.48	0.000	0.001	0.000
613	26.56	0.000	0.001	0.000
667	27.79	0.000	0.001	0.000
712	28.77	0.000	0.001	0.000
760	29.62	0.000	0.001	0.000
776	29.93	0.000	0.001	0.000
786	30.12	0.001	0.000	0.000
871	31.60	0.000	0.001	0.000
1306	38.46	0.000	0.000	0.001
1392	39.72	0.000	0.000	0.001
1420	40.20	0.000	0.001	0.000
1600	42.73	0.000	0.001	0.000

Mode	Frequency	Modal Participating Mass Ratios		
No.	(Hz)	X	Y	Z
1	4.48	0.000	0.018	0.000
2	4.58	0.015	0.054	0.000
3	4.59	0.055	0.015	0.000
4	4.61	0.066	0.000	0.000
5	4.74	0.010	0.334	0.000
6	4.90	0.401	0.010	0.000
7	5.01	0.002	0.019	0.000
8	5.02	0.022	0.000	0.000
9	5.20	0.000	0.003	0.000
10	5.29	0.000	0.060	0.001
12	5.39	0.000	0.004	0.000
13	5.46	0.000	0.076	0.000
14	5.47	0.012	0.007	0.000
15	5.86	0.031	0.000	0.000
16	6.02	0.001	0.006	0.002
18	6.19	0.006	0.006	0.000
20	6.41	0.000	0.036	0.000
23	6.72	0.000	0.002	0.003
26	6.96	0.020	0.000	0.000
27	6.99	0.000	0.017	0.000
28	7.23	0.004	0.001	0.003
30	7.45	0.000	0.026	0.010
32	7.49	0.000	0.003	0.000
33	7.58	0.001	0.004	0.008
34	7.96	0.048	0.000	0.000
35	8.04	0.015	0.000	0.000
36	8.09	0.002	0.000	0.000
38	8.16	0.012	0.015	0.008

Mode	Frequency	Modal Participating Mass Ratios		
No.	(Hz)	X	Y	Z
39	8.23	0.008	0.003	0.002
40	8.33	0.001	0.000	0.000
41	8.34	0.000	0.002	0.000
42	8.36	0.013	0.003	0.002
43	8.39	0.006	0.001	0.000
44	8.49	0.001	0.000	0.000
46	8.62	0.000	0.017	0.001
49	8.97	0.001	0.001	0.001
50	9.08	0.000	0.003	0.009
52	9.40	0.001	0.003	0.004
53	9.40	0.005	0.000	0.000
54	9.41	0.012	0.000	0.000
55	9.58	0.000	0.000	0.077
56	9.75	0.000	0.002	0.006
57	9.86	0.001	0.000	0.000
58	9.98	0.001	0.002	0.023
61	10.20	0.000	0.007	0.038
79	10.47	0.000	0.000	0.024
83	10.54	0.001	0.002	0.002
86	10.87	0.000	0.001	0.000
91	11.08	0.000	0.000	0.003
92	11.13	0.000	0.001	0.001
93	11.15	0.000	0.000	0.004
94	11.17	0.003	0.001	0.000
95	11.24	0.002	0.000	0.002
96	11.43	0.000	0.002	0.001
97	11.47	0.000	0.002	0.001
98	11.49	0.000	0.000	0.007

Mode	Frequency	Modal Participating Mass Ratios		
99	11.62	0.000	0.001	0.004
100	11.65	0.001	0.000	0.016
102	11.75	0.000	0.001	0.000
103	11.80	0.000	0.001	0.000
104	11.82	0.000	0.000	0.001
105	11.86	0.001	0.000	0.000
107	11.94	0.000	0.001	0.000
108	12.00	0.001	0.000	0.000
109	12.08	0.001	0.000	0.001
111	12.11	0.000	0.000	0.026
112	12.12	0.001	0.000	0.000
114	12.17	0.000	0.001	0.000
115	12.18	0.000	0.000	0.038
117	12.21	0.000	0.000	0.002
130	12.27	0.000	0.000	0.001
145	12.31	0.001	0.000	0.001
147	12.35	0.000	0.000	0.009
148	12.41	0.001	0.000	0.010
150	12.50	0.000	0.000	0.001
151	12.50	0.000	0.000	0.001
152	12.51	0.000	0.001	0.000
153	12.57	0.001	0.000	0.000
157	12.72	0.001	0.000	0.001
158	12.74	0.000	0.003	0.000
162	12.90	0.000	0.004	0.001
164	12.97	0.000	0.000	0.018
165	13.02	0.000	0.001	0.000
167	13.07	0.002	0.002	0.001

Mode	Frequency	Modal Participating Mass Ratios		
169	13.22	0.000	0.000	0.009
170	13.31	0.000	0.000	0.003
171	13.35	0.004	0.011	0.000
172	13.36	0.000	0.000	0.040
173	13.39	0.000	0.000	0.018
174	13.39	0.011	0.004	0.000
175	13.40	0.001	0.000	0.004
176	13.42	0.007	0.001	0.001
177	13.45	0.000	0.004	0.007
178	13.53	0.002	0.002	0.000
179	13.53	0.000	0.000	0.001
180	13.60	0.000	0.000	0.001
181	13.66	0.008	0.000	0.002
185	13.89	0.004	0.003	0.000
186	13.90	0.000	0.002	0.000
187	13.98	0.002	0.000	0.004
188	14.06	0.000	0.000	0.021
189	14.06	0.001	0.000	0.003
190	14.07	0.001	0.000	0.000
191	14.09	0.000	0.000	0.017
192	14.11	0.004	0.000	0.000
193	14.14	0.001	0.000	0.000
194	14.24	0.001	0.000	0.005
196	14.27	0.000	0.000	0.001
197	14.31	0.000	0.005	0.000
198	14.37	0.005	0.000	0.014
199	14.40	0.003	0.001	0.000
200	14.52	0.000	0.002	0.000

Mode	Frequency	Modal Participating Mass Ratios		
201	14.53	0.000	0.001	0.000
202	14.57	0.003	0.000	0.003
203	14.61	0.000	0.000	0.001
205	14.68	0.000	0.000	0.005
207	14.71	0.000	0.000	0.006
208	14.77	0.000	0.000	0.018
209	14.81	0.002	0.000	0.002
212	14.97	0.000	0.003	0.003
213	15.01	0.000	0.001	0.001
214	15.03	0.000	0.000	0.001
215	15.09	0.000	0.001	0.001
216	15.10	0.001	0.001	0.000
221	15.30	0.000	0.000	0.002
223	15.36	0.000	0.000	0.005
224	15.39	0.000	0.000	0.005
226	15.46	0.001	0.000	0.000
227	15.47	0.000	0.000	0.002
228	15.49	0.002	0.001	0.003
230	15.58	0.000	0.000	0.002
232	15.65	0.006	0.003	0.000
233	15.68	0.001	0.000	0.000
234	15.78	0.000	0.000	0.001
237	15.92	0.001	0.003	0.007
238	15.97	0.000	0.000	0.004
239	15.99	0.000	0.001	0.001
240	16.07	0.001	0.000	0.001
242	16.10	0.000	0.003	0.000
243	16.11	0.000	0.001	0.000

Mode	Frequency	Modal Participating Mass Ratios		
244	16.13	0.000	0.001	0.001
246	16.19	0.000	0.003	0.000
247	16.22	0.001	0.000	0.000
248	16.33	0.002	0.001	0.001
249	16.40	0.000	0.000	0.001
250	16.41	0.000	0.000	0.003
251	16.45	0.000	0.001	0.000
252	16.55	0.001	0.000	0.001
254	16.65	0.001	0.006	0.002
255	16.70	0.000	0.000	0.001
257	16.82	0.000	0.001	0.000
260	16.91	0.001	0.004	0.003
261	16.95	0.000	0.001	0.000
262	16.96	0.000	0.000	0.001
264	17.08	0.001	0.000	0.000
266	17.11	0.002	0.001	0.001
267	17.12	0.002	0.000	0.001
269	17.18	0.001	0.000	0.001
271	17.29	0.000	0.000	0.010
272	17.29	0.000	0.002	0.000
273	17.30	0.001	0.001	0.001
274	17.32	0.000	0.000	0.001
276	17.40	0.000	0.001	0.000
280	17.51	0.001	0.000	0.001
282	17.55	0.000	0.000	0.004
283	17.57	0.000	0.000	0.003
285	17.60	0.000	0.000	0.001
288	17.71	0.000	0.000	0.006

Mode	Frequency	Modal Participating Mass Ratios		
290	17.78	0.000	0.000	0.001
291	17.84	0.000	0.001	0.003
292	17.86	0.000	0.000	0.001
293	17.89	0.000	0.000	0.001
294	18.01	0.000	0.003	0.001
300	18.14	0.000	0.001	0.001
301	18.20	0.000	0.001	0.001
303	18.22	0.001	0.000	0.000
305	18.27	0.000	0.001	0.000
306	18.34	0.000	0.001	0.027
308	18.39	0.002	0.000	0.001
309	18.49	0.000	0.000	0.004
311	18.54	0.000	0.001	0.002
313	18.65	0.000	0.001	0.000
315	18.76	0.000	0.001	0.003
317	18.84	0.000	0.000	0.001
320	18.91	0.001	0.001	0.017
321	18.93	0.000	0.000	0.001
322	19.01	0.000	0.000	0.001
325	19.07	0.000	0.000	0.010
326	19.13	0.002	0.000	0.000
329	19.27	0.000	0.000	0.003
331	19.31	0.001	0.000	0.001
334	19.38	0.000	0.003	0.003
335	19.49	0.000	0.001	0.000
339	19.64	0.000	0.000	0.002
341	19.66	0.001	0.000	0.000
345	19.70	0.000	0.000	0.001

Mode	Frequency	Modal Participating Mass Ratios		
348	19.79	0.002	0.000	0.000
349	19.81	0.001	0.000	0.000
352	19.87	0.000	0.000	0.001
356	19.99	0.000	0.001	0.001
357	20.02	0.000	0.001	0.000
359	20.09	0.001	0.000	0.000
367	20.24	0.001	0.000	0.000
368	20.25	0.000	0.001	0.001
372	20.40	0.000	0.001	0.000
374	20.51	0.000	0.000	0.001
377	20.63	0.000	0.000	0.001
378	20.63	0.000	0.001	0.000
379	20.64	0.001	0.000	0.000
381	20.73	0.000	0.000	0.001
383	20.77	0.000	0.000	0.001
385	20.82	0.000	0.000	0.002
386	20.84	0.000	0.000	0.006
389	20.93	0.000	0.001	0.000
390	20.96	0.000	0.000	0.003
391	20.99	0.000	0.000	0.001
392	21.02	0.000	0.000	0.002
397	21.12	0.000	0.001	0.000
398	21.14	0.002	0.000	0.000
399	21.14	0.000	0.000	0.015
400	21.19	0.000	0.000	0.001
401	21.20	0.000	0.001	0.000
402	21.23	0.001	0.000	0.000
403	21.27	0.000	0.000	0.001

Mode	Frequency	Modal Participating Mass Ratios		
405	21.35	0.000	0.000	0.001
406	21.39	0.000	0.001	0.000
407	21.40	0.000	0.000	0.002
409	21.43	0.000	0.000	0.001
411	21.51	0.000	0.000	0.001
413	21.56	0.000	0.002	0.000
415	21.57	0.000	0.000	0.001
417	21.64	0.000	0.000	0.001
423	21.81	0.000	0.000	0.001
424	21.86	0.001	0.000	0.001
427	21.95	0.000	0.000	0.002
428	22.04	0.000	0.001	0.000
431	22.16	0.001	0.000	0.001
437	22.27	0.001	0.000	0.001
451	22.56	0.000	0.001	0.000
452	22.58	0.001	0.000	0.000
457	22.68	0.000	0.000	0.002
462	22.84	0.000	0.000	0.001
469	22.97	0.000	0.000	0.001
478	23.16	0.000	0.000	0.001
487	23.37	0.000	0.000	0.001
493	23.58	0.000	0.000	0.001
494	23.62	0.000	0.001	0.000
497	23.66	0.000	0.000	0.001
516	24.06	0.000	0.000	0.001
522	24.16	0.000	0.000	0.001
526	24.25	0.000	0.001	0.000
527	24.25	0.000	0.000	0.002

Mode	Frequency	Modal Participating Mass Ratios		
541	24.45	0.001	0.000	0.000
557	24.95	0.000	0.002	0.000
561	25.01	0.000	0.000	0.001
565	25.09	0.000	0.001	0.000
589	25.60	0.000	0.000	0.001
623	26.32	0.000	0.000	0.001
631	26.52	0.000	0.001	0.000
637	26.60	0.000	0.001	0.000
643	26.80	0.000	0.000	0.001
647	26.89	0.000	0.000	0.001
669	27.40	0.000	0.000	0.001
673	27.51	0.001	0.000	0.000
685	27.84	0.000	0.000	0.001
775	29.46	0.000	0.000	0.001
783	29.57	0.000	0.000	0.001
786	29.63	0.000	0.000	0.001
805	30.01	0.000	0.000	0.001
809	30.08	0.000	0.001	0.000
987	33.22	0.000	0.000	0.001
1154	35.81	0.000	0.000	0.001
1205	36.66	0.000	0.000	0.001
1345	38.92	0.000	0.000	0.002
1444	40.44	0.000	0.000	0.001
1661	43.70	0.000	0.000	0.001
1690	44.07	0.000	0.000	0.001
1967	47.97	0.000	0.000	0.001
1978	48.10	0.000	0.000	0.001
2010	48.48	0.000	0.000	0.001

Table 3.7.2-2—Deleted

Figure 3.7.2-14—Static FEM vs. Dynamic FEM Spectrum Comparison at Elev. +200 ft, 5 in (+61.09m) (Dome Apex) of Reactor Shield Building, 5% Damping, X-Direction

The sole purpose of this figure is to demonstrate dynamic compatibility between the dynamic and static models; it is not intended to be used as design information and it is not maintained as such.

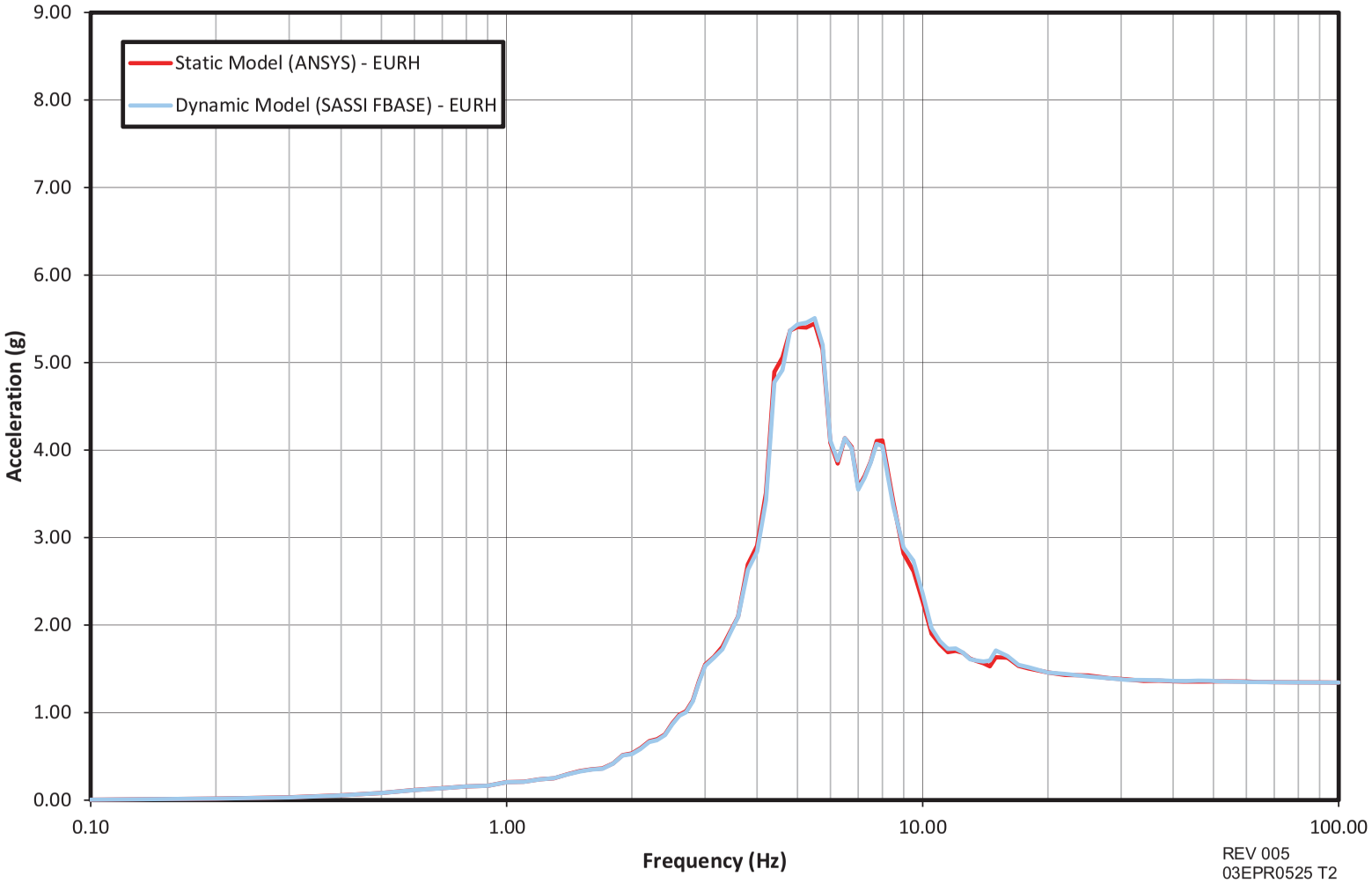

Figure 3.7.2-15—Static FEM vs. Dynamic FEM Spectrum Comparison at Elev. +200 ft, 5 in (+61.09m) (Dome Apex) of Reactor Shield Building, 5% Damping, Y-Direction

The sole purpose of this figure is to demonstrate dynamic compatibility between the dynamic and static models; it is not intended to be used as design information and it is not maintained as such.

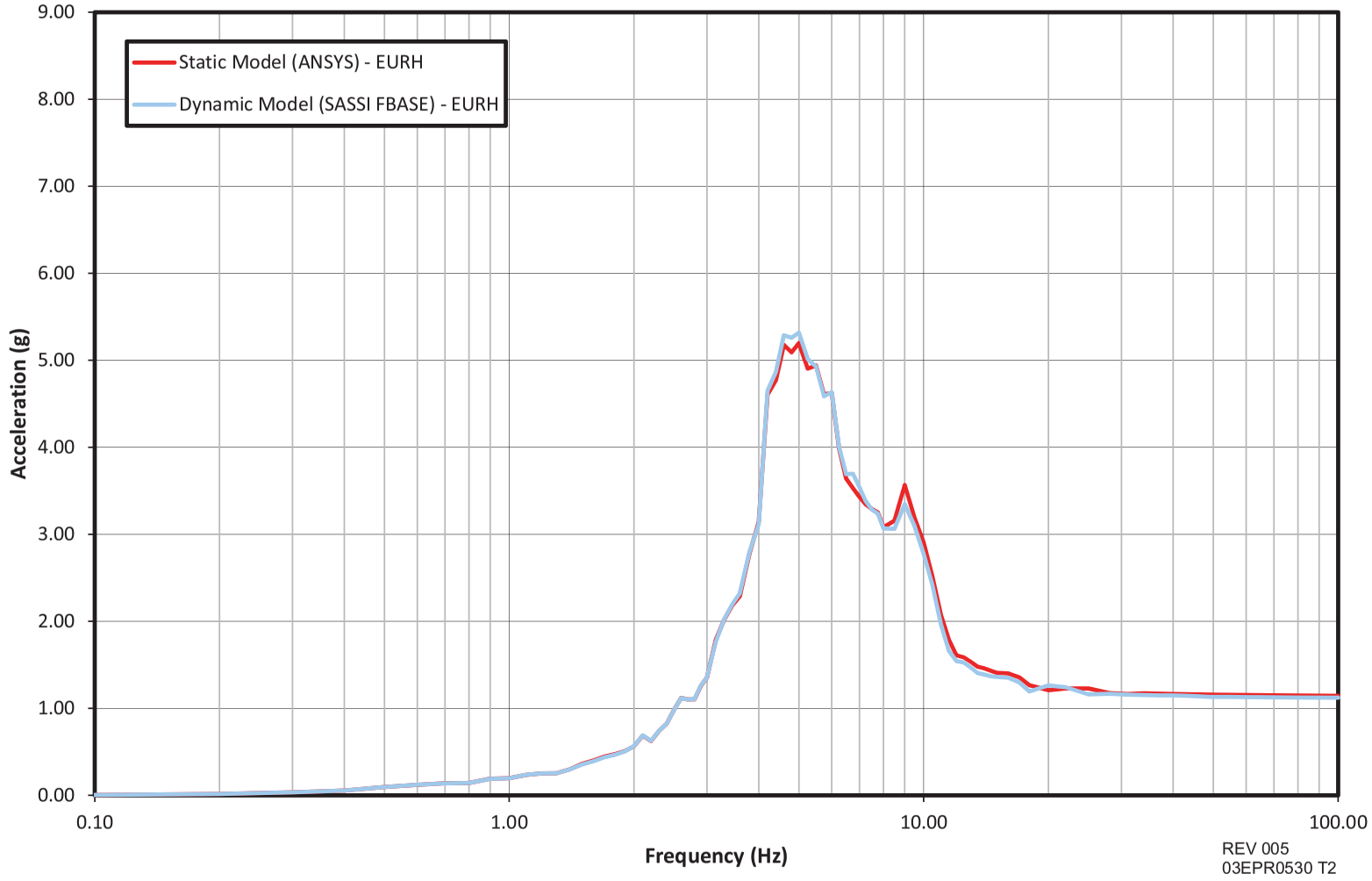

Figure 3.7.2-16—Static FEM vs. Dynamic FEM Spectrum Comparison at Elev. +200ft, 5 in (+61.09m) (Dome Apex) of Reactor Shield Building, 5% Damping, Z-Direction

The sole purpose of this figure is to demonstrate dynamic compatibility between the dynamic and static models; it is not intended to be used as design information and it is not maintained as such.

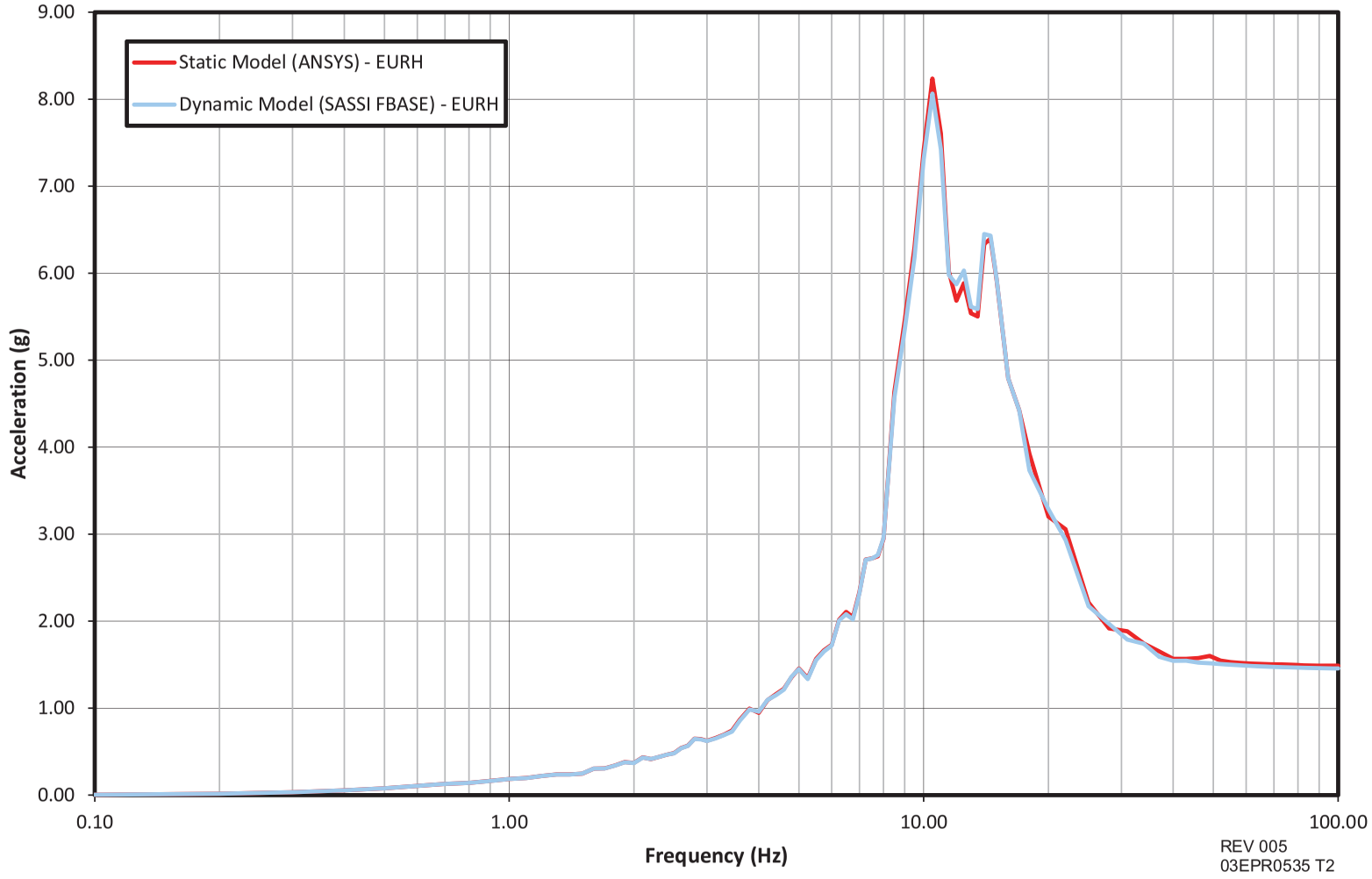

Figure 3.7.2-17—Static FEM vs. Dynamic FEM Spectrum Comparison at Elev. +95 ft, 1-3/4 in (+29.00m) - Safeguard Building 1, 5% Damping, X-Direction

The sole purpose of this figure is to demonstrate dynamic compatibility between the dynamic and static models; it is not intended to be used as design information and it is not maintained as such.

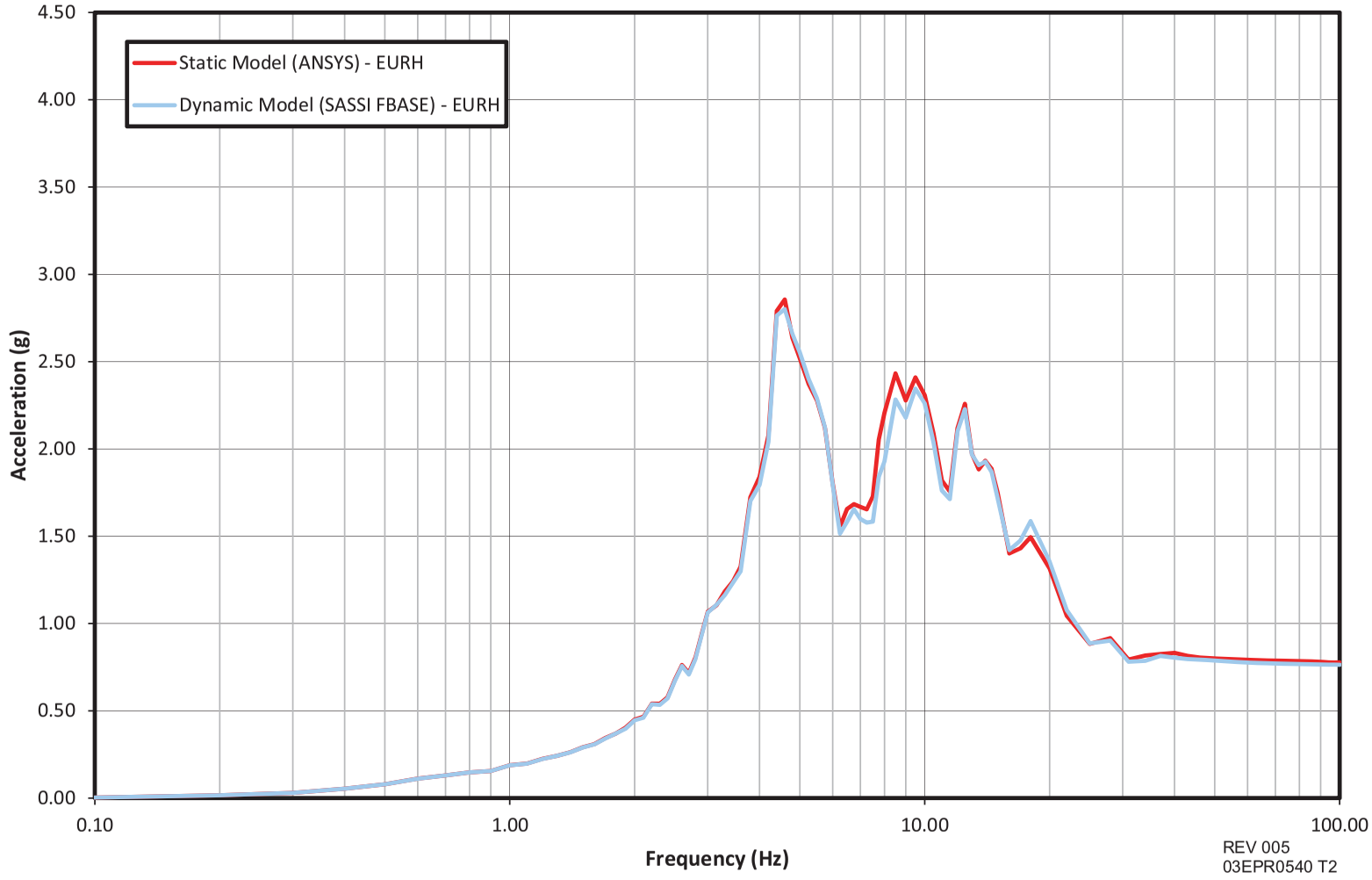

Figure 3.7.2-18—Static FEM vs. Dynamic FEM Spectrum Comparison at Elev. +95 ft, 1-3/4 in (+29.00m) - Safeguard Building 1, 5% Damping, Y-Direction

The sole purpose of this figure is to demonstrate dynamic compatibility between the dynamic and static models; it is not intended to be used as design information and it is not maintained as such.

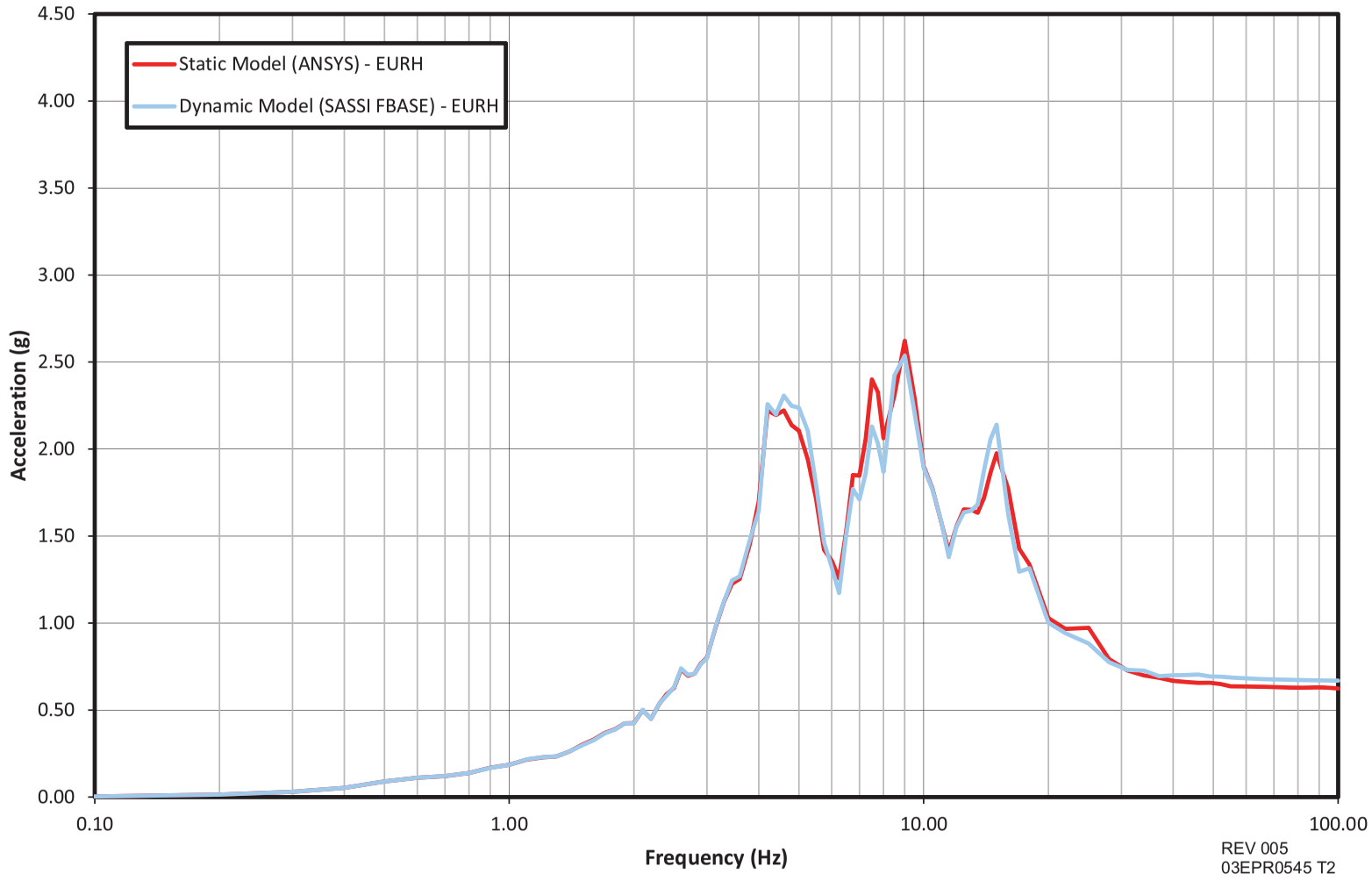

Figure 3.7.2-19—Static FEM vs. Dynamic FEM Spectrum Comparison at Elev. +95 ft, 1-3/4 in (+29.00m) - Safeguard Building 1, 5% Damping, Z-Direction

The sole purpose of this figure is to demonstrate dynamic compatibility between the dynamic and static models; it is not intended to be used as design information and it is not maintained as such.

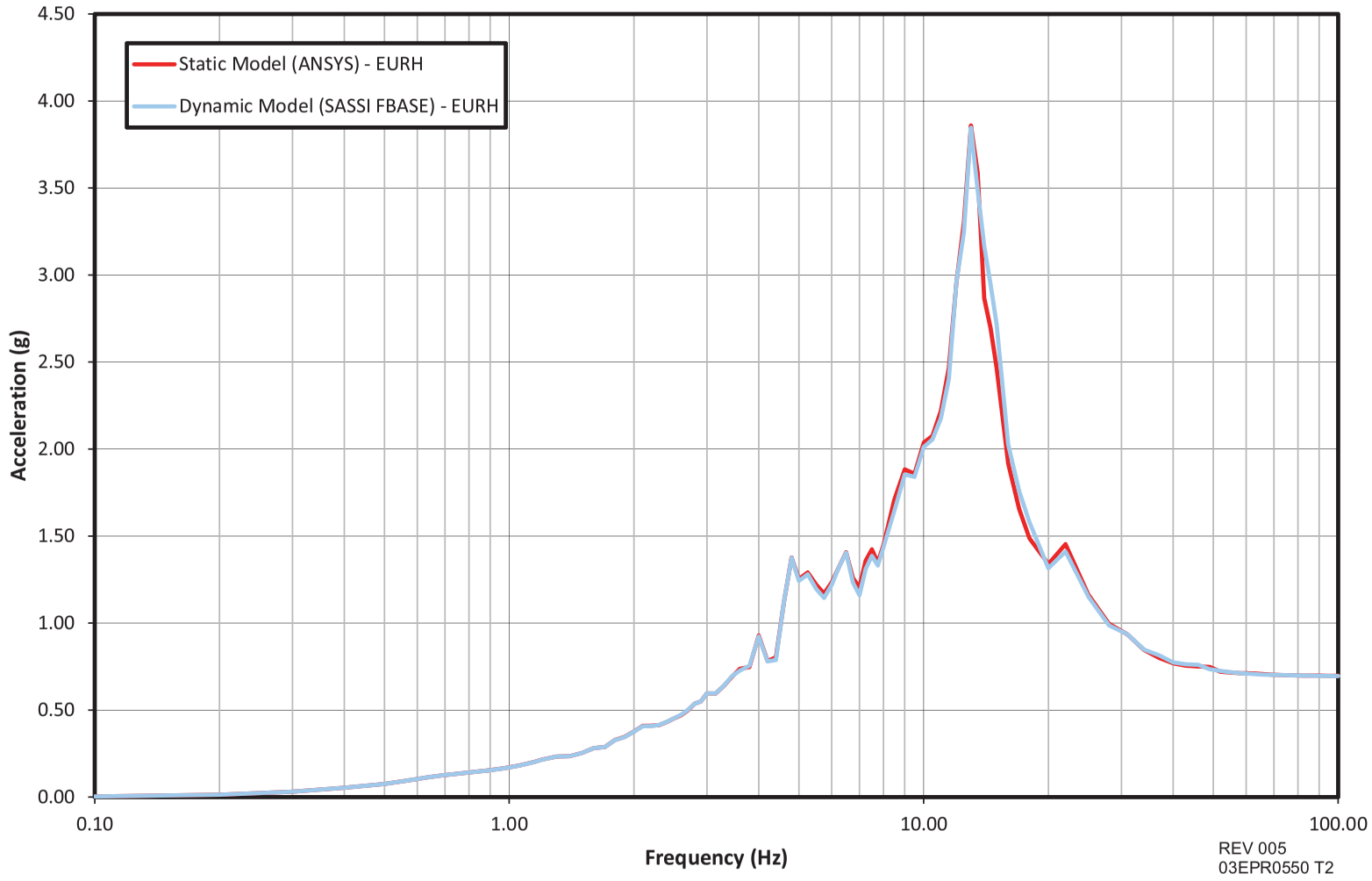

Figure 3.7.2-20—Static FEM vs. Dynamic FEM Spectrum Comparison at Elev. +26 ft, 3 in (+8.00m) - Safeguard Building 1, 5% Damping, X-Direction

The sole purpose of this figure is to demonstrate dynamic compatibility between the dynamic and static models; it is not intended to be used as design information and it is not maintained as such.

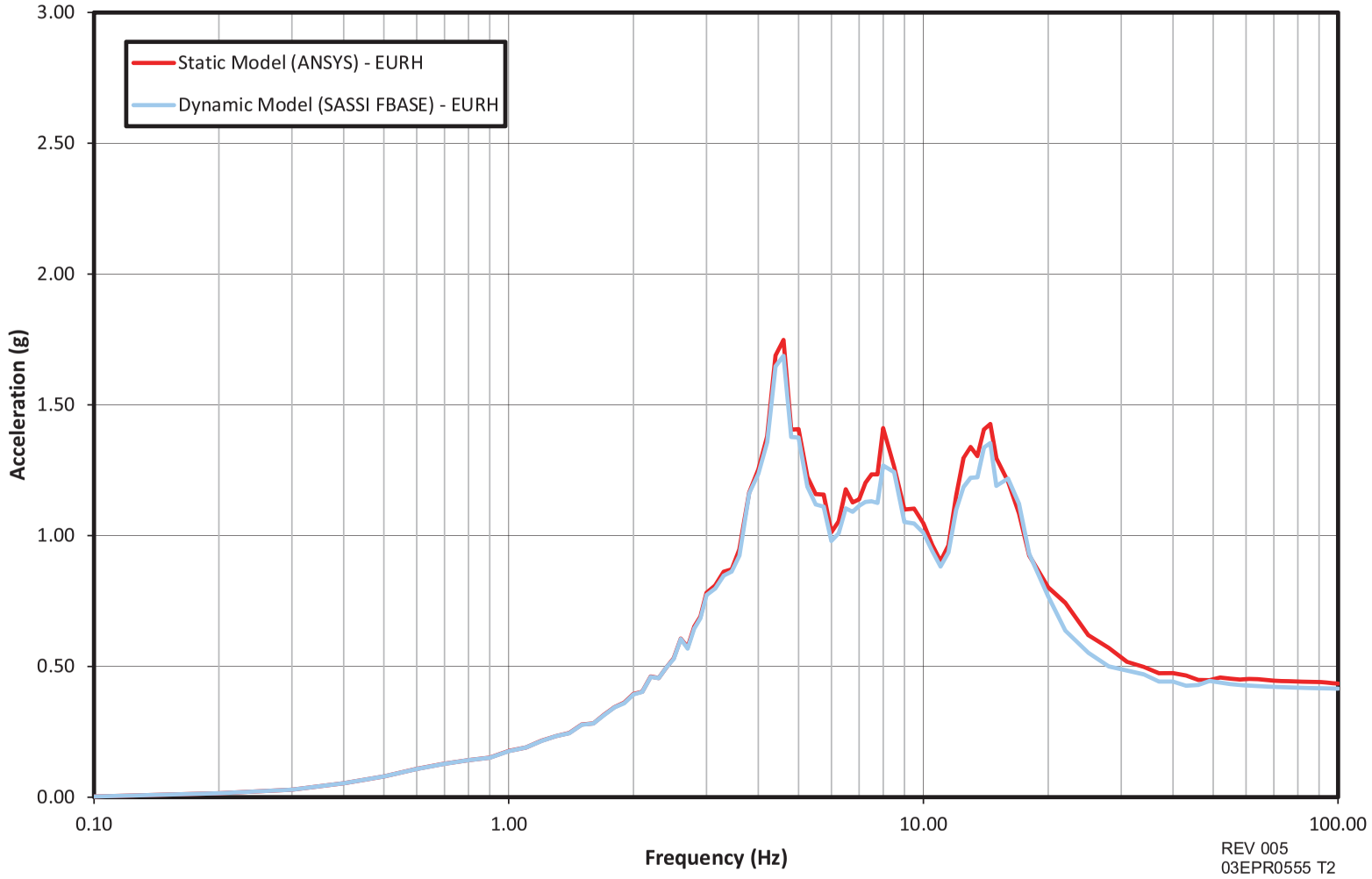

Figure 3.7.2-21—Static FEM vs. Dynamic FEM Spectrum Comparison at Elev. +26 ft, 3 in (+8.00m) - Safeguard Building 1, 5% Damping, Y-Direction

The sole purpose of this figure is to demonstrate dynamic compatibility between the dynamic and static models; it is not intended to be used as design information and it is not maintained as such.

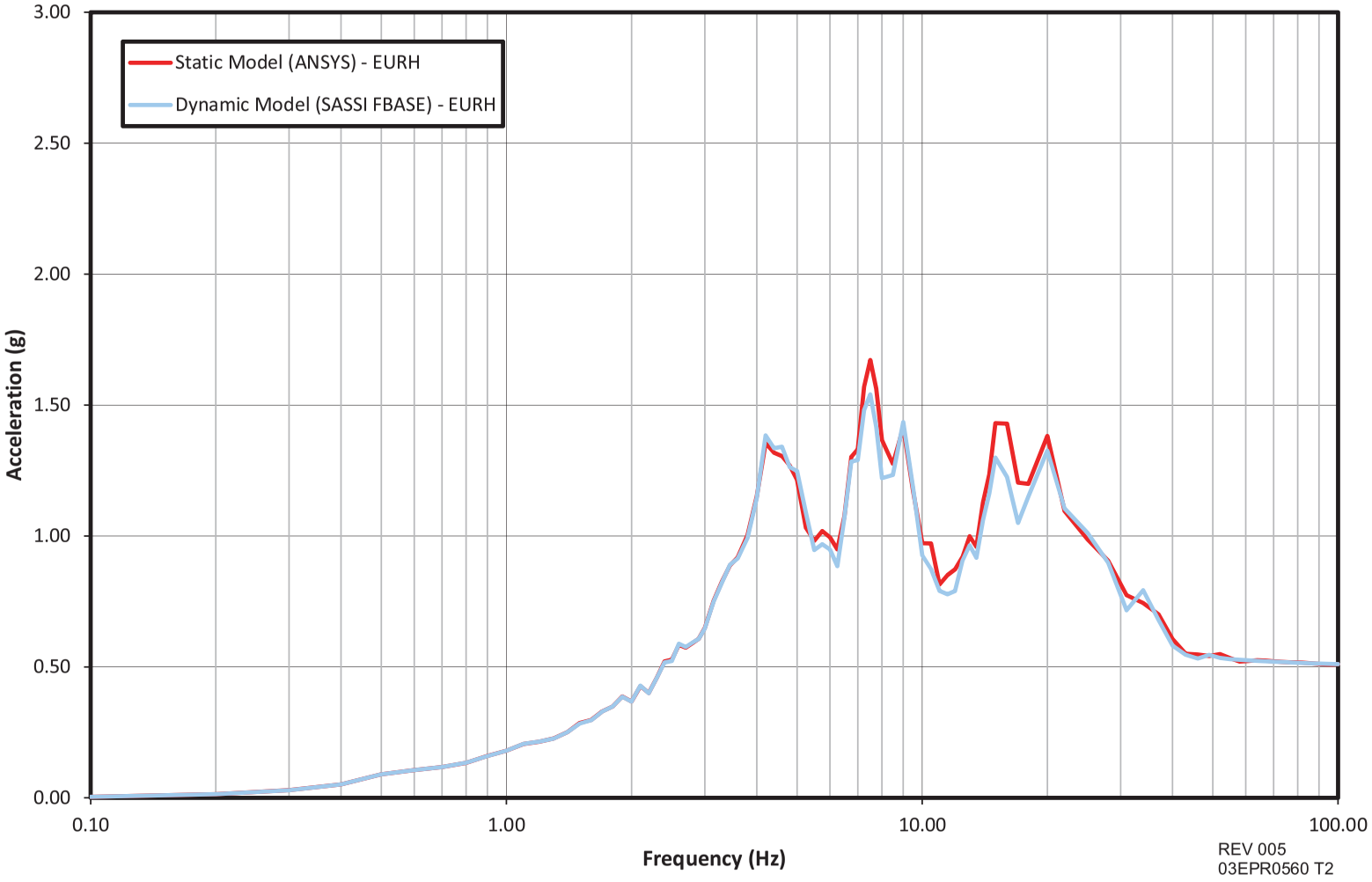

Figure 3.7.2-22—Static FEM vs. Dynamic FEM Spectrum Comparison at Elev. +26 ft, 3 in (+8.00m) - Safeguard Building 1, 5% Damping, Z-Direction

The sole purpose of this figure is to demonstrate dynamic compatibility between the dynamic and static models; it is not intended to be used as design information and it is not maintained as such.

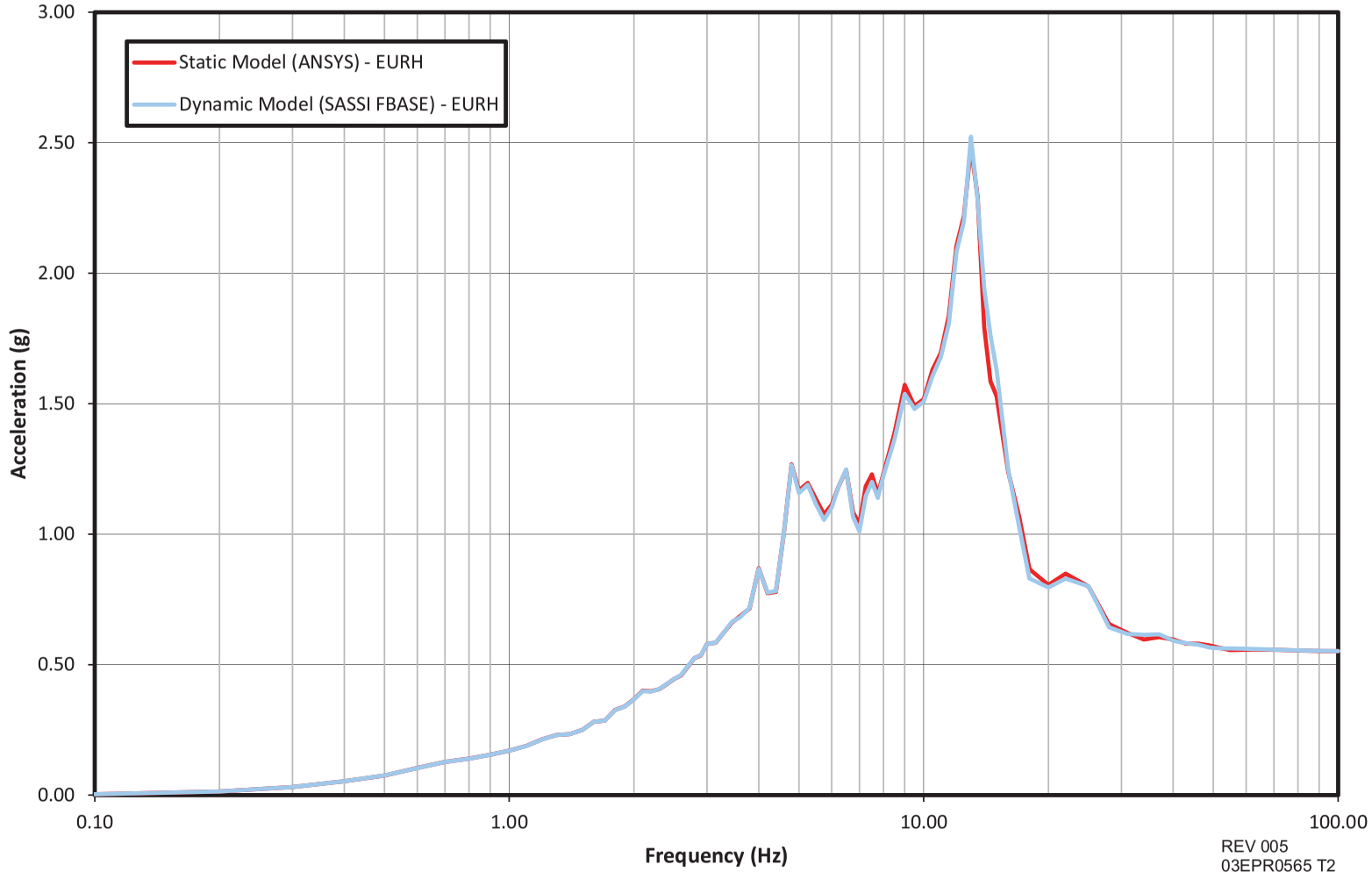

Figure 3.7.2-23—Static FEM vs. Dynamic FEM Spectrum Comparison at Elev. +95 ft, 1-3/4 in (+29.00m) - Safeguard Building 4, 5% Damping, X-Direction

The sole purpose of this figure is to demonstrate dynamic compatibility between the dynamic and static models; it is not intended to be used as design information and it is not maintained as such.

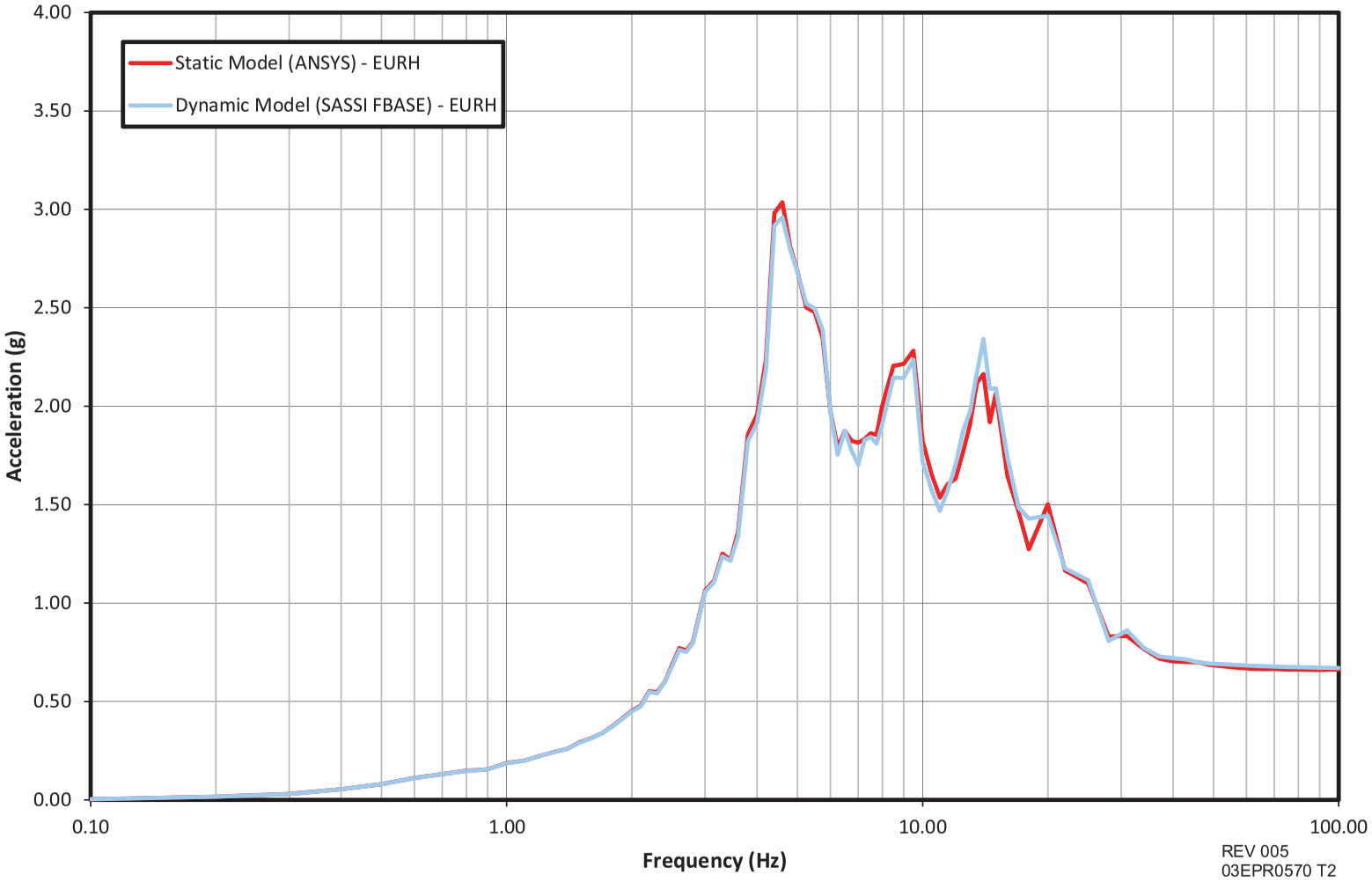

Figure 3.7.2-24—Static FEM vs. Dynamic FEM Spectrum Comparison at Elev. +95 ft, 1-3/4 in (+29.00m) - Safeguard Building 4, 5% Damping, Y-Direction

The sole purpose of this figure is to demonstrate dynamic compatibility between the dynamic and static models; it is not intended to be used as design information and it is not maintained as such.

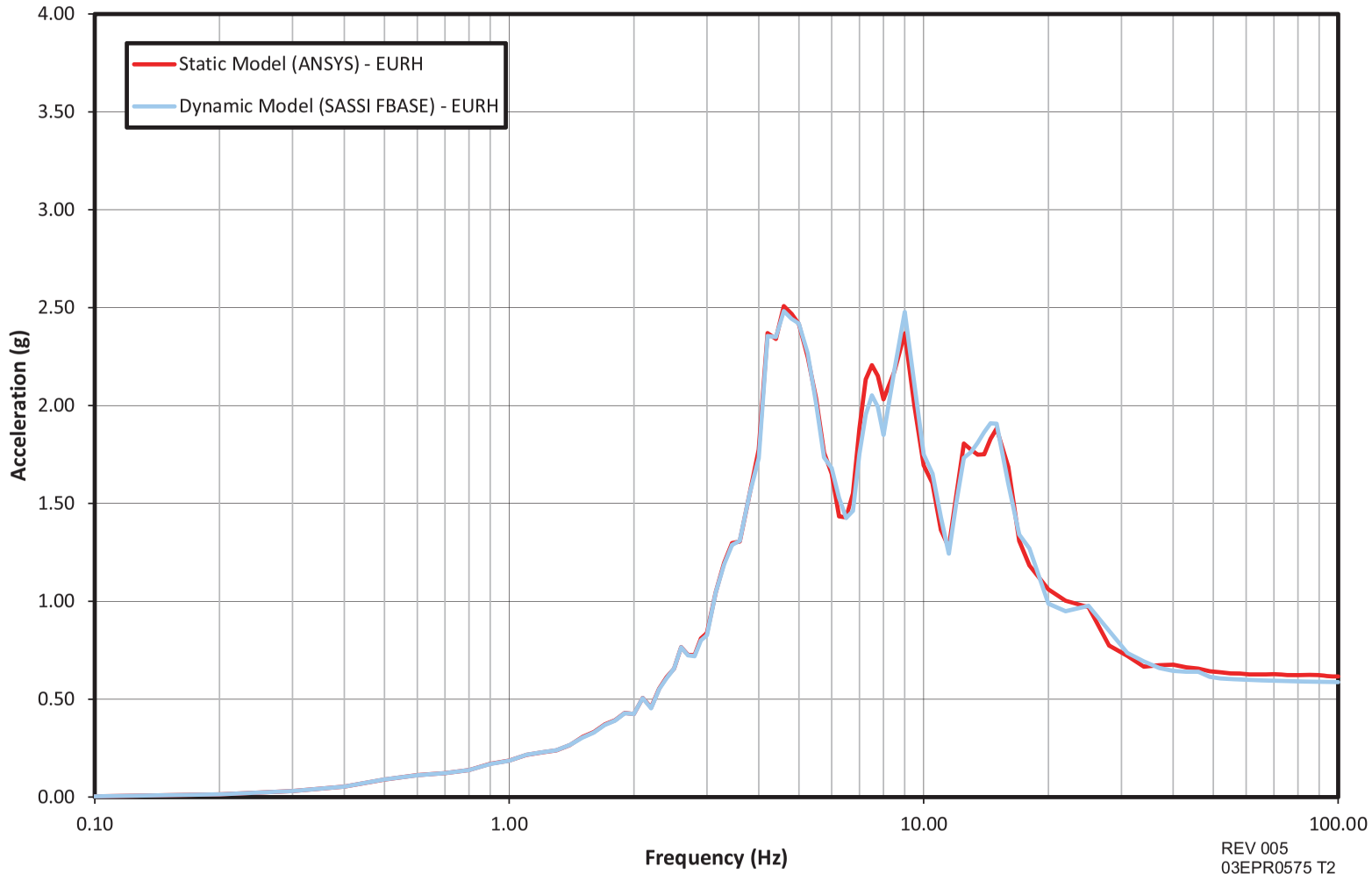

Figure 3.7.2-25—Static FEM vs. Dynamic FEM Spectrum Comparison at Elev. +95 ft, 1-3/4 in (+29.00m) - Safeguard Building 4, 5% Damping, Z-Direction

The sole purpose of this figure is to demonstrate dynamic compatibility between the dynamic and static models; it is not intended to be used as design information and it is not maintained as such.

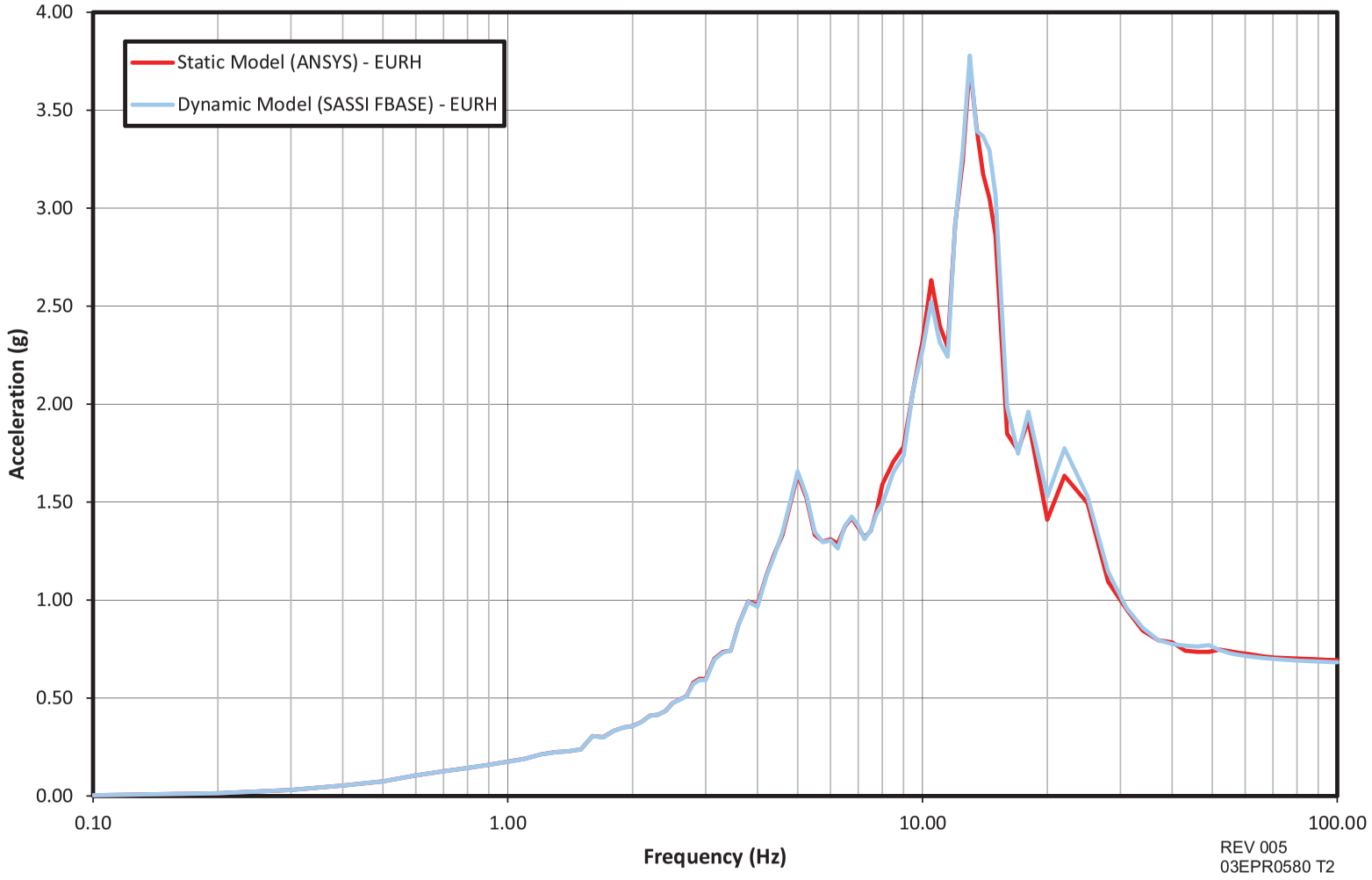

Figure 3.7.2-26—Static FEM vs. Dynamic FEM Spectrum Comparison at Elev. +26 ft, 3 in (+8.00m) - Safeguard Building 4, 5% Damping, X-Direction

The sole purpose of this figure is to demonstrate dynamic compatibility between the dynamic and static models; it is not intended to be used as design information and it is not maintained as such..

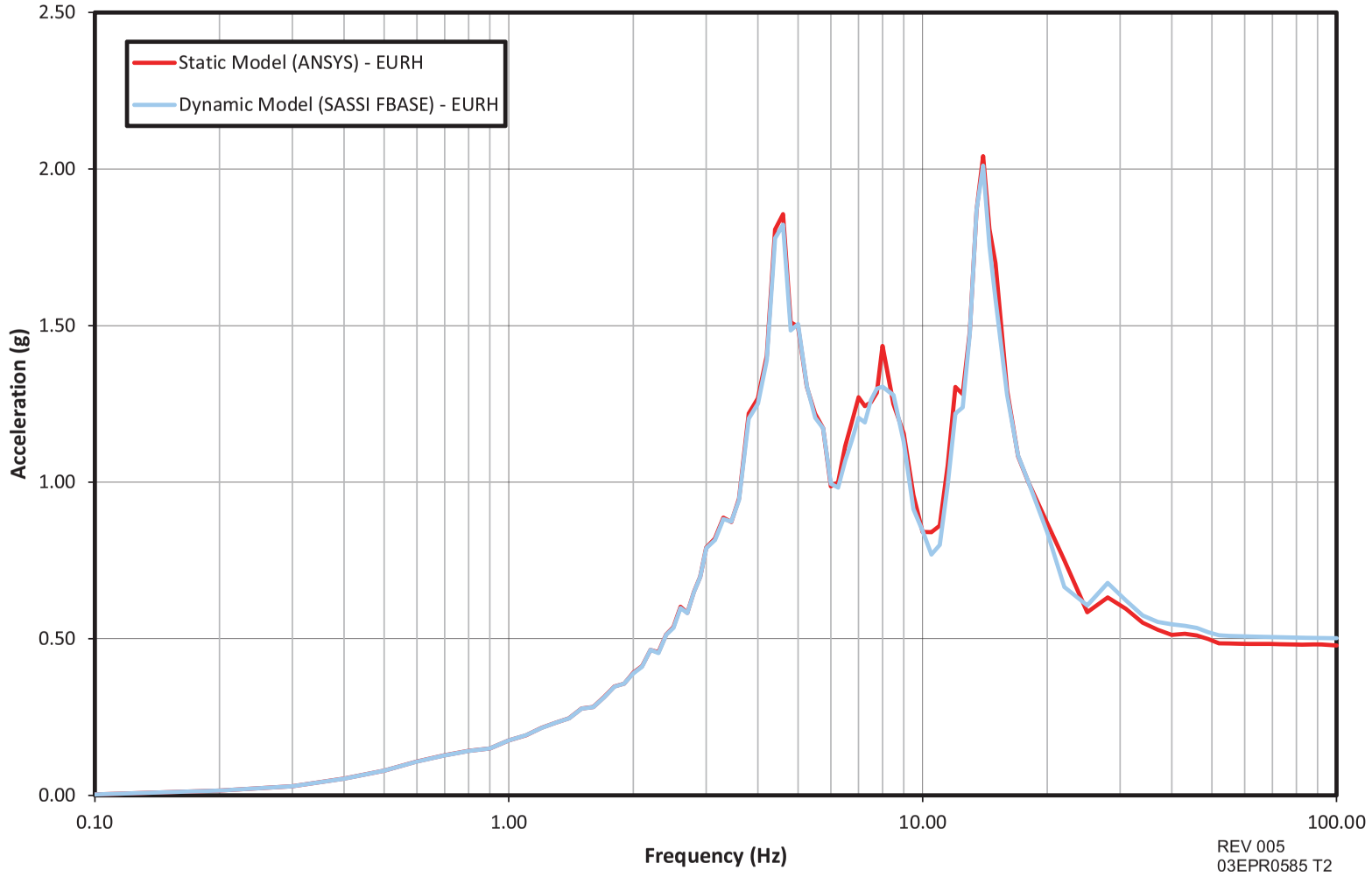

Figure 3.7.2-27—Static FEM vs. Dynamic FEM Spectrum Comparison at Elev. +26 ft, 3 in (+8.00m) - Safeguard Building 4, 5% Damping, Y-Direction

The sole purpose of this figure is to demonstrate dynamic compatibility between the dynamic and static models; it is not intended to be used as design information and it is not maintained as such..

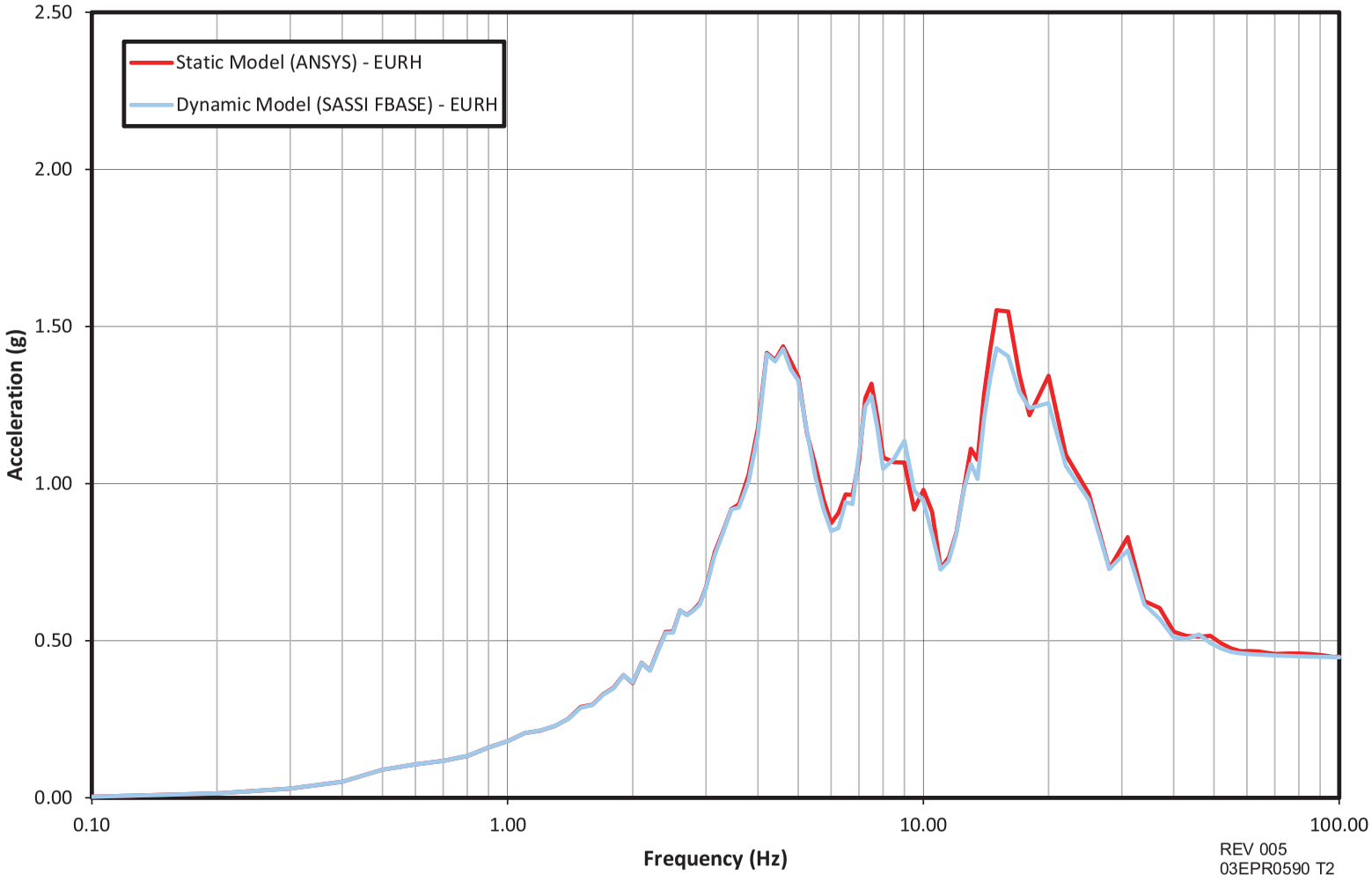

Figure 3.7.2-28—Static FEM vs. Dynamic FEM Spectrum Comparison at Elev. +26 ft, 3 in (+8.00m) - Safeguard Building 4, 5% Damping, Z-Direction

The sole purpose of this figure is to demonstrate dynamic compatibility between the dynamic and static models; it is not intended to be used as design information and it is not maintained as such.

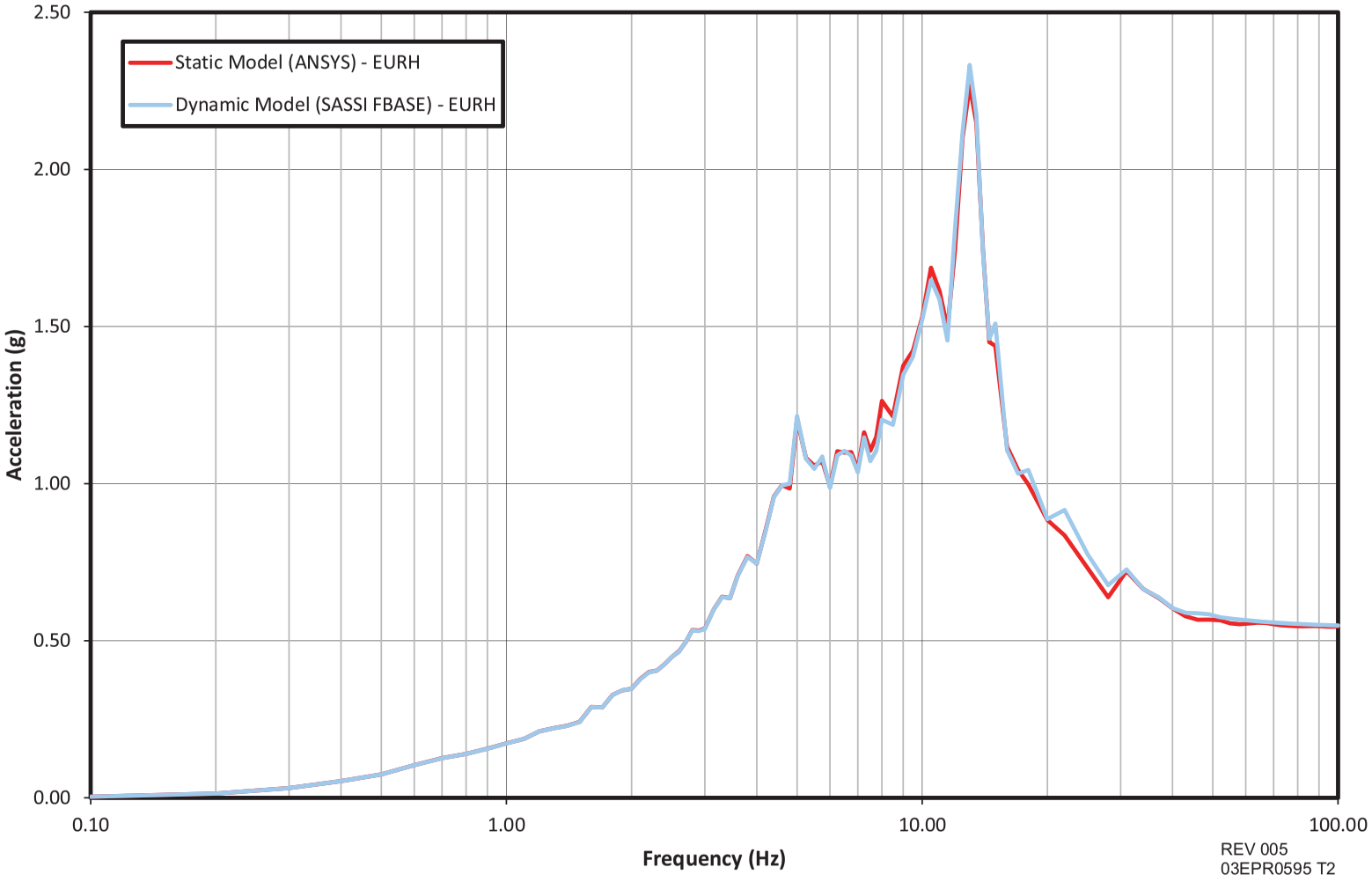

Figure 3.7.2-29—Static FEM vs. Dynamic FEM Spectrum Comparison at Elev. +68 ft, 10-3/4 in (+21.00m) - Safeguard Building 2/3, 5% Damping, X-Direction

The sole purpose of this figure is to demonstrate dynamic compatibility between the dynamic and static models; it is not intended to be used as design information and it is not maintained as such.

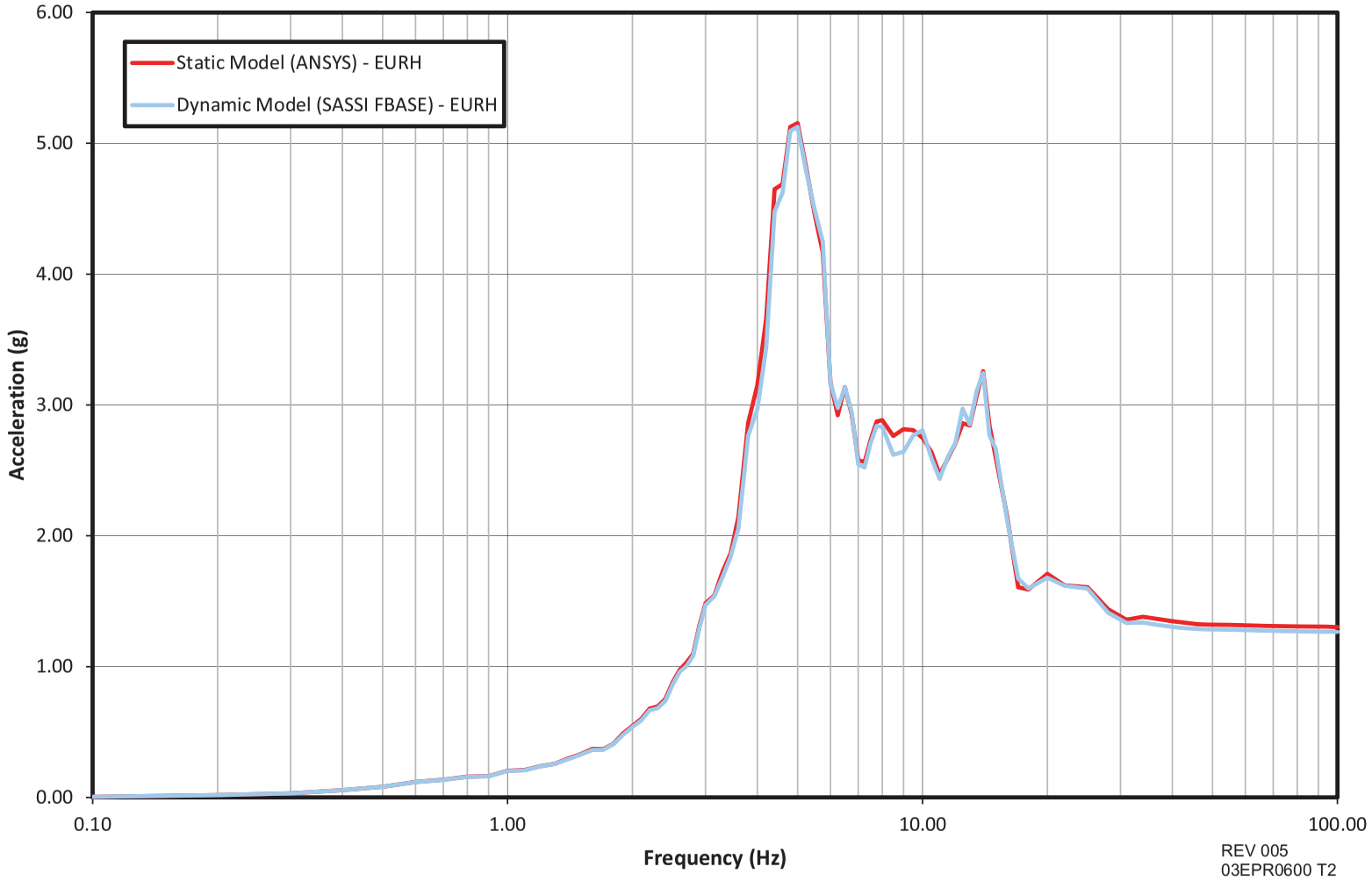

Figure 3.7.2-30—Static FEM vs. Dynamic FEM Spectrum Comparison at Elev. +68 ft, 10-3/4 in (+21.00m) - Safeguard Building 2/3, 5% Damping, Y-Direction

The sole purpose of this figure is to demonstrate dynamic compatibility between the dynamic and static models; it is not intended to be used as design information and it is not maintained as such.

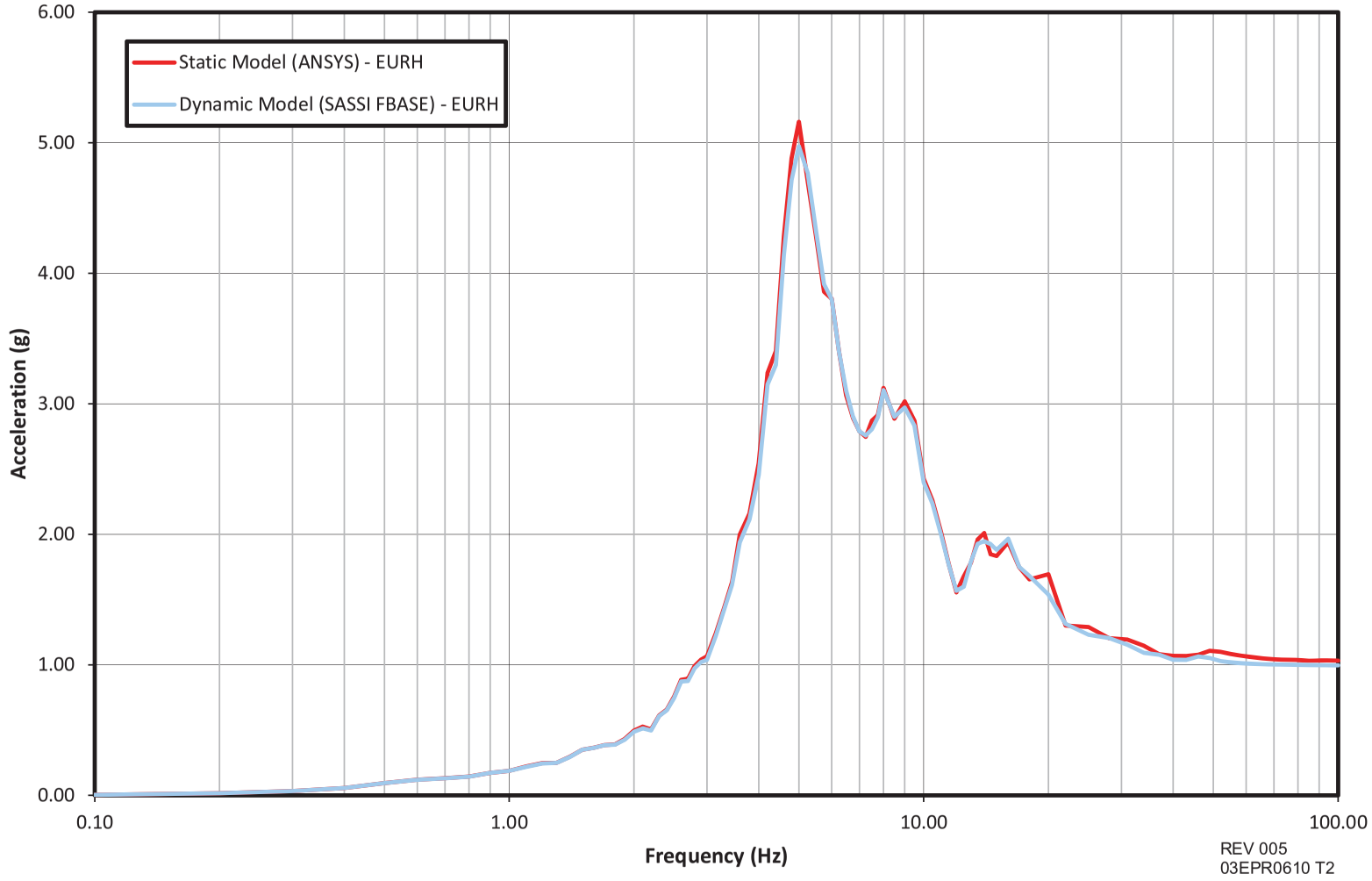

Figure 3.7.2-31—Static FEM vs. Dynamic FEM Spectrum Comparison at Elev. +68 ft, 10-3/4 in (+21.00m) - Safeguard Building 2/3, 5% Damping, Z-Direction

The sole purpose of this figure is to demonstrate dynamic compatibility between the dynamic and static models; it is not intended to be used as design information and it is not maintained as such.

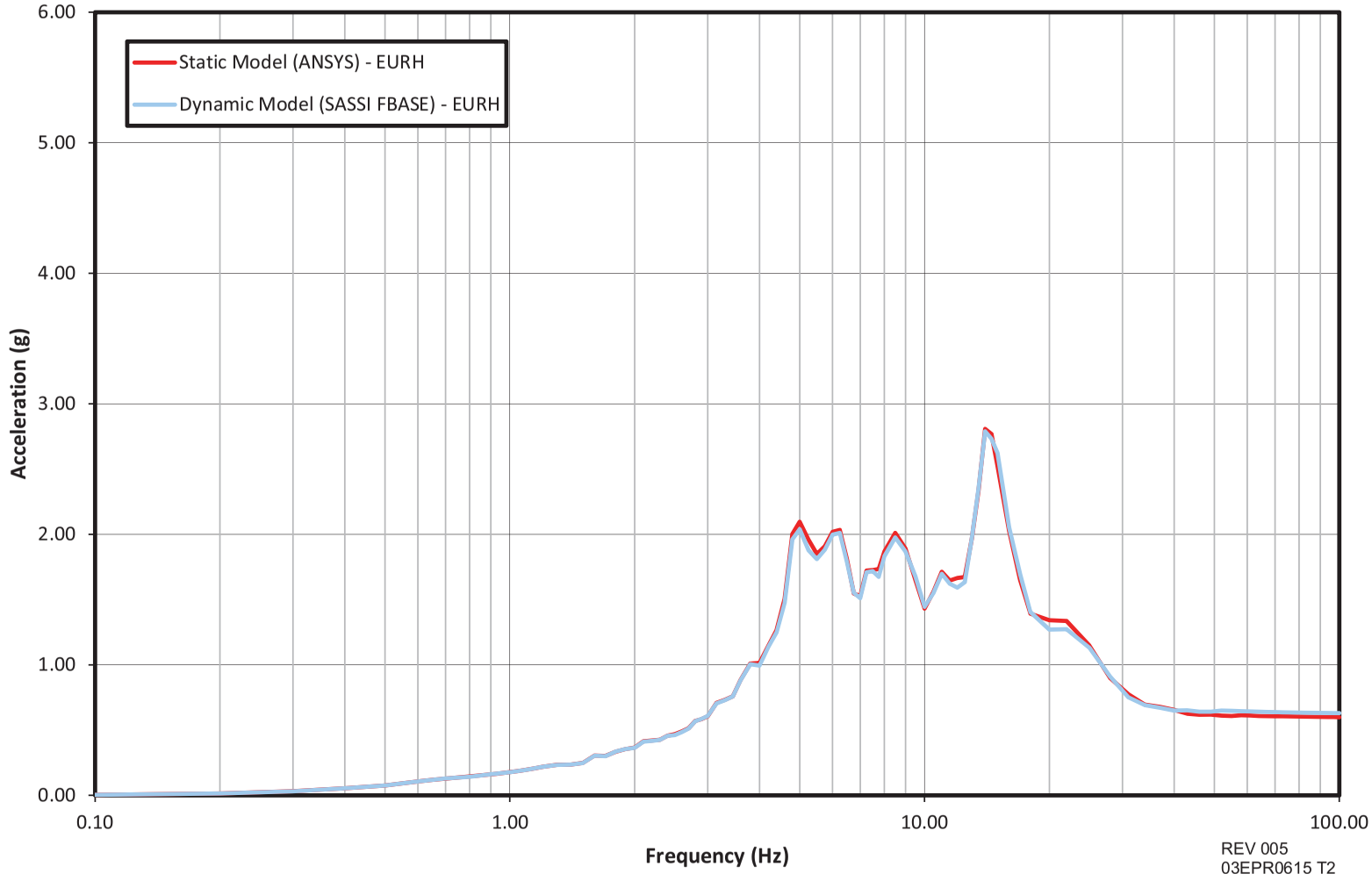

Figure 3.7.2-32—Static FEM vs. Dynamic FEM Spectrum Comparison at Elev. +26 ft, 3 in (+8.00m) - Safeguard Building 2/3, 5% Damping, X-Direction

The sole purpose of this figure is to demonstrate dynamic compatibility between the dynamic and static models; it is not intended to be used as design information and it is not maintained as such.

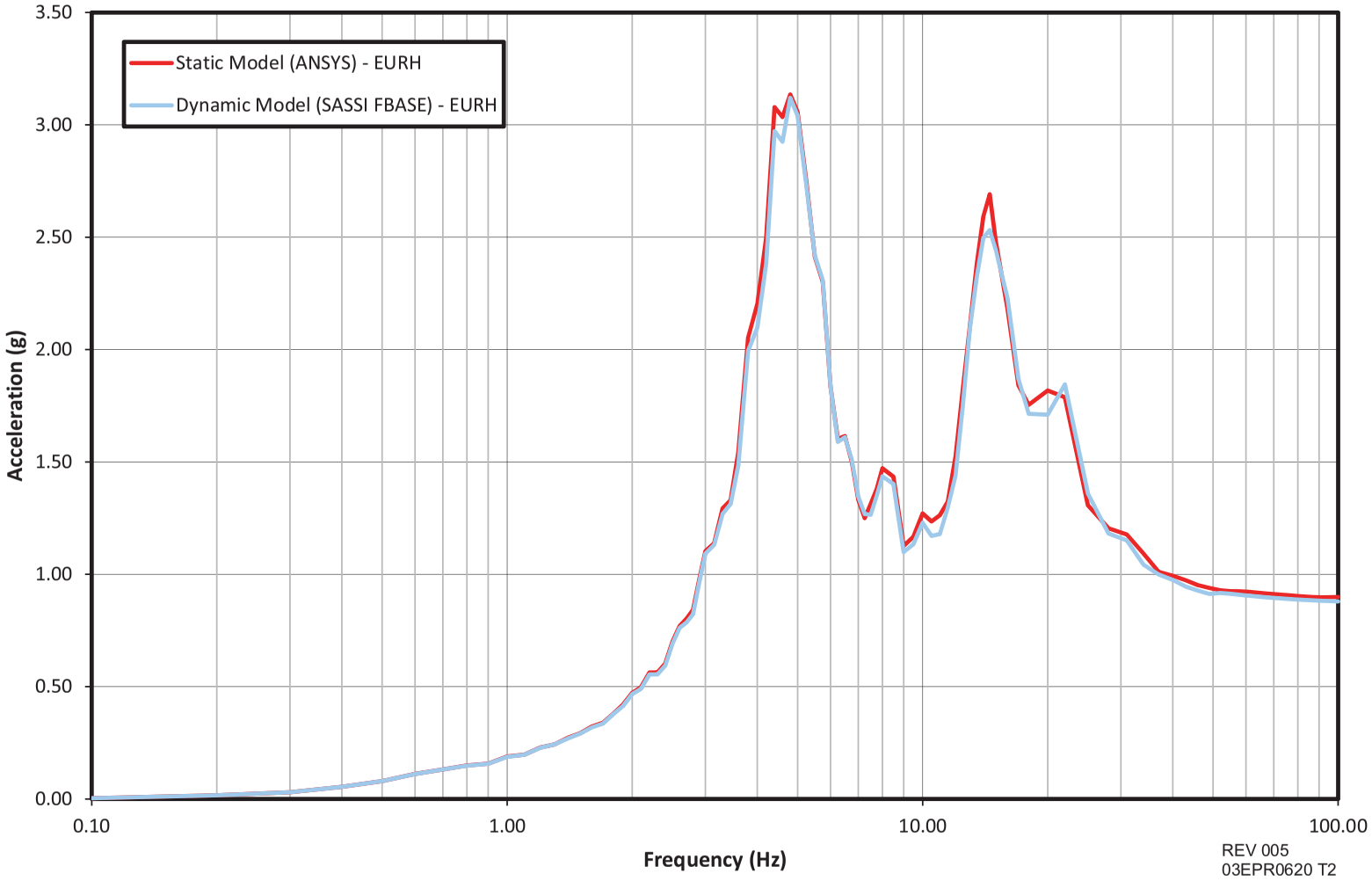

Figure 3.7.2-33—Static FEM vs. Dynamic FEM Spectrum Comparison at Elev. +26 ft, 3 in (+8.00m) - Safeguard Building 2/3, 5% Damping, Y-Direction

The sole purpose of this figure is to demonstrate dynamic compatibility between the dynamic and static models; it is not intended to be used as design information and it is not maintained as such.

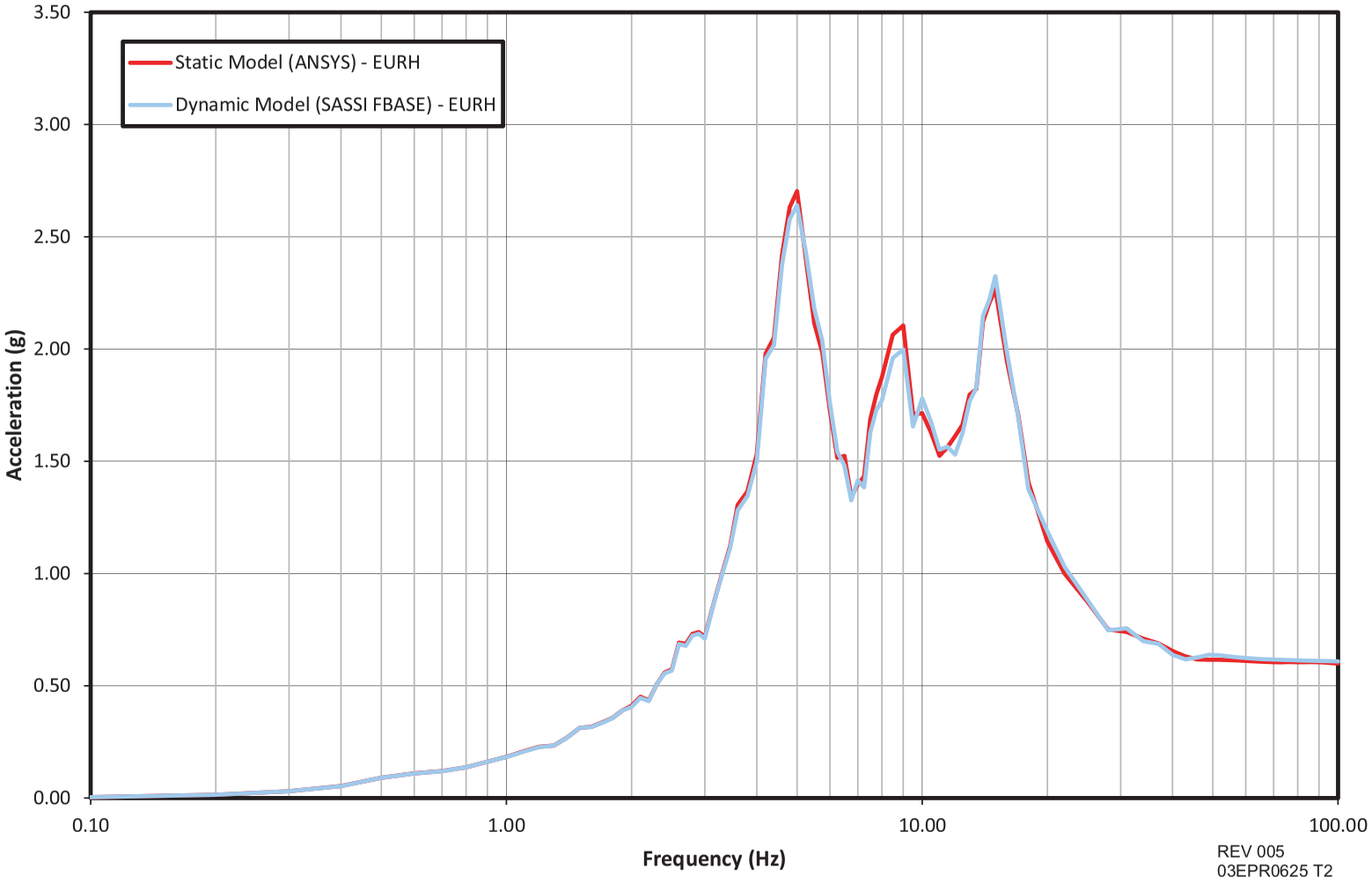

Figure 3.7.2-34—Static FEM vs. Dynamic FEM Spectrum Comparison at Elev. +26 ft, 3 in (+8.00m) - Safeguard Building 2/3, 5% Damping, Z-Direction

The sole purpose of this figure is to demonstrate dynamic compatibility between the dynamic and static models; it is not intended to be used as design information and it is not maintained as such.

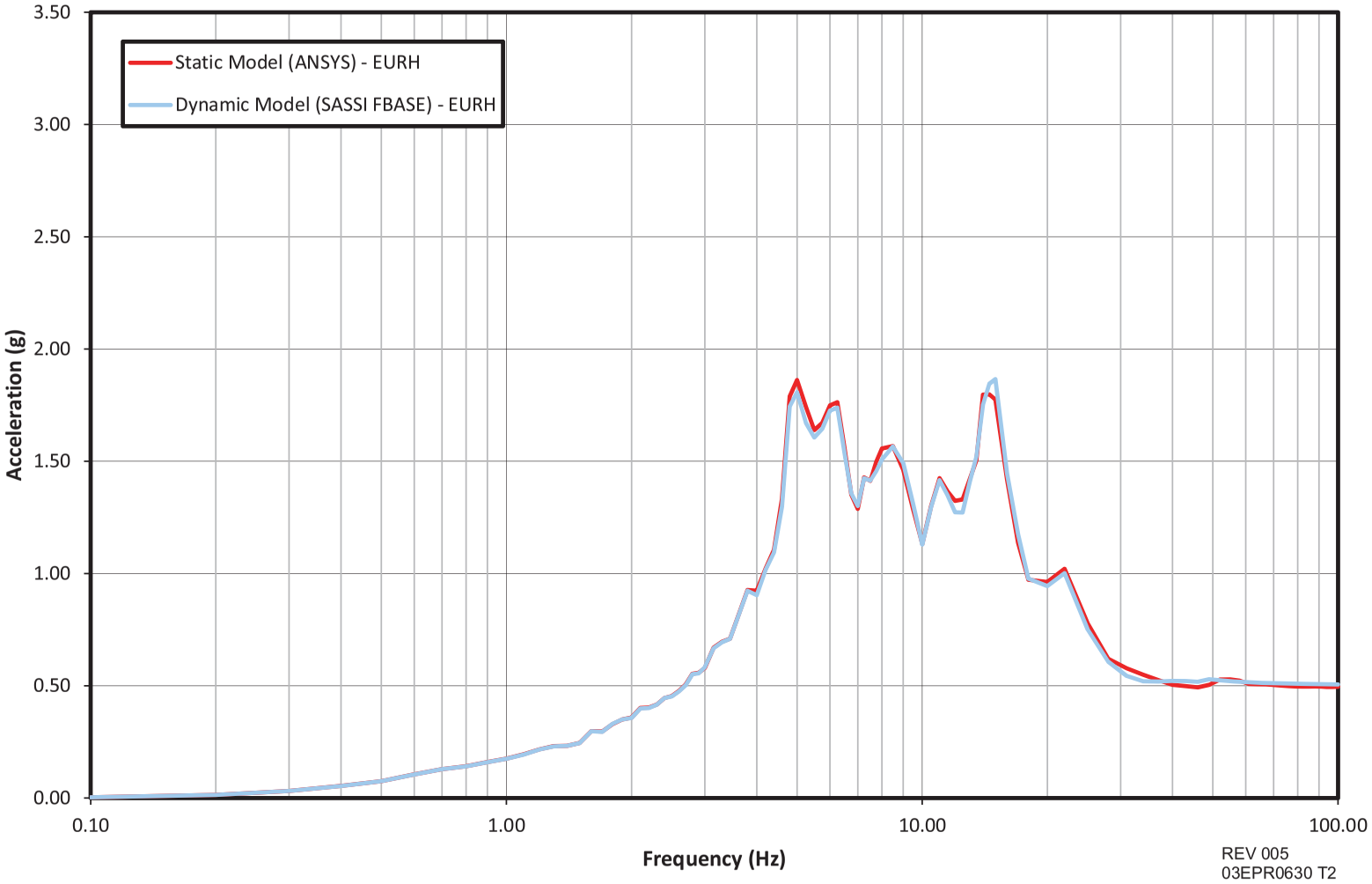

Figure 3.7.2-35—Static FEM vs. Dynamic FEM Spectrum Comparison at Elev. +62 ft, 4-1/4 in (+19.00m) - Fuel Building, 5% Damping, X-Direction

The sole purpose of this figure is to demonstrate dynamic compatibility between the dynamic and static models; it is not intended to be used as design information and it is not maintained as such.

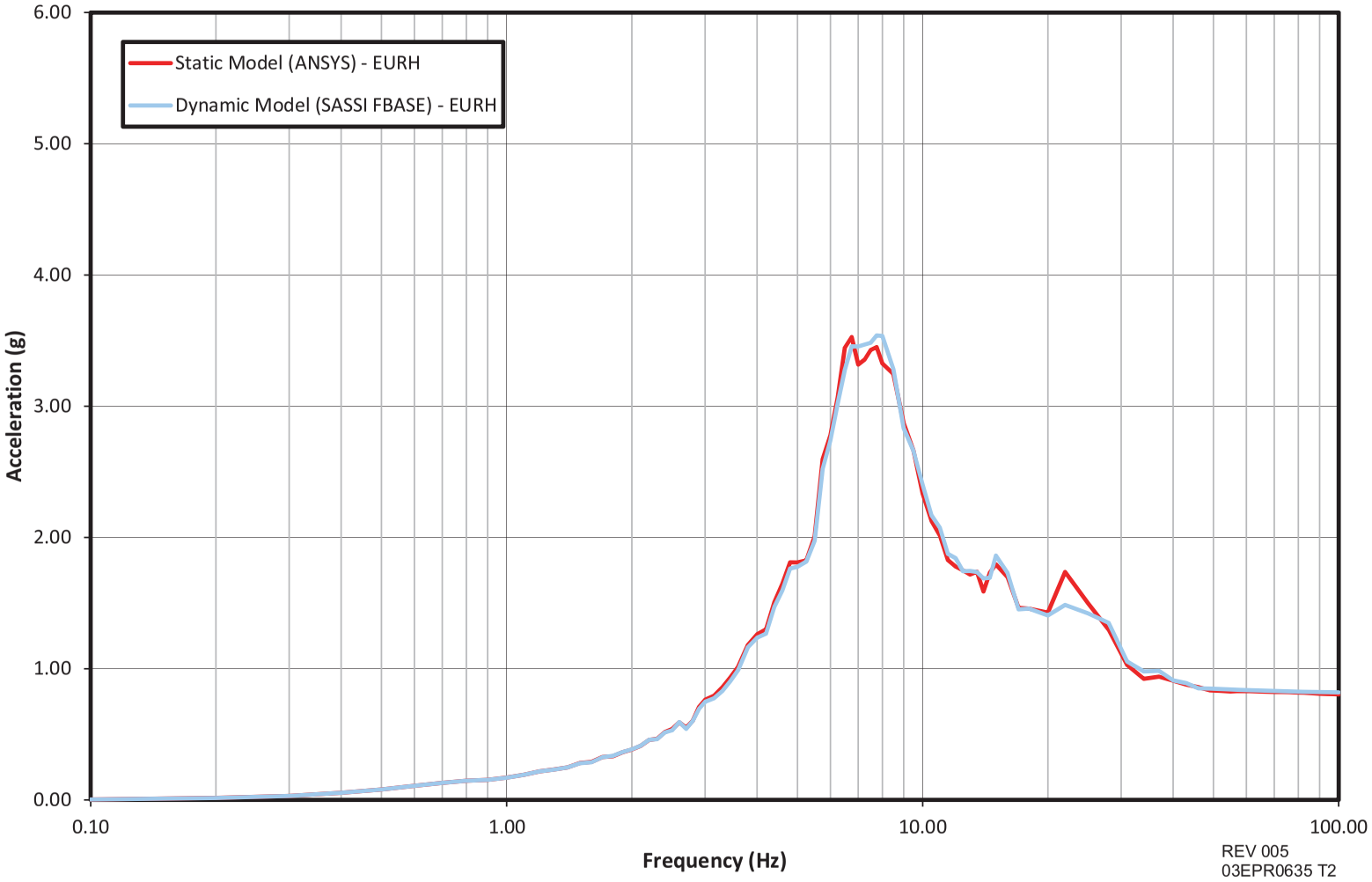

Figure 3.7.2-36—Static FEM vs. Dynamic FEM Spectrum Comparison at Elev. +62 ft, 4-1/4 in (+19.00m) - Fuel Building, 5% Damping Y-Direction

The sole purpose of this figure is to demonstrate dynamic compatibility between the dynamic and static models; it is not intended to be used as design information and it is not maintained as such.

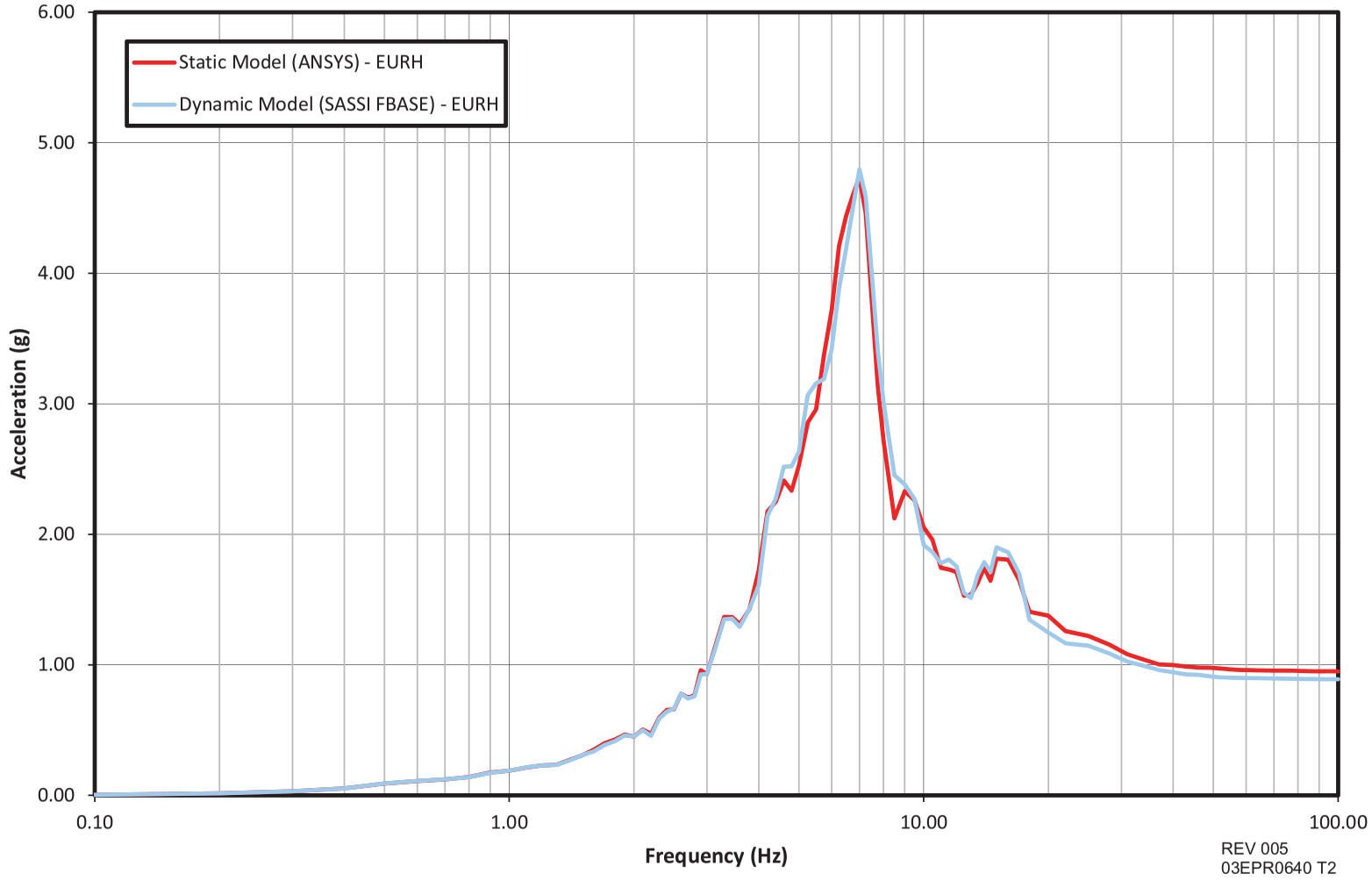

Figure 3.7.2-37—Static FEM vs. Dynamic FEM Spectrum Comparison at Elev. +62 ft, 4-1/4 in (+19.00m) - Fuel Building, 5% Damping, Z-Direction

The sole purpose of this figure is to demonstrate dynamic compatibility between the dynamic and static models; it is not intended to be used as design information and it is not maintained as such.

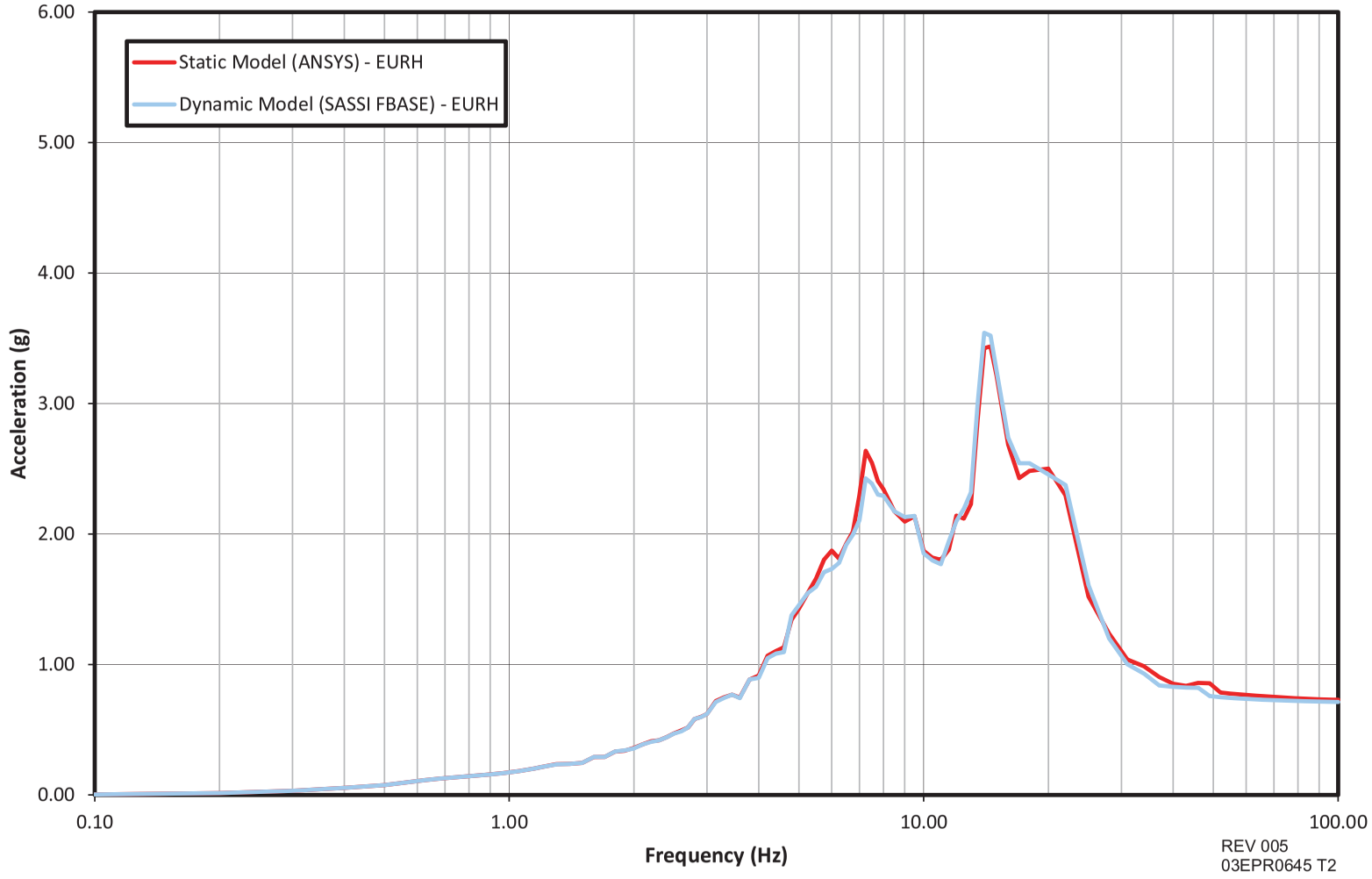

Figure 3.7.2-38—Static FEM vs. Dynamic FEM Spectrum Comparison at Elev. +23 ft, 7-1/2 in (+7.20m) - Fuel Building, 5% Damping, X-Direction

The sole purpose of this figure is to demonstrate dynamic compatibility between the dynamic and static models; it is not intended to be used as design information and it is not maintained as such.

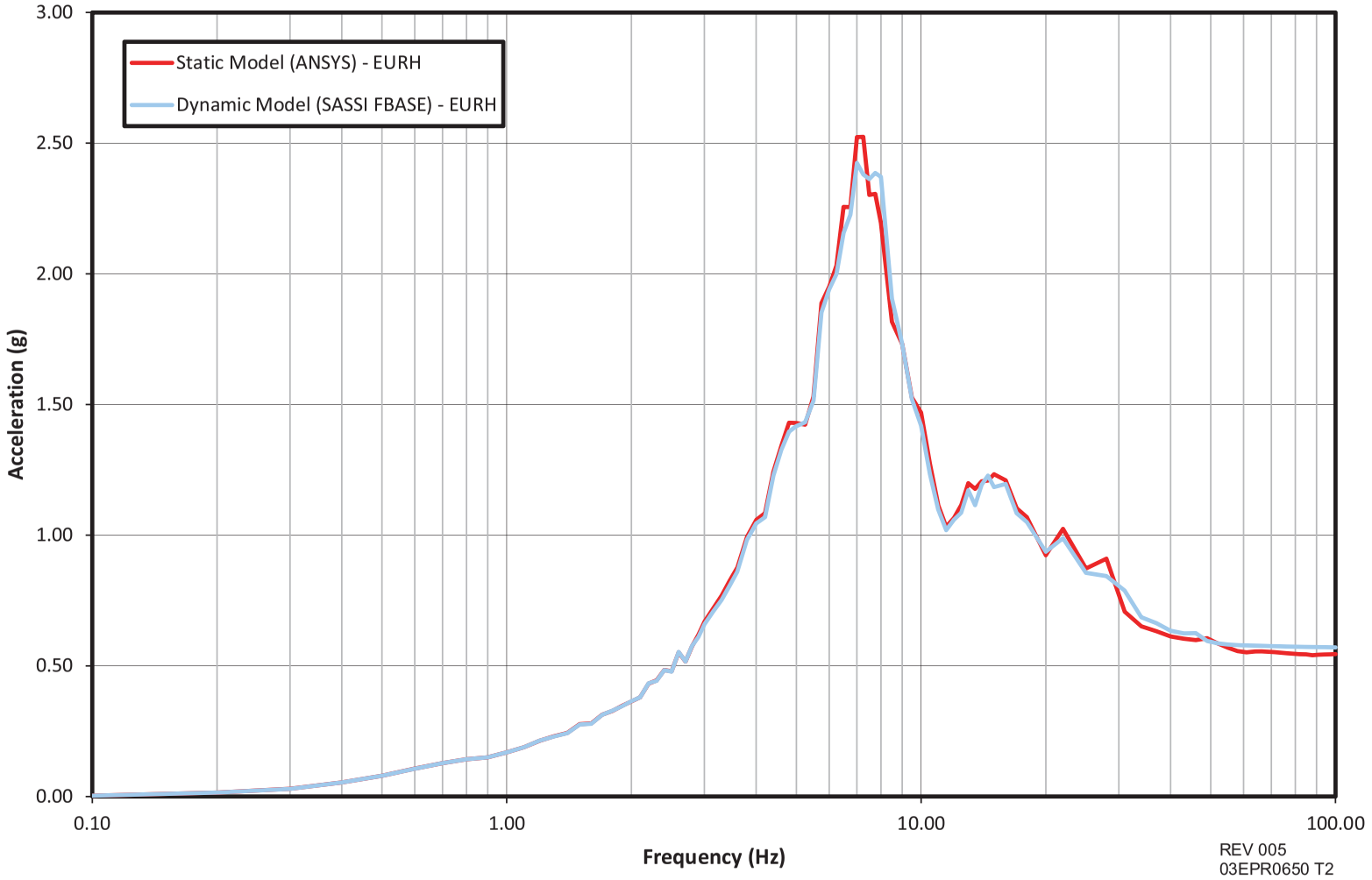

Figure 3.7.2-39—Static FEM vs. Dynamic FEM Spectrum Comparison at Elev. +23 ft, 7-1/2 in (+7.20m) - Fuel Building, 5% Damping, Y-Direction

The sole purpose of this figure is to demonstrate dynamic compatibility between the dynamic and static models; it is not intended to be used as design information and it is not maintained as such.

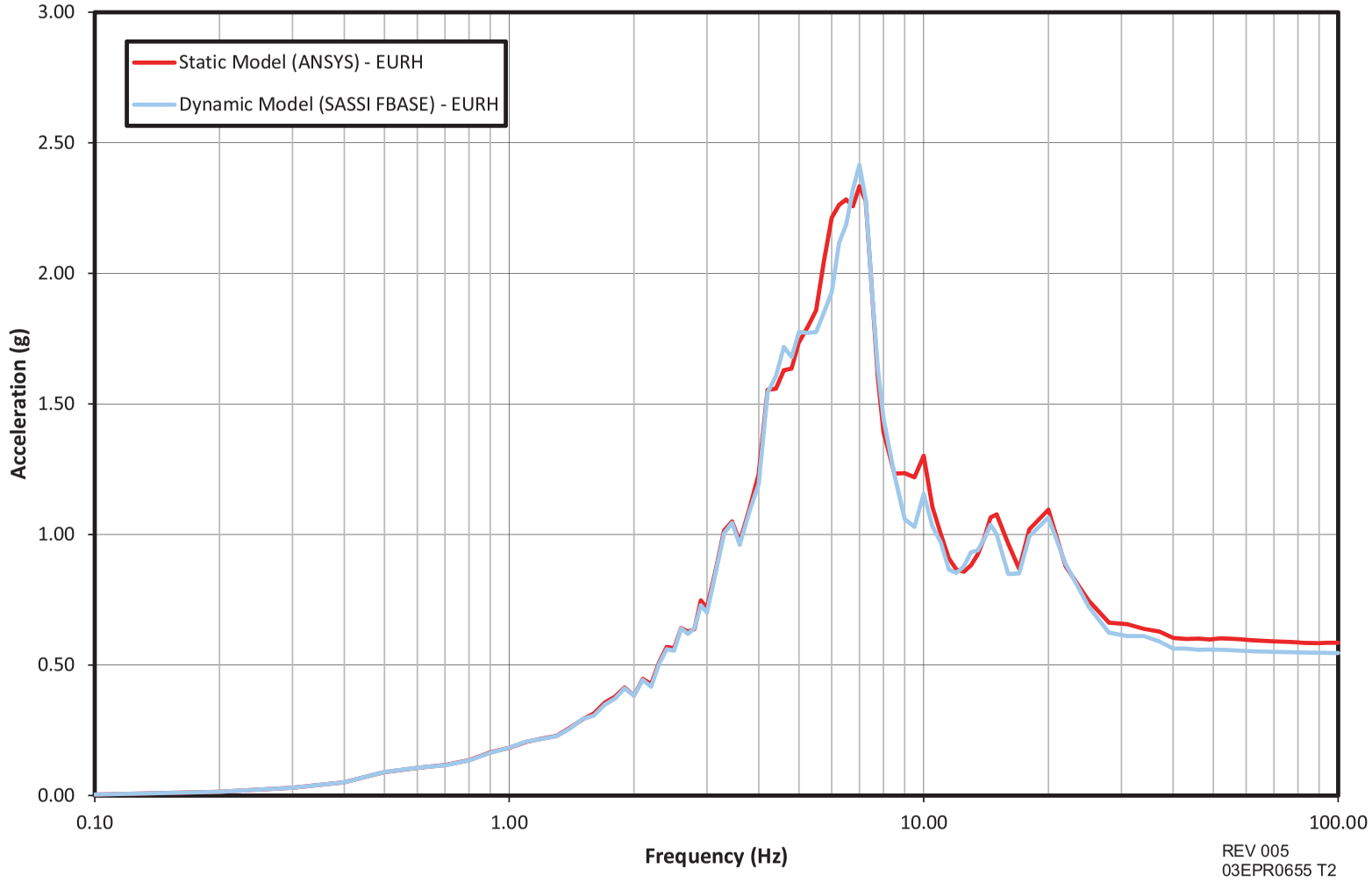

Figure 3.7.2-40—Static FEM vs. Dynamic FEM Spectrum Comparison at Elev. +23 ft, 7-1/2 in (+7.20m) - Fuel Building, 5% Damping, Z-Direction

The sole purpose of this figure is to demonstrate dynamic compatibility between the dynamic and static models; it is not intended to be used as design information and it is not maintained as such.

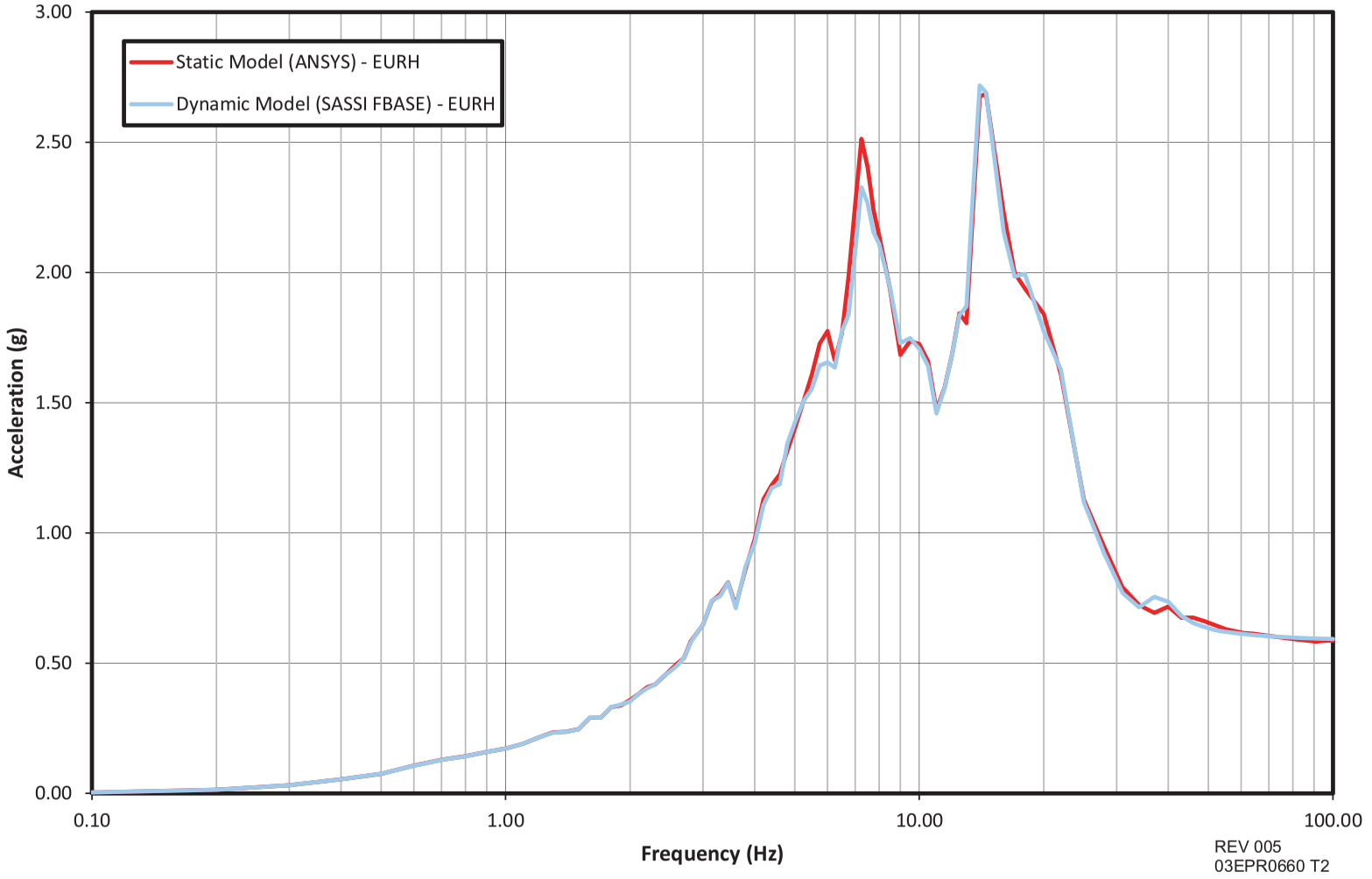

Figure 3.7.2-41—Static FEM vs. Dynamic FEM Spectrum Comparison at Elev. +190 ft, 3-1/2 in (+58.00m) - Containment Dome Apex, 5% Damping, X-Direction

The sole purpose of this figure is to demonstrate dynamic compatibility between the dynamic and static models; it is not intended to be used as design information and it is not maintained as such.

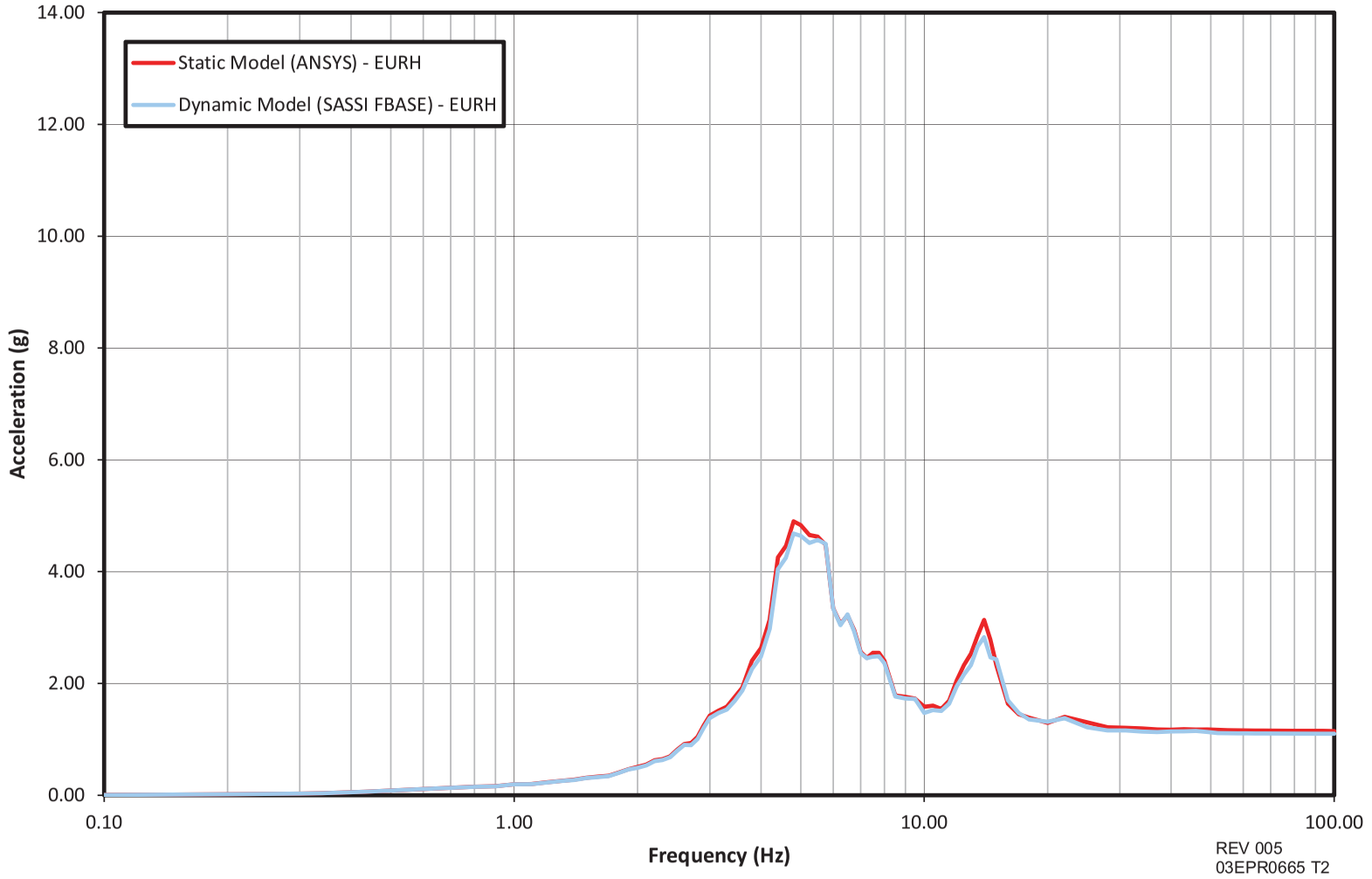

Figure 3.7.2-42—Static FEM vs. Dynamic FEM Spectrum Comparison at Elev. +190 ft, 3-1/2 in (+58.00m) - Containment Dome Apex, 5% Damping, Y-Direction

The sole purpose of this figure is to demonstrate dynamic compatibility between the dynamic and static models; it is not intended to be used as design information and it is not maintained as such.

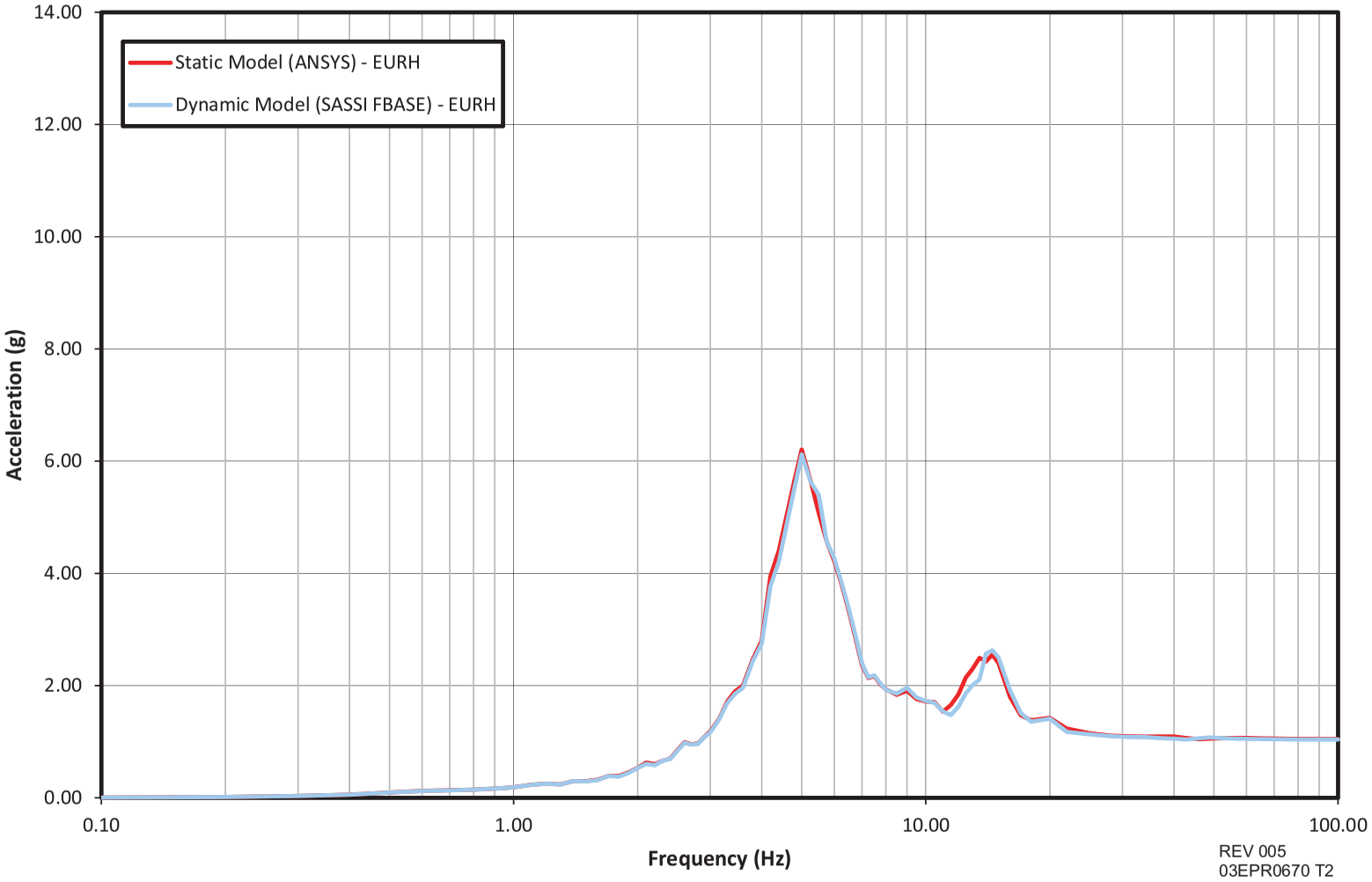

Figure 3.7.2-43—Static FEM vs. Dynamic FEM Spectrum Comparison at Elev. +190 ft, 3-1/2 in (+58.00m) - Containment Dome Apex, 5% Damping, Z-Direction

The sole purpose of this figure is to demonstrate dynamic compatibility between the dynamic and static models; it is not intended to be used as design information and it is not maintained as such.

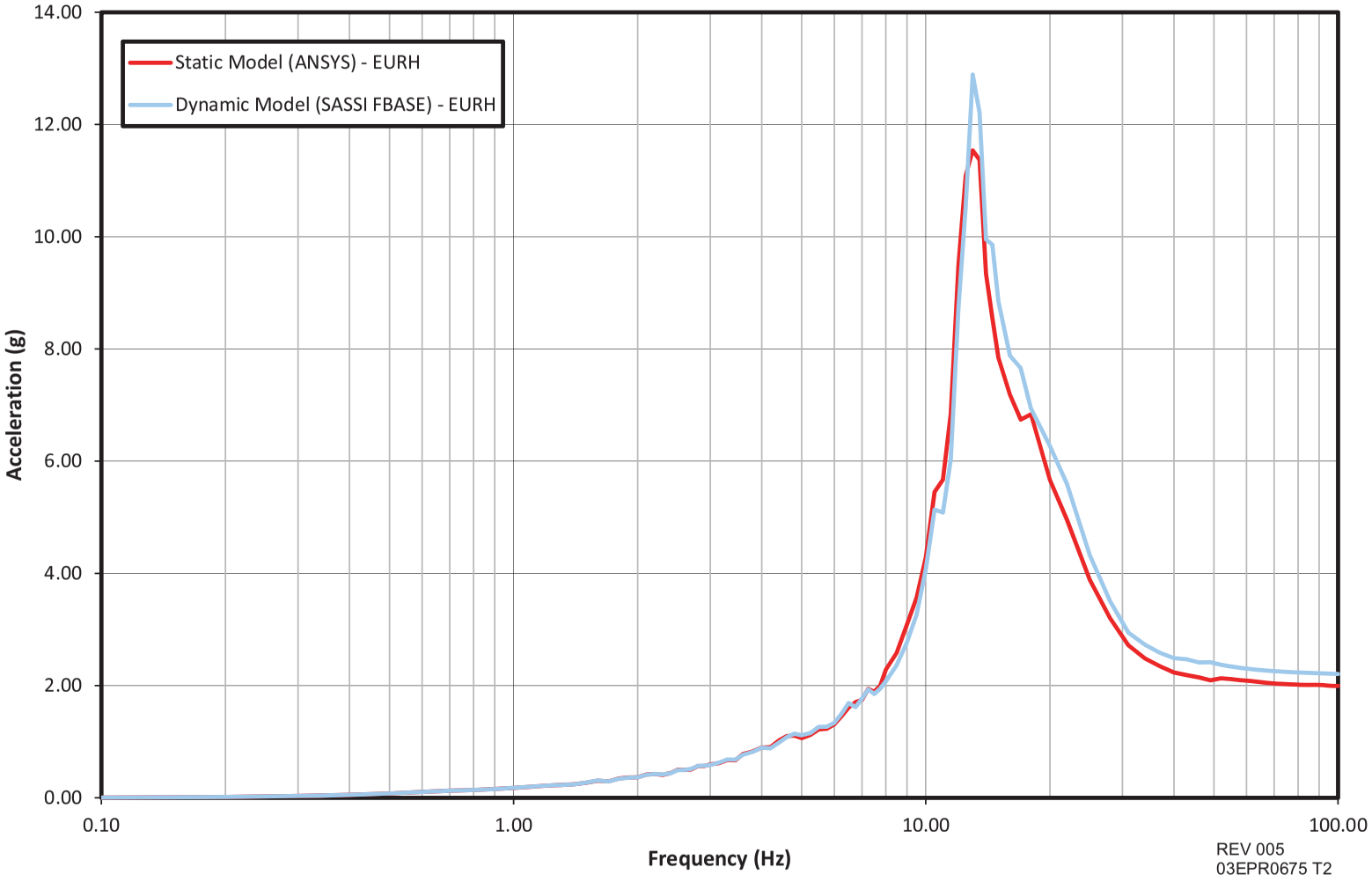

Figure 3.7.2-44—Static FEM vs. Dynamic FEM Spectrum Comparison at Elev. +123 ft, 4-1/4 in (+37.60m) - Containment Building, 5% Damping, X-Direction

The sole purpose of this figure is to demonstrate dynamic compatibility between the dynamic and static models; it is not intended to be used as design information and it is not maintained as such.

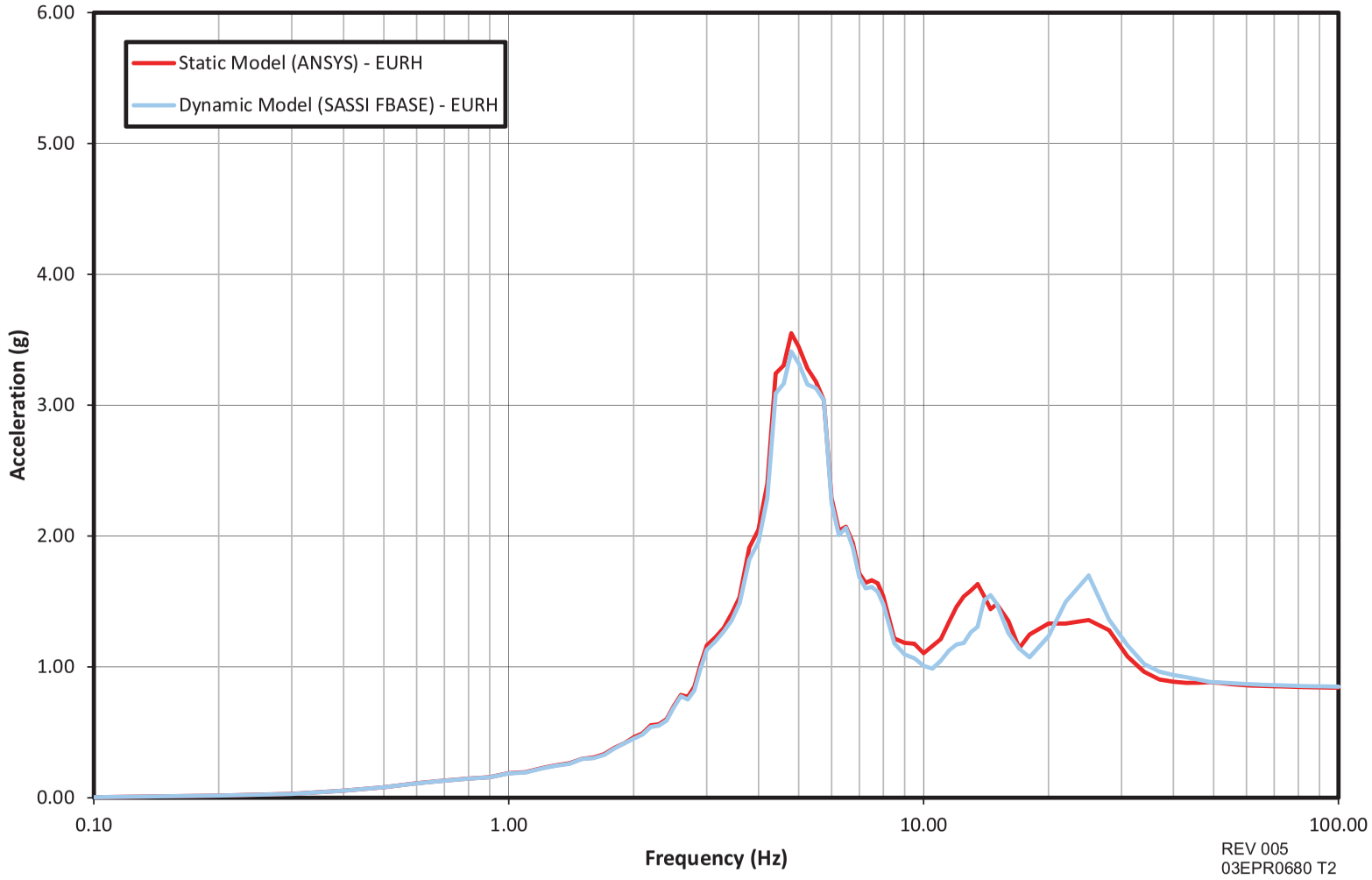

Figure 3.7.2-45—Static FEM vs. Dynamic FEM Spectrum Comparison at Elev. +123 ft, 4-1/4 in (+37.60m) - Containment Building, 5% Damping, Y-Direction

The sole purpose of this figure is to demonstrate dynamic compatibility between the dynamic and static models; it is not intended to be used as design information and it is not maintained as such.

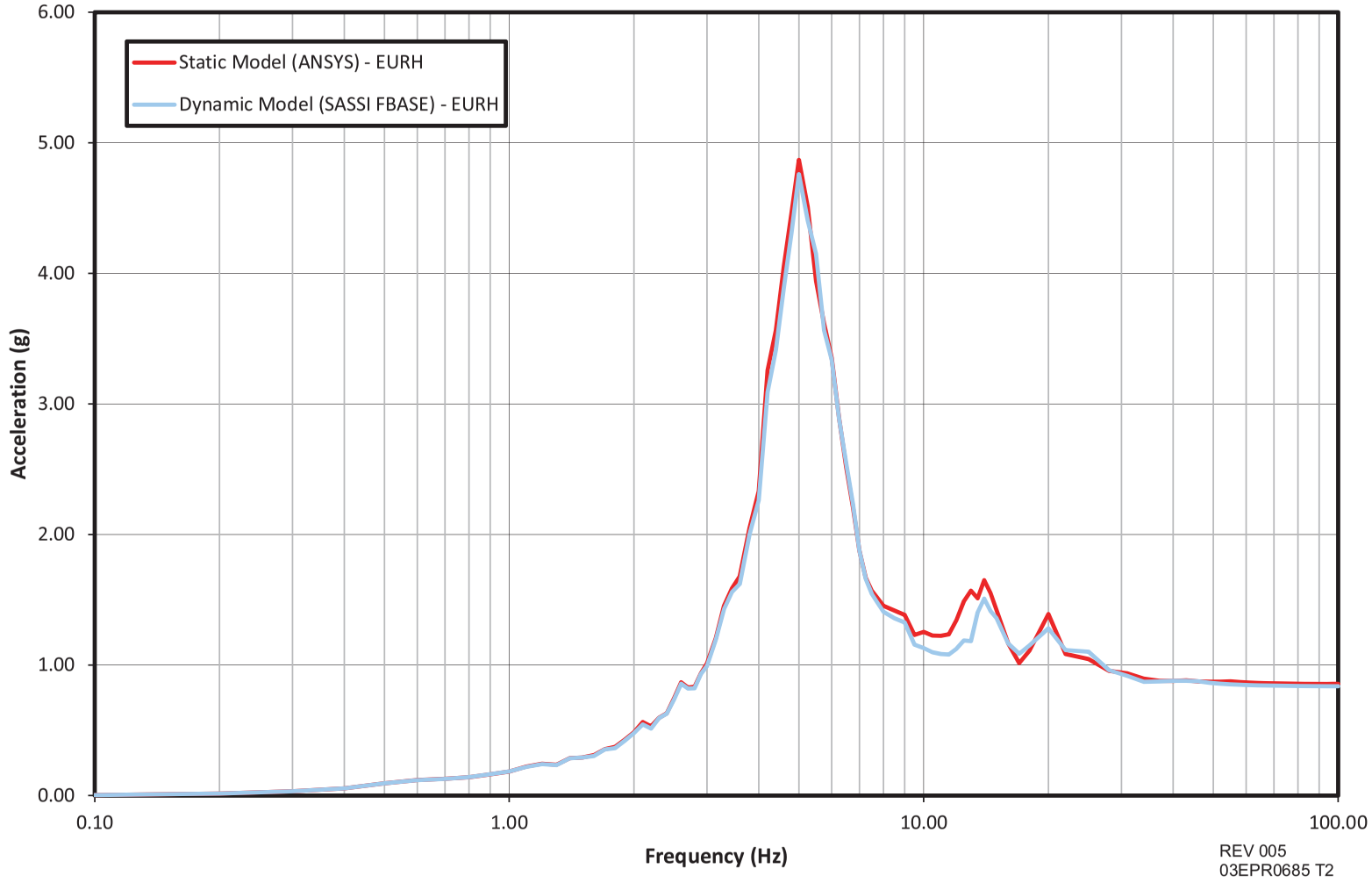

Figure 3.7.2-46—Static FEM vs. Dynamic FEM Spectrum Comparison at Elev. +123 ft, 4-1/4 in (+37.60m) - Containment Building, 5% Damping, Z-Direction

The sole purpose of this figure is to demonstrate dynamic compatibility between the dynamic and static models; it is not intended to be used as design information and it is not maintained as such.

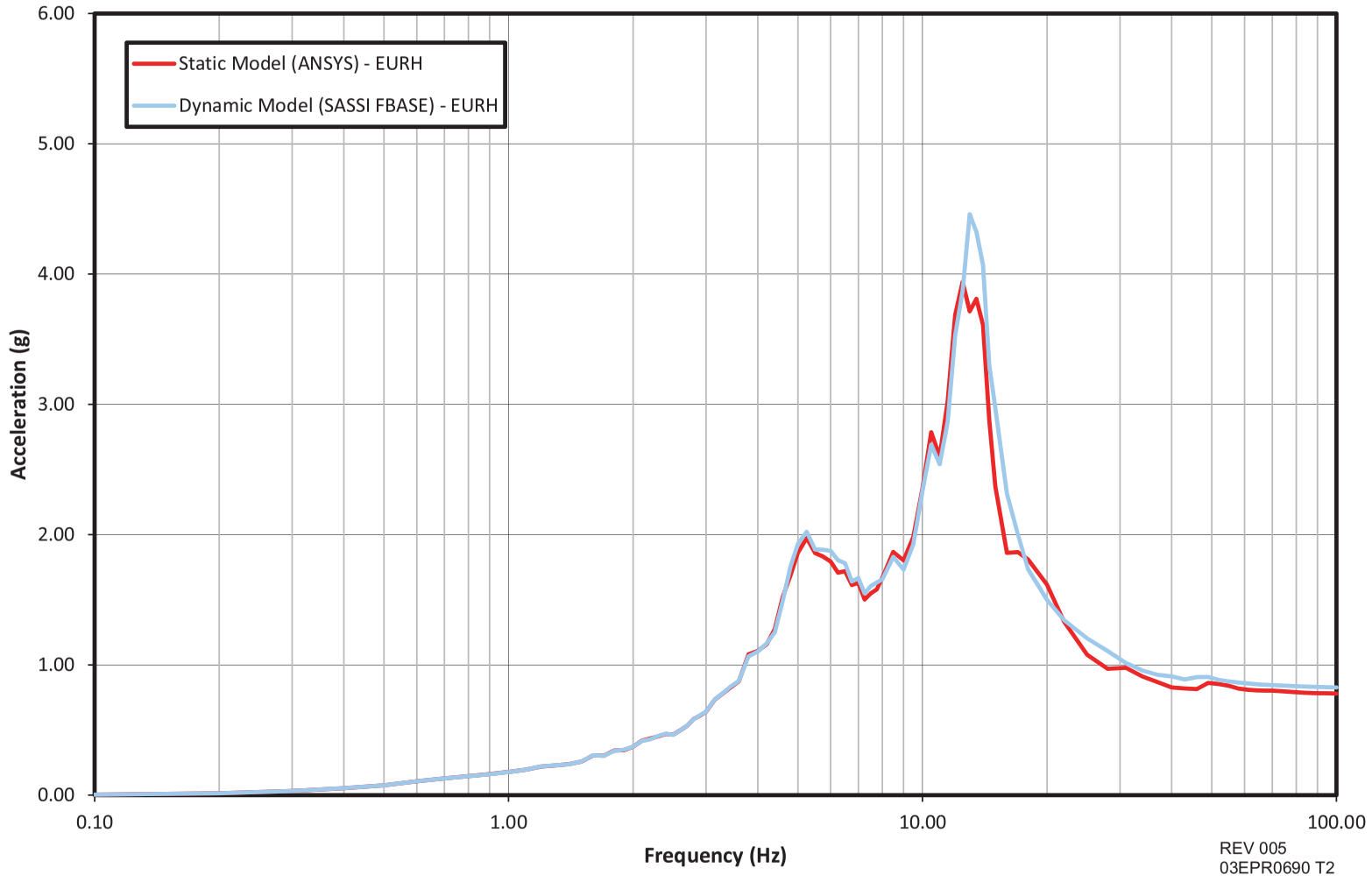

Figure 3.7.2-47—Deleted

Figure 3.7.2-48—Deleted

Figure 3.7.2-49—Deleted

Figure 3.7.2-50—Static FEM vs. Dynamic FEM Spectrum Comparison at Elev. +63 ft, 11-3/4 in (+19.50m) - Reactor Building Internal Structure, 5% Damping, X-Direction

The sole purpose of this figure is to demonstrate dynamic compatibility between the dynamic and static models; it is not intended to be used as design information and it is not maintained as such.

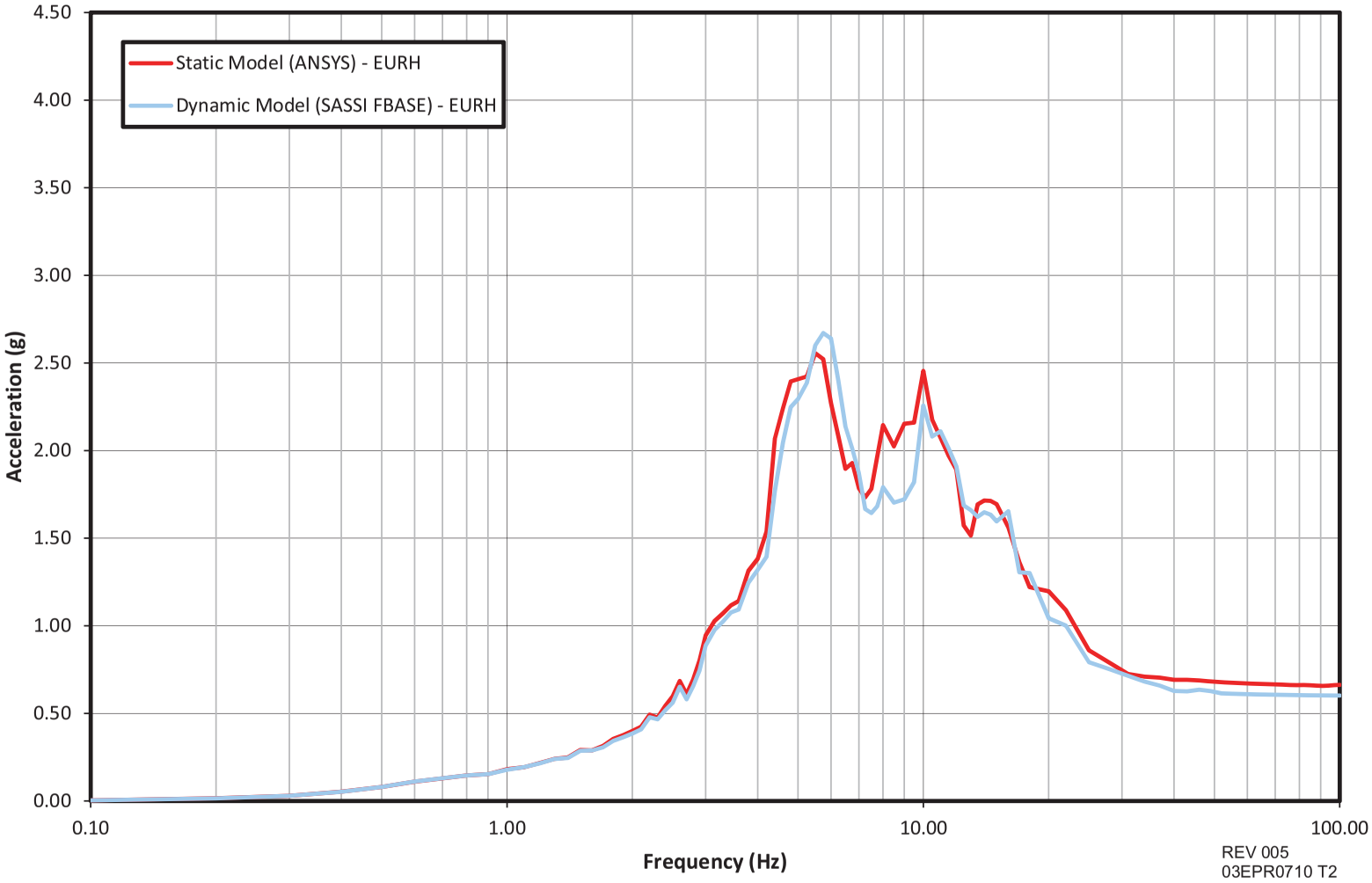

Figure 3.7.2-51—Static FEM vs. Dynamic FEM Spectrum Comparison at Elev. +63 ft, 11-3/4 in (+19.50m) - Reactor Building Internal Structure, 5% Damping, Y-Direction

The sole purpose of this figure is to demonstrate dynamic compatibility between the dynamic and static models; it is not intended to be used as design information and it is not maintained as such.

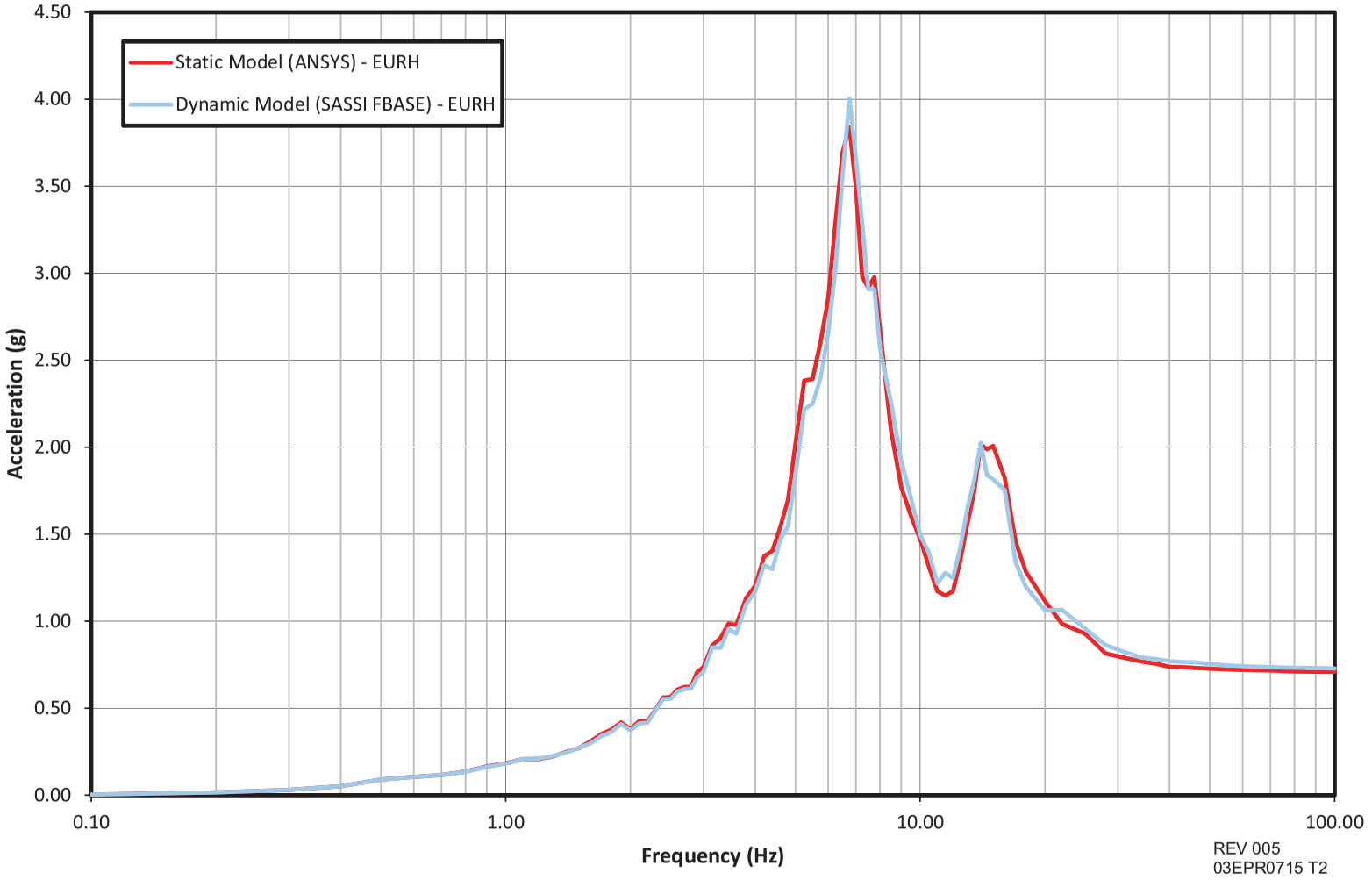

Figure 3.7.2-52—Static FEM vs. Dynamic FEM Spectrum Comparison at Elev. +63 ft, 11-3/4 in (+19.50m) - Reactor Building Internal Structure, 5% Damping, Z-Direction

The sole purpose of this figure is to demonstrate dynamic compatibility between the dynamic and static models; it is not intended to be used as design information and it is not maintained as such.

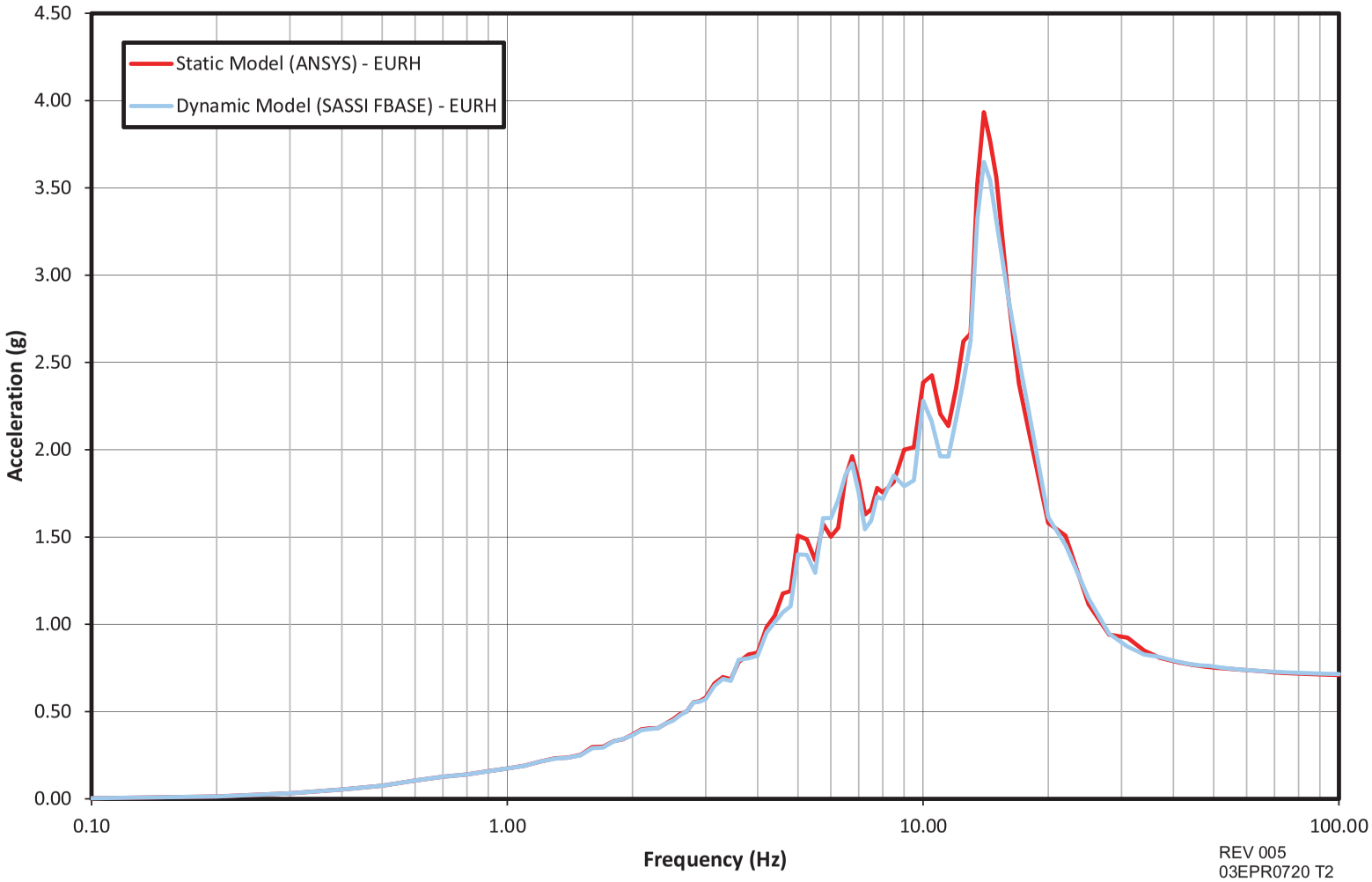

Figure 3.7.2-53—Static FEM vs. Dynamic FEM Spectrum Comparison at Elev. +16 ft, 10-3/4 in (+5.15m) - Reactor Building Internal Structure, 5% Damping, X-Direction

The sole purpose of this figure is to demonstrate dynamic compatibility between the dynamic and static models; it is not intended to be used as design information and it is not maintained as such.

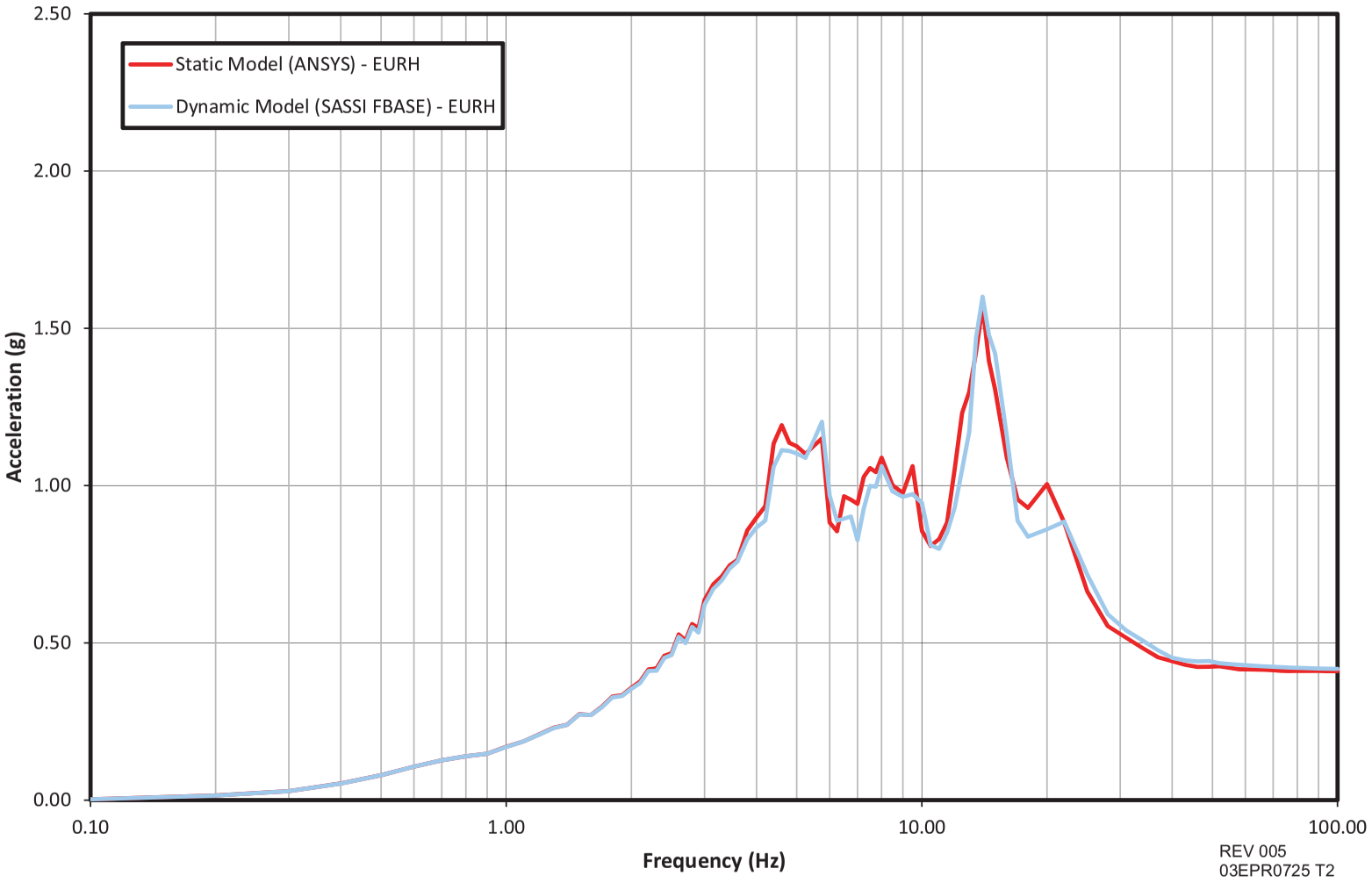

Figure 3.7.2-54—Static FEM vs. Dynamic FEM Spectrum Comparison at Elev. +16 ft, 10-3/4 in (+5.15m) - Reactor Building Internal Structure, 5% Damping, Y-Direction

The sole purpose of this figure is to demonstrate dynamic compatibility between the dynamic and static models; it is not intended to be used as design information and it is not maintained as such.

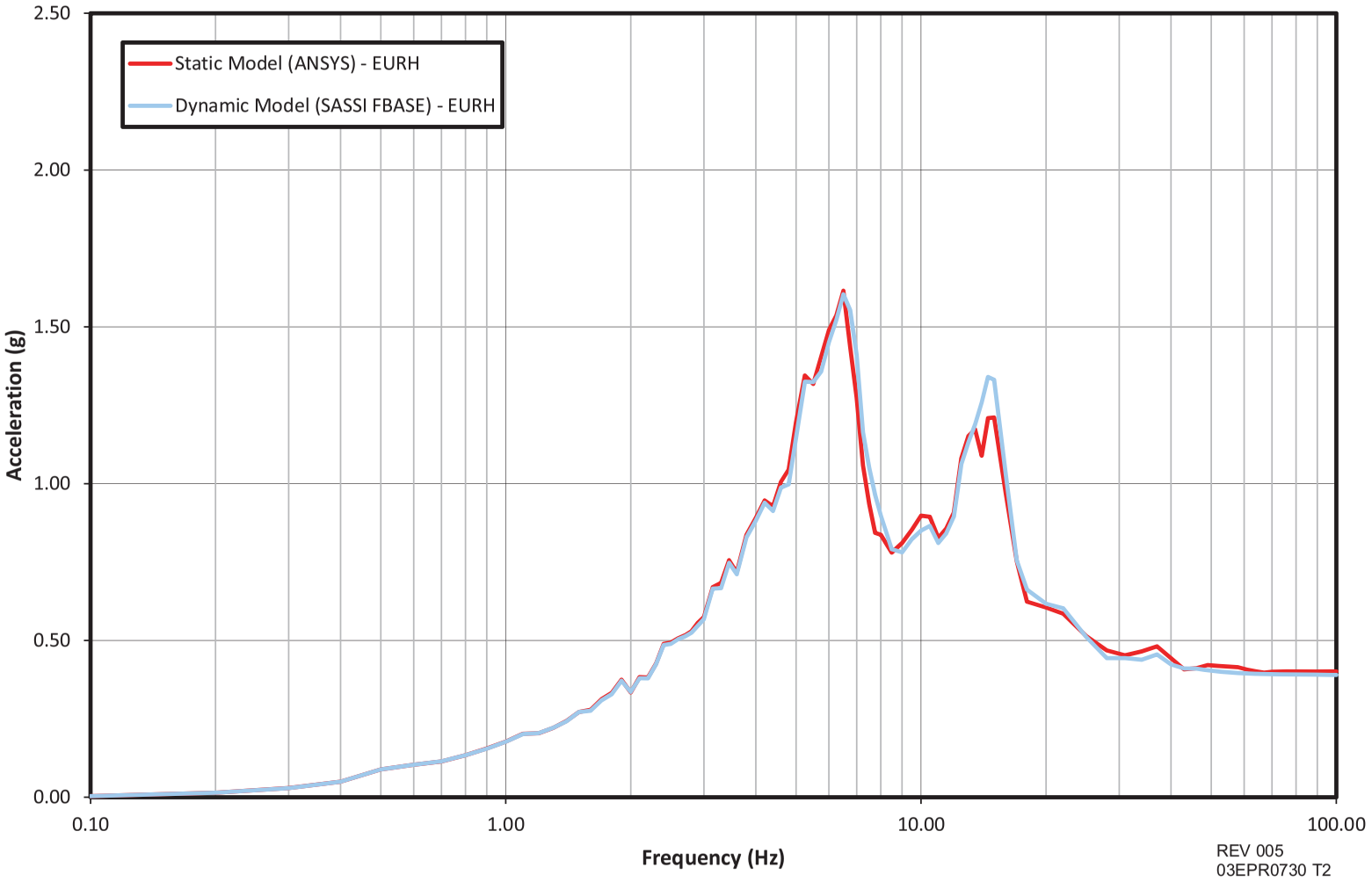

Figure 3.7.2-55—Static FEM vs. Dynamic FEM Spectrum Comparison at Elev. +16 ft, 10-3/4 in (+5.15m) - Reactor Building Internal Structure, 5% Damping, Z-Direction

The sole purpose of this figure is to demonstrate dynamic compatibility between the dynamic and static models; it is not intended to be used as design information and it is not maintained as such.